POLITECNICO DI MILANO

Facoltà di Ingegneria dei Sistemi

Corso di Laurea Specialistica in Ingegneria Biomedica

Drowsiness detection through spectral estimation of ElectroEncephaloGraphic (EEG) signals

Relatore: Prof. Sergio Cerutti

Correlatori: Prof. Jacques Verly

Ing. Matteo Migliorini

Ing. Clementine François

Tesi di Laurea di:

DANIELA MAZZEO 783251

Anno Accademico 2013-2014

ABSTRACT

OBJECTIVES

In the last years, an increasing interest about drowsiness detection is emerging. This is due to the fact that drowsiness causes a reduction of vigilance, which can affect everybody's normal daily activities.

Drowsiness is defined as the passage from wakefulness to sleep, which leads to a decrease of alertness. The main causes of sleepiness are the duration of sustained activities, sleep deprivation, circadian rhythm, the environment and individual's personal characteristics. In particular, sleep deprivation or elongated nocturnal sleep reduction, implies a strong cognitive impairment. Indeed, a sleep-deprived subject tends to take longer to react to stimuli. Besides, behavioral and physiological consequences are emerged too: reduced processing speed and information storage, weak performances for normal tasks.

This work has aimed at detecting drowsiness through the spectral analysis of electroencephalographic (EEG) signals. These signals have been acquired from volunteers while performing reaction time tests. During each test, the participant was supposed to react to stimuli, randomly presented on the screen of a computer as little circles, by clicking on the mouse, as soon as possible.

As regards spectral analysis employed for features extraction, it has been implemented by three different approaches: non-parametric, parametric and according to singular spectrum analysis ("SSA").

Secondly, performances of the three developed methods have been compared, in order to individuate which one is able to provide the best features, in terms of class's discrimination.

Finally, it was verified if the protocol is appropriate for drowsiness detection and, more specifically, if collected data mirror the purposes of this work.

MATERIALS AND METHODS

Experimental protocol

All the experimental data used in this work have been collected in the laboratory "INTELSIG" of the Department of Electrical Engineering and Computer Science (Montefiore Institute), of the Faculty of Applied Science of the University of Liège, in Belgium.

Experiments have been performed on 21 subjects, 9 males and 12 females, in an age range between 19-32 years (mean age 23.9) and in good health. The participants were selected according to the following exclusion criteria: alcohol or drugs addicted; regular smokers; recently medicated people or medical drugs consumers during the 2 weeks before the test; changing schedule workers; people with sleep disorders; people with jet lag in the 2 weeks before the test; people with the requirement of wearing glasses for driving (wearing contact lenses was allowed) or with skin allergies related to cosmetics or lotions.

Finally, it was asked to participants not to assume any stimulants (coffee or tea) between 6,00 pm on the first day until the end of the last test.

Subjects were supposed to perform three visual reaction-time (RT) tests, each lasting 15 minutes, over two days.

After a normal night of sleep, each subject realized the first reaction time test (RT1) between 8,00 am and 10,00 am on the first day.

Then, the subject wore an actimetry sensor, in order to monitor her/his sleep/awake cycle but was free to carry out daily activities, until 11,00 pm when the subject came back to the laboratory. During that night, the subject was not allowed to sleep and she/he no longer wore the actimeter. On the second day, the subject performed the second RT test (RT2) between 2,00 and 4,00 am and, after having breakfast, she/he performed the third and last RT test (RT3) between 11,00 am and 1,00 pm.

As regards the execution of each test, the participant sat in front of a computer. Throughout the whole test, a large number of stimuli was randomly presented to the volunteer on the screen of the computer. Each stimulus lasted 400 msec and the subject was supposed to react to each stimulus by clicking on the mouse of the computer as quickly as possible after having detected the onset of the stimulus. During each test, electroencephalogram (EEG), electrooculogram (EOG), electromyogram (EMG) and electrocardiogram (ECG) have been

recorded. In particular, EEG signals have been acquired with a sampling frequency of 512 Hz through electrodes Ag/AgCl disposed on central, frontal and parietal regions, C3, C4, Cz, Fz, Pz respectively, plus an electrode at the earlobe as reference and a ground electrode, placed according to the standard traditional 10/20 system. Data related to the tester's performance during each session, have been computed with respect to a minute scale and some of them, like mean reaction time and number of lapses (500 msec≤reaction time≤2 sec) have been employed in order to label each minute of test as "drowsy", "transition", "alert". The so-defined dataset resulted to be composed of 812 epochs, divided into 60 "drowsy" cases, 404 "transition" cases and 348 "alert" cases.

Signal pre-processing

The original signal has been firstly pre-processed as follows:

- mean value removal;
- band-pass filtering in the range [0.5, 35] Hz in order to eliminate more suitably the DC contribute (already drastically reduced through mean value removal) and very low frequency contribute not of interest for this work, noise due to network interference. It has been performed through a band-pass Butterworth filter of 5^{th} order so that it is possible to get the flattest frequency response amplitude in the passing band and monotonicity in the passing and stopping bands;
- zero-phase filtering obtained by processing data in both the forward and reverse directions, in order to eliminate problems related to the phase distortion (caused by the Butterworth filter): after filtering the signal in the forward direction, this filter reverses the filtered sequence and runs it back through the filter, leading to zero-phase distortion and a filter order that is double the order of the previous filter;
- signal resampling from the original sampling frequency of 512 Hz to a more appropriate frequency of 80 Hz.

Spectral analysis

Spectral analysis has been performed in three different ways: non-parametric, parametric, singular spectrum analysis (SSA).

Non-parametric analysis

The most traditional way of getting the spectrum of a signal is the periodogram, defined as the squared module of the Discrete Fourier Transform (DFT) of the signal, normalized to the number of data points employed for the computation of the DFT.
In this work, the signal has been divided into K=4 smaller segments, each of whom is long M=1200 samples, with an overlapping of 50% among adjacent segments. Then, 4 periodograms, mutually independent, have been obtained and a triangular Bartlett window has been applied in order to get the correspondent modified periodograms.
Finally, the spectral estimator has been calculated by averaging on the K modified periodograms.
Once the spectral estimator of the entire frequency range has been computed, the spectrum for each frequency band of the EEG signal has been gained as well. Since the bands of interest for this work are θ band (4-8 Hz), α band (8-13 Hz), β band (13-30 Hz), 3 additional spectra have been used in order to extract later the correspondent features. Δ band has been excluded because it is generally associated to the deep sleep.
The algorithm just described has been applied on 14 epochs of signal, test per test and subject per subject, for all the 5 acquisition channels of the EEG (C3, C4, Cz, Fz, Pz).

Parametric analysis

Parametric analysis is based on the concept that the spectrum of a signal can be computed as the spectrum of the output signal of a LTI (linear time-invariant) system receiving a white noise in input.
AR model has been preferred as model family in order to correctly represent EEG signals. According to the AR model, the amplitude of a signal at a given instant can be obtained by summing up the different amplitudes of previous samples, plus an additional noise taking into account all the sources of error.
The optimum order p of the AR model has been individuated according to the Akaike information criterion (AIC). Then, the Anderson's whiteness test was also realized on the prediction error. This test involves to check if the prediction error results to be white and so if its autocorrelation function (ACF) is maximum at lag=0 and around zero elsewhere. If the order suggested by AIC does not satisfy the condition of the Anderson's test, the order

needs to be incremented until the residual error becomes white, paying attention in order to avoid problems of over-fitting.

Finally, by summing up all the squared values of the prediction errors on the N samples of the signal, a "cost function", called J, can be obtained. This figure of merit is a function of the coefficients of the model so that the coefficients are determined through Yule Walker's equations that are based on the minimization of the function J using Levinson-Durbin recursion.

Once the estimated coefficients $\hat{a}_k$ of the model have been determined, that are as many as the order of the model, it is possible to compute the power spectrum of the signal. All the operations described until now have been run for all the 14 epochs of the signal considered, subject per subject and test per test, including all the signals coming from the 5 acquisition channels of the EEG (C3, C4, Cz, Fz, Pz).

Singular spectrum analysis

Singular spectrum analysis exploits the advantages of both singular value decomposition (SVD) and principal component analysis (PCA)in order to decompose the original series into a sum of a few components that represent the main content of the signal, such as a slowly varying trend, oscillatory components and the background noise. SSA is characterized by the fact that neither a parametric model or stationarity hypothesis are assumed for the time series so it is a model-free technique.

In this work, it has been employed in order to extract "monocomponent" signals, related to a certain frequency band, and a filtered version of the original signal.

The algorithm has been implemented through two main steps: decomposition and reconstruction.

The first step includes two additional substeps:

1. "Embedding step": the time series is embedded into multidimensional series, long L that is the window length. This is the important parameter to determine in this step because it influences the frequency resolution of the method. It was chosen to have a frequency resolution of 4Hz because this is the minimum width of each frequency band, resulting in L=20. It is possible to obtain K L-lagged vectors, where K = N-L+1, in order to compute the so-said trajectory matrix, which is a Hankel matrix. Then, the correspondent covariance matrix can be gained.

2. SVD: eigenvalues and eigenvectors of the covariance matrix have been obtained. Starting from them, the number of principal components (k=6), that are able to explain well (less than 5%) the variance of the signal, are individuated in order to eliminate most of the background noise.

The second step includes two substeps through which it is possible to reconstruct the final signals.

1. Grouping: principal components are computed and for each of them a non-parametric spectrum has been computed, by using the same devices as already described for non-parametric analysis. Through the spectral content, some indices are defined in order to obtain after the final signals: filtered original signal and monocomponent signals for θ, α, β bands.
2. Reconstruction: it consists in bringing back the new signals to the original time-scale.

For each new signal, the correspondent spectrum has been computed in order to extract features. The algorithm has been repeated for 14 epochs of signal, test per test and subject per subject, including all the signals from the 5 acquisition channels (C3, C4, Cz, Fz, Pz).

Features extraction

The EEG features selected for drowsiness detection are the percentage power in each frequency band, $log\ (\frac{P\%}{1-P\%})$, the ratio between α band activity and β band activity, the ratio between the sum of the activities in θ and α bands and the activity in β band (meaning the ratio between LF and HF), dominant peak and dominant frequency for each frequency band. As regards these last two features, the way of computing them has varied according to which method was considered.
The set of such features has been gained for 14 epochs of signal, test per test and subject per subject, for all the 5 acquisition channels (C3, C4, Cz, Fz, Pz).

Statistical analysis

The content of the 80 features (16x5 channels) has been preliminarily analyzed through ROC (receiver operating characteristic) curves. Features have been firstly normalized in order to belong to the range [0,1], by subtracting their minimum value and dividing to their

maximum value. The cut-off step has been defined according to the size of each feature while a significance value of 95% has been chosen. The parameter that has been used is the AUC (area under curve): an AUC > 0.7 indicates a good performance of the feature.
The second and decisive statistical test that has been employed is the non-parametric Kruskal-Wallis test: non-parametric because no specific probability distribution has been assumed a-priori, by Kruskal-Wallis because it allows to easily managing groups with different sizes as in this case.
In both tests, two different cases have been considered: the ability of a certain feature to discriminate between two classes, excluding the remaining one, and to distinguish a class with respect to the combination of the other two ones.

Classifier

As regards the classifier, a feed-forward neural network has been preferred, with a hidden layer and sigmoid activation function, because this work aims at identifying three distinct classes. The number of neurons for the input and the hidden layers has been fixed the same as the number of features selected through the previous statistical tests; the output layer instead is always composed of three neurons, as much as the number of classes to identify.
Data have been firstly processed so that the targets matrix contains three binary vectors where 1 indicates epochs related to the current class and 0 in the other cases, for each vector. The features matrix has been created time after time in order to contain only the selected features for the current method. The neural network has been trained according to Levenberg-Marquardt algorithm. Besides, it was thought to repeat 10 times a 5-fold cross-validation in order to moderate the effects due to the random initialization of the classifier and the random distribution of the dataset into 5 subsets. Therefore the 80% of the dataset has been employed for training the network and the remaining 20% to test it, varying 5 times the distribution of data into training set and testing set and this operation has been repeated 10 times. For each iteration, a k-Cohen coefficient has been computed and at the end 50 k-Cohen coefficients were available. In order to compare the three developed methods, the mean value and standard deviation of the k-Cohen coefficient have been considered, for each method.

RESULTS

Statistical tests, which have been used in order to select the features providing the best separation among classes, have led to the following results.

For non-parametric analysis, 11 features with a significance level of 95% have been individuated:

1. dominant peak in θ band, parietal area
2. percentage power in θ band, frontal area
3. $log\ (\frac{P\%}{1-P\%})$, frontal area
4. dominant frequency in the whole range, frontal area
5. dominant peak in the whole range, frontal area
6. dominant frequency in the whole range, central area
7. dominant peak in θ band, central area
8. percentage power in θ band, left central area
9. $log\ (\frac{P\%}{1-P\%})$, left central area
10. dominant frequency in the whole range, left central area
11. dominant peak in the whole range, left central area.

For the parametric analysis, the following 4 features have resulted to be statistically significant at 95%:

1. percentage power in θ band, frontal area
2. $log\ (\frac{P\%}{1-P\%})$, frontal area
3. percentage power in θ band, left central area
4. $log\ (\frac{P\%}{1-P\%})$, left central area.

For singular spectrum analysis (SSA), only 3 features have showed a significance level of 95%:

1. dominant peak in the whole range, frontal area
2. domain peak in the whole range, central area
3. dominant peak in θ band, left central area.

From k-Cohen coefficients it emerged that the first non-parametric method results to be the one which is associated the greatest accuracy for classes identification, because a mean value of the k-Cohen coefficient of 0.5087 with a standard deviation of 0.0194 has been obtained.

Finally, from the analysis of all the subjects through the non-parametric method, resulted to be the best one, it emerged that, from a physiological point of view, dominant peak and dominant frequency in θ band and in the whole range are optimal features, together with $log\ (\frac{P\%}{1-P\%})$,as regards frontal and central (both C3, Cz) EEG derivations, and only for dominant peak in θ, also the parietal area.

DISCUSSION AND CONCLUSION

According to results of the statistical tests, it is possible to state that this work has allowed individuating a subset of features that are able to distinguish, with a significance level of 95%, among the desired classes: alertness, "transition", drowsiness.

In particular, the unbalanced number of features obtained for each method (11,4,3) has absolutely favored an appropriate training of the neural network in the case of non-parametric analysis but not in the other cases.

In addition, the dataset has not provided a high number of drowsy cases so that this aspect has surely influenced the performance of both the methods and the classifier to correctly discriminate drowsiness with respect to the other two ones.

It must be observed that the SSA method has however provided optimal performance in individuating the energy distribution for each frequency band.

As future proposals, it could be interesting to possibly repeat such analysis with richer and more varied datasets, in terms of classes, in order to verify if the performances of the methods stay the same or they improve.

In addition, since during reaction time tests subjects reacted by clicking on the mouse, that movement causes the sensorimotor cortex activation. Therefore, it could be interesting to take into account the event-related synchronization/ desynchronization (ERS, ERD), by exploiting data regarding the time of stimulus presentation and of reaction to it, which were not available for this work.

Finally, a last suggestion for the future could be to try to develop an automatic data labelling of the minutes of test (i.e. through unsupervised machine learning), instead of the manual approach implemented in this research.

SOMMARIO

OBIETTIVI

Negli ultimi anni, sta emergendo un sempre più acuto interesse verso la rilevazione della sonnolenza. Tale fenomeno è responsabile della diminuzione della vigilanza che può influenzare la capacità di ognuno di effettuare normalmente le attività quotidiane.

La sonnolenza è definita come quello stato di passaggio dalla veglia al sonno che comporta un abbassamento del livello di vigilanza. Tra le principali cause che conducono alla sonnolenza si annoverano la durata di attività continuative, la privazione di sonno, il ritmo circadiano, l'ambiente e le caratteristiche personali di ciascun individuo. In particolare, la privazione o eccessiva e prolungata riduzione della quantità del sonno notturno comporta un elevato deficit cognitivo con gravi conseguenze. Di fatto, una persona privata del sonno impiega mediamente più tempo a reagire agli stimoli. Inoltre anche delle conseguenze di tipo comportamentale e fisiologico sono emerse: una ridotta velocità di elaborazione e immagazzinamento di informazioni, riduzione della vigilanza e scarse prestazioni nello svolgere abituali attività.

Questo studio è stato finalizzato alla rilevazione della sonnolenza attraverso l'analisi spettrale di segnali elettroencefalografici (EEG). Tali segnali sono stati acquisiti da soggetti volontari che si sono offerti di effettuare dei test di tempi di reazione. Ogni test prevedeva che il partecipante reagisse agli stimoli, presentati in modo casuale sullo schermo di un computer come dei piccoli cerchi, cliccando sul mouse il più velocemente possibile.

Per quanto riguarda l'analisi spettrale adoperata per l'estrazione delle caratteristiche, essa è stata implementata secondo tre differenti approcci: non parametrico, parametrico, secondo l'analisi degli spettri singolari ("SSA").

Secondariamente, sono state confrontate le perfomances dei tre metodi sviluppati, con lo scopo di individuare quello in grado di fornire i descrittori caratterizzati da prestazioni e potere discriminatorio migliori.

Per concludere, si è voluto valutare se il protocollo proposto è adatto o meno a rilevare la sonnolenza e in particolare, se i dati raccolti rispecchiano le intenzioni di questa ricerca.

MATERIALI E METODI

Protocollo sperimentale

Tutti i dati sperimentali utilizzati nel presente lavoro sono stati raccolti presso il laboratorio "INTELSIG" del Dipartimento di Ingegneria Elettrica e Computer Science (Istituto Montefiore), della Facoltà di Scienze Applicate dell'Università di Liège, in Belgio.

Gli esperimenti sono stati effettuati su 21 soggetti, di cui 9 maschi e 12 femmine, in un intervallo di età tra i 19-32 anni (età media 23.9) e in buona salute. Per la selezione dei partecipanti, si è tenuto conto dei seguenti criteri di esclusione: dipendenti da alcool e droghe, fumatori abituali, persone con medicazioni o che hanno assunto medicine nelle due settimane precedenti al test, lavoratori con scheduling variabile, persone con disordini del sonno, jet lag nelle due settimane precedenti al test, con prescrizione ad indossare occhiali da vista (le lenti a contatto erano ammesse), con allergie cutanee legate a cosmesi e lozioni varie. Infine, veniva richiesto ai volontari di non assumere alcuno stimolante (caffè o tè) tra le 6 pm del primo giorno di test fino alla fine dell'ultimo giorno di test.

Ogni partecipante ha svolto tre test visivi di tempi di reazione (RT), ciascuno della durata di 15 minuti, nell'arco di due giorni. Il primo test (RT1) è stato effettuato tra le 8,00 e le 10,00 del mattino del primo dei due giorni previsti per l'esperimento, dopo una normale notte di sonno. A partire dalla fine del test, veniva richiesto al soggetto di indossare un sensore di actimetria in modo da poter monitorare il proprio ciclo di sonno/veglia, senza però condizionare il normale svolgimento delle attività quotidiane. Alle 11 di sera, il tester ritornava in laboratorio e si interrompeva il monitoraggio tramite actimetro. Durante la notte che seguiva, al soggetto veniva richiesto di non dormire. Quindi, tra le 2,00 e le 4,00 di mattina (inizio del secondo giorno), egli eseguiva il secondo test (RT2). Infine, dopo aver fatto colazione, svolgeva il terzo e ultimo test (RT3), tra le 11,00 di mattina e l'1 di pomeriggio.

Il test prevedeva che il soggetto stesse seduto di fronte un computer e che una certa quantità random di stimoli, della durata di 400 msec, fosse inviata. Durante ogni test, venivano acquisiti i segnali elettroencefalografici (EEG), elettromiografici (EMG), elettrooculografici (EOC), elettrocardiografici (ECG). In particolare l'EEG è stato acquisito con una frequenza di campionamento di 512 Hz e tramite 5 canali (C3, C4, Cz, Fz, Pz per le regioni centrale, frontale e parietale dello scalpo), secondo il sistema standard

10-20. I dati riferiti alle prestazioni del tester per ogni sessione sono stati calcolati sulla scala del minuto e alcuni di questi, come il tempo di reazione medio e il numero di "sbagli" (500 msec ≤tempo di reazione ≤2 sec), sono stati utilizzati per definire le etichette di ogni minuto di test ("assonnato", "in transizione", "sveglio"). Il dataset, così etichettato, risulta composto di 812 epoche divise in 60 casi di "assonnato", 404 di "in transizione" e 348 di "sveglio".

Pre-elaborazione dei segnali

Il segnale originale è stato innanzitutto pre-elaborato nel seguente modo:

- rimozione del valore medio;
- filtraggio passa-banda nell'intervallo [0.5, 35] Hz per eliminare più adeguatamente il contributo in continua (già drasticamente ridotto con la rimozione del valor medio) e quello in bassissima frequenza. Si è usato un filtro passa-banda di Butterworth di quinto ordine, in modo da ottenere una risposta in frequenza il più piatta possibile in modulo nella banda passante e monotonicità in banda passante e arrestata;
- filtraggio a fase zero, ottenuto filtrando prima il segnale in una direzione e poi applicando lo stesso filtro ma a coefficienti invertiti. Questa tecnica consente di eliminare i problemi causati dalla distorsione di fase introdotta dal filtro di Butterworth e conduce a un filtro con ordine doppio rispetto al precedente;
- ricampionamento del segnale da 512 Hz a 80 Hz.

Analisi spettrale

L'analisi spettrale è stata effettuata in tre differenti modi: non parametrico, parametrico, secondo il metodo dell'SSA.

<u>Analisi non parametrica</u>

Il modo più tradizionale per ottenere lo spettro del segnale è il calcolo del periodogramma, definito come il modulo quadrato della trasformata del segnale diviso per il numero di punti utilizzati per il calcolo della trasformata stessa. In questo lavoro, si è scelto di suddividere il segnale in K=4 segmenti più piccoli, ognuno di M=1200 campioni ciascuno, con una sovrapposizione del 50% tra segmenti adiacenti. Quindi 4 periodogrammi,

reciprocamente indipendenti, vengono ottenuti applicando una finestra triangolare di Bartlett per ricavare i corrispondenti periodogrammi modificati. Infine lo stimatore spettrale si ottiene mediando sui K periodogrammi modificati.
Una volta ottenuto lo stimatore spettrale sull'intero intervallo di frequenze [0.5, 35]Hz, si è voluto calcolare lo spettro su ogni banda di frequenza del segnale EEG. Ricordando che le bande considerate in questo lavoro sono la banda θ (4-8 Hz), α (8-13 Hz), β (13-30 Hz), si ottengono 3 spettri aggiuntivi da cui verranno successivamente estratte le corrispondenti caratteristiche. La banda δ è stata esclusa perché generalmente associata al sonno profondo. L'algoritmo appena descritto è applicato a tutte e 14 le epoche di segnale, test per test e soggetto per soggetto, in riferimento ai 5 canali di acquisizione dell'EEG (C3, C4, Cz, Fz, Pz).

Analisi parametrica

L'analisi parametrica si basa sul concetto che lo spettro di un segnale può essere calcolato come lo spettro dell'uscita di un sistema lineare tempo-invariante (LTI) che riceva in ingresso un rumore bianco.
Come famiglia di modelli per rappresentare un segnale EEG si è preferito usare il modello AR, secondo il quale l'ampiezza di un segnale ad un dato istante è esprimibile come la somma dello stesso agli istanti precedenti, più l'aggiunta di un rumore che tenga conto dell'imperfezione della stima e di ogni fonte di disturbo.
Per quanto riguarda l'ordine ottimo, esso è stato individuato utilizzando il criterio di ottimalità di Akaike (AIC= Akaike information criterion), in combinazione con il test di Anderson di bianchezza dell'errore di predizione. Con il test di Anderson, si è andato a controllare che l'errore di predizione commesso dallo stimatore sia bianco, ovvero che il modello sia stato in grado di spiegare il processo in modo esaustivo. Se però il test di Anderson non risultava verificato, l'ordine del modello veniva incrementato fintantoché il rumore non diventasse bianco, evitando però di incrementarlo eccessivamente e rischiare il problema di overfitting. Infine si è calcolata la funzione di costo come la somma dei quadrati degli errori di predizione commessi sugli N campioni. Minimizzando tale cifra di merito, che è una funzione dei coefficienti del modello, questi possono essere ricavati attraverso le equazioni di Yule Walker, utilizzando il metodo ricorsivo di Levinson Durbin. Una volta stimati i coefficienti $\hat{a}_k$ del modello (tanti quanto l'ordine ottimo p), si ricava lo

stimatore spettrale del segnale. Anche in questo caso, una volta calcolato lo spettro nell'intero intervallo, è stato calcolato anche lo spettro per ogni banda di frequenza. Tale algoritmo è stato applicato a tutte le 14 epoche di segnale, test per test e soggetto e per soggetto, in riferimento ai 5 canali di acquisizione dell'EEG (C3, C4, Cz, Fz, Pz).

Singular spectrum analysis

L'analisi degli spettri singolari si propone di sfruttare i vantaggi della scomposizione ai valori singolari (SVD) e l'analisi delle componenti principali (PCA) per scomporre la serie temporale originale nella somma di poche componenti che racchiudono le informazioni principali: componente lentamente variabile, componente oscillatoria e rumore di sottofondo. Il grande vantaggio nell'impiego di tale metodo è il fatto che si tratta di una tecnica "model-free", a fronte però di un costo computazionale elevato. In questo lavoro, essa è stata impiegata con l'obiettivo di estrarre dei segnali "monocomponente" che fossero legati, ciascuno, ad una certa banda di frequenza di interesse e inoltre per ottenere un segnale EEG ripulito dal rumore. L'algoritmo è stato implementato secondo i seguenti due passaggi: la scomposizione e la ricostruzione del segnale.
Il primo può essere ulteriormente scomposto in due step secondari:

1. "Embedding step": la serie temporale è incorporata in serie multidimensionali di dimensione L. Tale dimensione rappresenta il parametro critico da definire a questo livello in quanto influenza la risoluzione in frequenza del metodo. Si è scelto di avere una risoluzione in frequenza di 4Hz, che è l'ampiezza minima di ogni banda di frequenza, imponendo L=20. Si ottengono quindi K vettori ritardati di L, con K=N-L+1, dai quali si ricava la cosiddetta matrice traiettoria, che è un matrice di Hankel. Da quest'ultima si può ottenere la corrispondente matrice di covarianza.
2. SVD: si ottengono gli autovalori e gli autovettori della matrice di covarianza, a partire dai quali è stato ricavato il numero di componenti principali (k=6) che spiegano adeguatamente (a meno del 5%) la varianza del segnale e permettono di eliminarne gran parte del rumore di sottofondo.

Il secondo passaggio riguarda i due momenti tramite i quali è possibile ricostruire i segnali finali.

1. Raggruppamento: si ricavano le componenti principali e per ognuna si calcola uno spettro non-parametrico secondo le stesse modalità precedentemente spiegate. In base ad esso si definiscono degli indici che sono stati in seguito usati per ricavare i segnali finali: segnale originale filtrato e segnali monocomponente relativi a θ, α, β.
2. Ricostruzione: consiste nel riportare il segnale scomposto e rielaborato nella scala temporale originale.

Su ogni segnale è stato infine calcolato il corrispondente spettro per ricavarne dei descrittori. L'algoritmo è stato ripetuto per 14 epoche di segnale, test per test e soggetto per soggetto, in riferimento ai 5 canali di acquisizione dell'EEG (C3, C4, Cz, Fz, Pz).

Estrazione di descrittori

Le caratteristiche individuate per la rilevazione della sonnolenza sui segnali EEG sono state la potenza percentuale in banda, $log\ (\frac{P\%}{1-P\%})$, il rapporto tra l'attività in banda α e in banda β, il rapporto tra la somma delle attività in banda α e θ e l'attività in banda β (inteso come rapporto tra LF e HF), picco dominante e frequenza dominante per ogni banda di frequenza e su tutto l'intervallo considerato. Per quanto riguarda queste ultime due caratteristiche, la modalità con cui sono state ottenute è variata a seconda del metodo di analisi spettrale considerato. L'insieme di descrittori appena elencato è stato ricavato per 14 epoche di segnale, test per test e soggetto per soggetto, per tutti e 5 i canali di acquisizione dell'EEG (C3, C4, Cz, Fz, Pz).

Analisi statistica

Il contenuto degli 80 descrittori (16x5canali) è stato preliminarmente analizzato tramite curve ROC (receiver operating characteristic). Essi sono stati innanzitutto normalizzati in modo da rientrare nell'intervallo [0,1], con sottrazione del valore minimo e divisione per il valore massimo. Il passo di cut-off invece è stato definito in base alla taglia di ciascun descrittore mentre si è scelto un livello di significatività del 95%. Il parametro utilizzato è stato l'AUC (area under curve): un AUC > 0.7 indicava una buona prestazione del descrittore.

Il secondo e decisivo test statistico impiegato è stato il test non parametrico di Kruskal-Wallis: non parametrico perché non si è assunta alcuna distribuzione di probabilità a priori, di Kruskal-Wallis in quanto esso permette di gestire facilmente gruppi di taglie differenti,

come in questo caso. In entrambi i test, sono state valutate due situazioni differenti: capacità delle caratteristiche di discriminare tra due classi con esclusione della restante e di distinguere una classe rispetto alla combinazione delle altre due.

Classificatore

Per il classificatore, la scelta è caduta su una rete neurale feed-forward, con uno strato nascosto e funzione di attivazione la funzione sigmoide, in quanto si vuole distinguere tra tre differenti classi. Il numero di neuroni per lo strato di ingresso e nascosto è stato fissato pari al numero di descrittori selezionati tramite i precedenti test statistici; lo strato di uscita invece contiene sempre 3 neuroni tanto quanto il numero di classi che si vuole identificare.
Innanzitutto i dati sono stati rielaborati in modo che la matrice dei target contenesse tre vettori binari in cui 1 indicasse le epoche relative alla classe corrente e 0 negli altri casi, per ciascun vettore. La matrice delle caratteristiche è stata creata di volta in volta per contenere le sole caratteristiche selezionate per ogni metodo. La rete è stata addestrata secondo il metodo di Levenberg-Marquardt. Inoltre si è scelto di ripetere una cross-validazione 5-fold per dieci volte in modo da lenire ogni effetto legato all'inizializzazione casuale della rete e alla ripartizione casuale del dataset in 5 basi. Quindi si è utilizzato l'80% del dataset per addestrare la rete e il restante 20% per testarla, variando per cinque volte la ridistribuzione dei dati in training set e testing set e poi ripetendo il tutto per 10 volte. Ad ogni iterazione inoltre è stato calcolato un coefficiente k di Cohen per un totale di 50 coefficienti. Per confrontare quindi i tre metodi si è utilizzati il valore medio e la deviazione standard del coefficiente k di Cohen, relativo ad ogni metodo.

RISULTATI

I test statistici adoperati per selezionare i descrittori in grado di fornire il migliore potere discriminante tra classi hanno condotto ai seguenti risultati.
Per l'analisi non parametrica sono state individuati 11 descrittori con un livello di significatività del 95%:

1. picco dominante in banda θ, area parietale
2. potenza percentuale in banda θ, area frontale

3. $log\ (\frac{P\%}{1-P\%})$, area frontale
4. frequenza dominante nell'intero range, area frontale
5. picco dominante nell'intero range, area frontale
6. frequenza dominante nell'intero range, area centrale
7. picco dominante in banda θ, area centrale
8. potenza percentuale in banda θ, area centrale sinistra
9. $log\ (\frac{P\%}{1-P\%})$, area centrale sinistra
10. frequenza dominante nell'intero range, area centrale sinistra
11. picco dominante nell'intero range, area centrale sinistra.

Per l'analisi parametrica sono risultate statisticamente significative al 95% le seguenti 4 caratteristiche:

1. potenza percentuale in banda θ, area frontale
2. $log\ (\frac{P\%}{1-P\%})$, area frontale
3. potenza percentuale in banda θ, area centrale sinistra
4. $log\ (\frac{P\%}{1-P\%})$, area centrale sinistra.

Per l'analisi degli spettri singolari, solo 3 descrittori hanno mostrato un livello di significatività del 95%:

1. picco dominante nell'intero range, area frontale
2. picco dominante nell'intero range, area centrale
3. picco dominante in banda θ, area centrale sinistra.

Dai valori dei coefficienti k di Cohen è emerso che il primo metodo non parametrico risulta quello a cui è associata la maggiore accuratezza nell'identificazione delle tre classi, avendo ottenuto un valore medio del k di Cohen pari a 0.5087 con una deviazione standard di 0.0194.

Infine dall'analisi di tutti i soggetti tramite metodo non parametrico, risultata la più prestante, e le caratteristiche corrispondenti selezionate, è emerso che, da un punto di vista fisiologico, picco dominante e frequenza dominante sia in banda θ che nell'intero range sono degli ottimi descrittori, insieme con il $log\ (\frac{P\%}{1-P\%})$, relativamente alle derivazioni

EEG frontale e centrale (Cz, C3) e solo per il picco dominante in banda θ anche dall'area parietale.

DISCUSSIONE E CONCLUSIONI

Secondo i risultati ottenuti dai test statistici si può concludere che questo lavoro ha consentito di individuare un sottoinsieme di descrittori in grado di distinguere, con una significatività del 95%, tra le classi desiderate: allerta, "transizione", sonnolenza. In particolare il fatto di aver ottenuto un numero sbilanciato di descrittori tra i vari metodi (11, 4, 3) ha decisamente favorito un buon addestramento della rete neurale nel caso del metodo di analisi non parametrica, a discapito degli altri due.

A questo bisogna aggiungere il fatto che il dataset utilizzato non ha fornito un elevato numero di casi di sonnolenza per cui anche questo aspetto ha sicuramente influenzato le prestazioni e dei metodi e del classificatore a discriminare correttamente tale classe rispetto alle altre.

Va detto però che per quanto riguarda la capacità di individuare la distribuzione di energia per ogni banda di frequenza, il metodo SSA ha comunque fornito ottime prestazioni.

Come sviluppo futuro, sarebbe interessante ripetere eventualmente tale analisi nel caso di dataset più ricchi e diversificati in termini delle tre casistiche, al fine di verificare se le prestazioni dei vari metodi vengano confermate o presentino dei miglioramenti.

Inoltre, dal momento che durante i test di reazione, i soggetti reagiscono con un click sul mouse, tale movimento comporta una certa attivazione della corteccia sensorimotoria. Sarebbe pertanto interessante tenere conto della sincronizzazione/desincronizzazione evento-correlata, conseguenziale al movimento, sfruttando i dati riguardanti l'istante di presentazione dello stimolo e di reazione ad esso, che in questo studio non erano purtroppo consultabili.

Infine, un ultimo suggerimento per il futuro potrebbe essere quello di tentare di sviluppare in modo automatico l'etichettatura dei minuti di test (ad esempio mediante tecniche di machine learning non supervisionato), sostituendola all'approccio manuale implementato in tale lavoro.

Index

Glossary

AIC = Akaike Information Criterion

ACF = AutoCorrelation Function

ANN = Artificial Neural Network

ANOVA = Analysis Of Variance

AUC = Area Under Curve

AR = Auto Regressive

ARMA = Auto Regressive Moving Average

C3 = Left central area of the brain

C4 = Right central area of the brain

Cz = Median central area of the brain

DC = Direct Current

DFT = Discrete Fourier Transform

ECG = ElectroCardioGraphic/ElectroCardioGram

EEG = ElectroEncephaloGraphic/ElectroEncephaloGram

EMG = ElectroMyioGraphic/ElectroMyoGram

EOG = ElectroOculoGraphic/ElectroOculoGram

EOF = Empirical Orthogonal Function

ERD = Event-Related Desynchronization

ERS = Event-Related Synchronization

Fz = Median frontal area of the brain

FPE = Final Prediction Error

FFT = Fast Fourier Transform

FWHM = Full Width Half Maximum

HF = High Frequency

Hz = Hertz

KSS = Karolinska Sleepiness Scale

LF = Low Frequency

LCD = Liquid Crystal Display

LTI = Linear Time Invariant

No = number

MA = Moving Average

MDL = Minimum Description Length

Msec = milliseconds

NaN = Not a Number

NREM = Non REM sleep (see REM meaning)

N1 = 1st NREM sleep stage

N2 = 2nd NREM sleep stage

N3 = 3rd NREM sleep stage

OSS = Objective Sleepiness Scale

PC = Principal Component

PSD = Power Spectral Density

Pz = Median parietal area of the brain

P% = Percentage Power

PCA = Principal Component Analysis

PSG = PolySomnoGraphic/ PolySomnoGraphy

REM = Rapid Eye Movement

ROC = Receiver Operating Characteristic

RT = Reaction-time Test

RT1 = Reaction-time Test no. 1

RT2 = Reaction-time Test no.2

RT3 = Reaction-time Test no.3

R&K = Rechtschaffen and Kales sleep scale

SSA = Singular Spectrum Analysis

SCN = SupraChiasmatic Nuclei

Sec = seconds

SVM = Support Vector Machine

SWA = Slow Wave Activity

VPE = Variance Prediction Error

W = Wakefulness sleep stage

WN = White Noise

1. State of art

In the recent years, an increasing interest for drowsiness detection is emerging. This phenomenon, that is not yet the sleep but something that anticipates the real and proper sleep, is responsible of a decreased vigilance, which can influence the normal capability of individuals to carry out everyday tasks [1].

This study focuses on drowsiness detection through EEG signals spectral analysis, acquired from volunteers that have performed reaction time tests. These tests involve subjects to react to stimuli, randomly presented on the screen of a computer in the form of little circles, by clicking on the mouse of the computer, as soon as possible.

In order to better understand what drowsiness is, it is worthy to introduce a brief review on sleep, its macrostructure and the physiological meaning of each frequency band.

In addition, it is appropriate to mention the correlation between motor acts and their evidences on EEG signals because subjects' reactions consist of movements of clicks on the mouse of the computer.

Lastly, as drowsiness detection is realized through EEG spectral analysis, a panorama of results of several methods of spectral analysis, applied to EEG in order to study drowsiness, is provided.

1.1 Sleep physiology and EEG

Sleep is a primary need that assumes a central role in everybody's life therefore a quantitative and qualitative evaluation of it can be very useful. It is defined as a nervous, rhythmic and active process, regulated by the so-called "circadian pacemaker". A correct balance sleep/wakefulness contributes to the following functions: energetic recovery, temperature decrease, immune defense, memory and learning enhancement.

The polysomnography (PSG) represents the classical approach in order to monitor several physiological parameters and signals (EEG, EOG, EMG, ECG), related to sleep. It is normally performed in specialized sleep centers or by home: throughout a night of sleep, the above-mentioned signals are recorded and then analyzed. More specifically, the PSG involves experienced physicians to visually distinguish the several stages of sleep.

The possibility of continuous recordings of the brain electrical activity, through electroencephalographic signals (EEG), during sleep and wakefulness, has revealed specific activity patterns for each vigilance state. As emerged from literature, wakefulness is characterized by low voltage and fast frequency activities, also referred as beta band (13,30 Hz). When eyes close in preparation for sleep, alpha activity (8-13 Hz) becomes prominent, mainly in the occipital area of the scalp. Just after the so-called stage W, NREM sleep starts. It is subdivided into different stages: a transitional state, stage 1 (N1), characterized by an alpha disappearing activity, gradually substituted by a low-voltage mixed-frequency EEG pattern with prominent theta activity (4-8 Hz). Stage 1 moves to NREM sleep stage 2 (N2), where the EEG is characterized by sleep spindles (12-15 Hz). Finally, NREM sleep stage 3 (N3) follows, where the EEG shows high voltage and slow frequency waves at around 1-2 Hz, so that it is also known as slow wave sleep [49, 50]. The several sleep stages are tightly regulated and a correct alternation is heavily influenced by humoral factors, previous wakefulness, psychological and environmental aspects. For further details, it is suggested to read Appendix A.

Once a fast panoramic of sleep is introduced, it is possible to understand why somnolence can be located in between the so-called stage W, related to wakefulness, and the early instants of NREM sleep.

1.2 Somnolence characterization

Drowsiness is the transition state between awakening and sleep during which vigilance level generally decreases. One of the main factor that can lead to drowsiness is the fatigue. This is the reason why the terms ‘sleepiness’ and ‘fatigue’ are often used as synonymous to indicate the result of neurobiological processes regulating circadian rhythms and the sleep [5]. It emerged from several studies that there are various causes that lead to drowsiness such as duration of continuous tasks, sleep deprivation, circadian rhythm, the environment and personal characteristics of each individual. The main effect of total sleep deprivation, and even of the prolonged reduction in sleep, causes cognitive impairment, with strong practical consequences [49]. A sleep-deprived person tends to take longer to react to stimuli, especially when tasks are monotonous and require weak emotional involvement. In addition, it leads to behavioral and physiological modifications (Figure 1.1) such as decreased processing speed and memory capacity, drastic changes in task performance,

reduction in vigilance, slower reaction time [1]. Therefore, since sleep deprivation produces more than just decreased alertness, drowsiness occurring can represent a serious problem when a sustained attention is needed to perform some tasks.

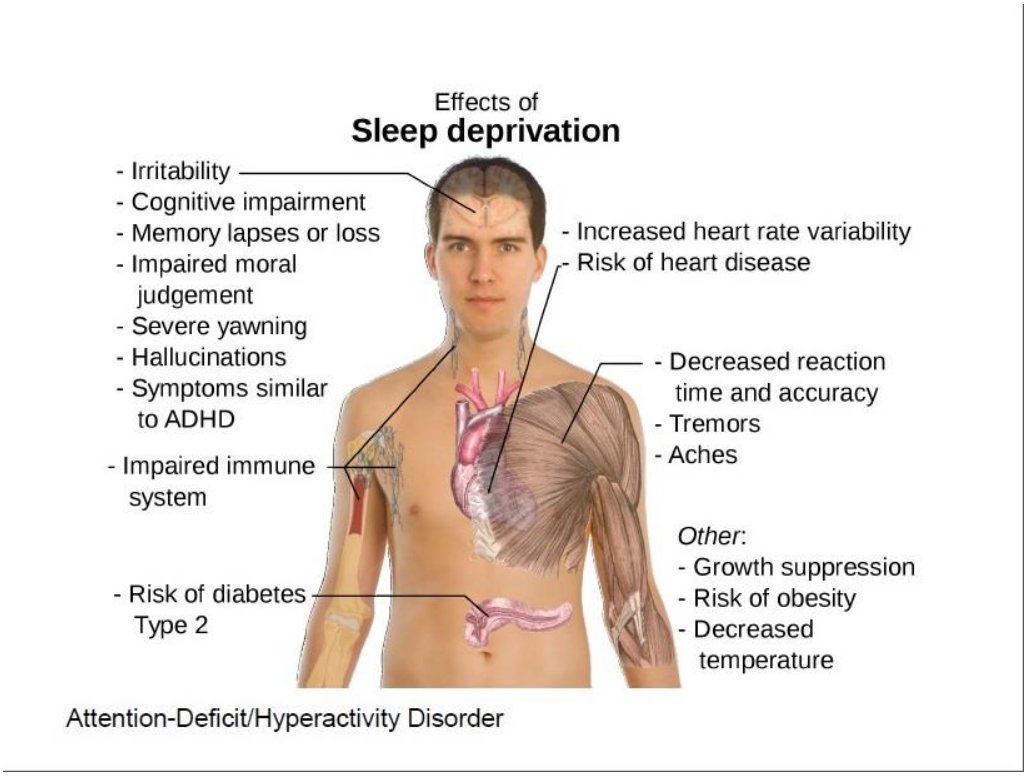

Figure 1.1: Effects of sleep deprivation.

As regards physiological modifications in cerebral activity, they can be detected through the electroencephalography (EEG). As already said, the EEG signal is a measure of electrical brain activity and it is acquired by means of electrodes placed on the scalp, according to the 10-20 standard traditional system. The number of EEG channels, used to monitor drowsiness, depends on the researchers' choice. On one hand, using a large number of EEG channels allows to get a high spatial resolution [44, 45]. On the other hand, since the employment of many electrodes is time-consuming, using only a few EEG channels allows to less computational costs.

Drowsiness can be observed in the EEG spectrum as an increase of activity in the frequency bands (8-13 Hz) (alpha band) and (4-8 Hz) (theta band) occurs, mainly in the parietal and central regions of the brain. Simultaneously, a diminution of activity in the beta band (13-26 Hz) is generally present, because beta activity is related to vigilance and alertness. This has been shown in several studies [46, 47, 48].

Thanking to an increasing interest in drowsiness, mainly due to the emerged relationship between car accidents on the highways and drowsiness manifestations, many scales of drowsiness classification exist but none of them is standardized. Moreover, there are no standardized rules to differentiate the levels of drowsiness as the Rechtschaffen and Kales rules (Rechtschaffen & Kales, 1968) for the study of sleep. This may be due to the quite recent interest on drowsiness compared to the sleep analysis and the difficulty to collect drowsiness data. There are two kinds of scales: subjective sleepiness scales like the Karolinska Sleepiness Scale (KSS) [47], which allows subjects to directly evaluate their own drowsiness and Objective Sleepiness Scales (OSS) which is used by expert doctors to evaluate drowsiness level (after driving).

Objective sleepiness score	α and θ cumulative duration	Blinks and eye movements
0	Negligible	Normal
1	Less than 5s	Normal
2	Less than 5s or Less than 10s	Slow Normal
3	Less than 10s or More than 10s	Slow Normal
4	More than 10s	Slow

Table 1.1: OSS Criteria

In this study, we employ none of these scales because we exploit data coming from reaction time tests. Decisions are made every 60s of test and depend on the mean reaction times and number of lapses [57].

Several researches have focused on other physiological indicators such as the electrocardiogram (ECG) to monitor heart rate [54, 53] or the temperature [52] or the combination of electrooculogram EOG and images of eye.

This study focuses on the drowsiness detection caused by sleep deprivation, by analyzing EEG signals collected from subjects that have participated to reaction time tests, under different conditions of vigilance. According to what has been said so far, drowsiness is strictly linked to reduced reaction times so the passage from a well-awake condition to a transitional state to drowsy state is investigated.

Finally, in order to perform an automatic drowsiness analysis, it is convenient to compute the EEG power spectrum, from which it is possible to obtain some features. Drowsiness decision can be made using EEG features, subsequently employed as inputs to a classifier.

1.3 Movement physiology and EEG

Motor acts result from neuronal pulses coming from the sensorimotor cortical area that is located, more or less, in correspondence of the central zone of the cortex.

Since electrodes from these areas have been employed also to acquire EEG signals for drowsiness detection, it is appropriate to clarify the relationship between EEG spectrum amplitude and motor tasks.

Since several years, the activity of cortical regions for the control of movement has been investigated. Cortical activation related to movement preparation and execution leads to a phenomenon called event-related desynchronization (ERD) which consists of a desynchronization of the mu rhythm. ERD in hand movement predominates in the contralateral sensorimotor areas during motor preparation and spreads bilaterally after the movement has started. In addition, a second phenomenon can be detected: it is called "event-related synchronization" (ERS) and it occurs in the 10 Hz band over areas not involved in the task, during movement preparation and execution, or over the same areas that previously displayed in ERD, after movement execution [42, 62].

Similar results have been obtained by Leocani et all. (1996) [43]. They have studied the event-related desynchronization/synchronization (ERD/ERS) when performing self-paced movements of the right index finger. Results have permitted to state that movement preparation and execution produce ERD over the sensorimotor areas at 10 Hz (in alpha band) and 20 Hz (in beta band), followed by ERS. ERD corresponded spatiotemporally to the frontocentral areas recruitment. For both frequency bands, ERD began over the contralateral sensorimotor areas and became bilateral with the onset of movement.

Another important issue that has been investigated is the difference between the case of motor preparation, that implies planned movements, and the absent of intentionality for motor tasks performance. In addition, another parameter can influence results and it is the required force level to keep an object. In order to discriminate among these different situations, Zaepffel et all. [42] used a pre-cueing paradigm in which a GO signal is preceded by a cue providing partial, complete or no information about these two above-

mentioned parameters for grasping tasks: the grip type to grasp an object and the overall strength required for pulling it. Results reflected a beta modulation according to different conditions of movements.

It is actually possible to state that, if there is motor preparation, the spectrum in alpha and beta bands decreases just before the movement and increases after the movement because of a desyncronization and a synchronization in each frequency band, respectively. If no planned movement are supposed, it can be observed a reduction in alpha and beta spectra only after that the stimulus is presented.

This last phenomenon is related to the so-called "beta-rebound". Beta rebound indicates the short-lasting burst of activity in beta band (13–35 Hz) that is present after movement or in response to somatosensory stimulation. It is typically found in Rolando areas over the motor and somatosensory cortex, but also around the supplementary motor area and the prefrontal cortex. Therefore, the beta rebound should actually reflect the active neurons inhibition once that a motor program is concluded, that can be motor planning, motor execution, or motor imagery.

In this study, the tasks were performed without any movement planning since the subjects were supposed to click on the mouse after detecting a stimulus, that was *randomly* presented. Therefore, it was expected to find a diminution of the alpha and beta spectrum amplitude when the motor task was going on, followed by an increase. Unfortunately, either information about the instant when the subject reacted by clicking on the mouse, nor the time when the stimulus was presented, are available therefore this information couldn't be taken into account for further evaluations.

1.4 Spectral analysis of EEG signals

As mentioned in paragraph 1.2, it is convenient to compute the EEG power spectrum in order to study drowsiness. Physiological events generally cause changes into the EEG spectrum.

Among several analysis methods, spectral analysis methods are, without doubts, really important because they highlight changes in frequencies and in characteristics of brain waveform, depending on the cerebral function. Over the years, several methods of spectral analysis have been experienced in order to individuate the best possible performance to produce powerful and meaningful features, with an appropriate frequency resolution.

In this work, some of the existing methods are considered in order to firstly extract features and then compare their performances.

One of the considered method is the traditional approach of EEG spectral analysis: the Fourier Transform-based method also referred as "non-parametric" analysis. It involves the employment of the periodogram, which is the squared module of the Fourier transform of the signal (divided to the number of data points). Several researchers preferred to use this classical method to easily get features and then they implemented more robust classifiers to obtain a classification as good as possible. An interesting study was published by Mervyn et all. [37]: they extracted features after computing EEG spectrum by using a Fast Fourier Transform (FFT) and a Hann window, with an overlapping of 50% and the features extracted have been used as inputs for a Support Vector Machine (SVM) classifier. Instead, in our case, a FFT with a Bartlett window and an overlapping of 50% has been chosen in order to extract features to give in input to an Artificial Neural Network (ANN) classifier.

In addition, some of the features computed by Mervyn et all. have been used in this work in order to extract information from EEG signals. In particular, dominant peak and the related dominant frequency have been considered. For more details about the way of computing them, see [37] and reference therein.

Another approach that has been included in this study is the parametric analysis: it consists in expressing the spectrum of the signal as the spectrum of the output of an LTI system that receives in input a white noise process. In this case, problems related to spectral leakage and statistical consistence are overcome. In reverse, a higher computational cost is required, due to the individuation of the right order of the model, the choice of the right

model family and the computation of the coefficients of the model, from which the real and proper spectrum is computed. Normally, for EEG analysis, AR or eventually ARMA models are preferred.

Historically, the first application of the parametric approach to EEG signals is associated to Isaakson, who investigated most of the factors that can cause EEG spectral variations (age, mental state, region of the brain, influences on the brain, disturbances), by employing multi-variable parametric analysis. In particular, he firstly discriminated changes in the EEG, according to several conditions of vigilance such as wakefulness, drowsiness, sleep [68,69].

Thereafter, Cerutti et all. employed multi-variable AR approach for the computation and coherence analysis in order to study synergy between locally active cortical areas in the brain, after applying a combination of visual and somatosensory stimulation [72]. In particular, they analyzed electrical potentials from four experimental conditions: closed eyes without stimulus through (EEG), visual stimulus (VEP), somatosensory stimulus (SEP), visual and somatosensory stimulus (mix). The use of multi-variable AR approach resulted to be really useful because of its ability to process short-length data series, especially for stimulus-related potentials [72].

Some studies have been realized in order to compare results coming from both the non-parametric and parametric methods. Akin et all. [17] realized a research similar to the one developed in this work of thesis. Indeed, they tried to apply periodogram and AR spectral analysis to EEG signals, in order to compare their performances, concluding that AR models allow gaining clearer spectra, useful for clinical purposes as well. Another study of the Indian Institute of Science [55] has proposed a different way of employing AR spectra-based concepts. Starting from the observation that the energy in the EEG data segment is concentrated somewhere in between the initial and the final positions, they exploited least squares waveshaping filter in order to identify the position where the energy is concentrated. The knowledge of this position can be used in making a better spectral estimation of short segments of EEG data. In addition, they showed that the performance of such method and conventional AR method become comparable as the length of data segment increases.

More recently, new methods of EEG analysis have been experienced, aiming to get better and better performances, such as the “singular spectrum analysis” approach. It has been

originally employed for climatic, meteorological, geophysical time series analysis. Thereafter, it has been successfully applied to medicine and engineering as well. According to such promising characteristics, also SSA has been developed for features extraction in this work.

The debut of SSA is usually associated with Broomhead and King's work [19]. The fascinating aspect of this method is the fact that neither hypothesis for a parametric model or stationarity conditions have to be assumed so it can be considered as a model-free technique. SSA proposes to decompose the original series into a sum of a few components: a slowly varying trend, oscillatory components and the background noise. It is based on the singular-value decomposition (SVD) of the matrix constructed upon time series and it finally leads to reconstructed signal that can be considered as filtered version of the original one. This method applies a sort of adaptive filter to the time series. Since there are several papers published on methodological aspects and applications of SSA, it is suggested to see [19-27] and references therein for more information.

Many researchers have employed SSA for EEG analysis. Aydın et all. [23] have applied SSA on EEG signals in order to analyze sleep in patients with insomnia or paradoxical insomnia. The resulting singular spectra computed for both C3 and C4 recordings were given as input features to an Artificial Neural Network (ANN) for EEG classification. The sleep stages that the classifier had to distinguish were "awake", "REM", "stage1" and "stage2". Three clinical groups have been successfully classified by using the corresponding singular spectra. The results confirmed that the SSA can be applied to sleep EEG series for researching about insomnia, if ten trials are available for the specific sleep stages. In addition, another interesting study has regarded the field of readiness potentials identification, by applying SSA [27]. They used an approach similar to the one developed in this work of thesis, with interesting results. Differentially from the previous article, where singular spectra have been directly assigned as features to use as input for a classifier, in this case singular spectra were employed in order to individuate the principal components more able to explain the most variance of the signal. Instead, the remaining ones were associated to noise and therefore excluded. Starting from principal components, signals for each frequency band were obtained and in addition a filtered new signal was computed as well. It aimed at individuating the different stages during a motor program:

preparation, execution and post-movement. The results of this work were promising so that we developed a similar strategy, as regards this method.

From the results of previous studies in drowsiness detection, it emerged that there are particularly powerful features to employ in order to extract meaningful information from EEG signals. Several studies proposed to monitor some ratios between different EEG power bands. Hong J. Eoh et all. [5] studied drowsiness resulting from sleep deprivation, in simulated driving. They suggested to monitor the following ratios: the ratio between the alpha activity (8-13 Hz) and the theta activity (4-8 Hz) on the beta activity (13-22 Hz), that is [(alpha+theta)/beta]; the ratio of beta activity on alpha activity. EEG α, β, β/α and (α+θ)/β indices resulted significantly different for the several tasks. In addition, they analyzed EEG variations before and after car accidents, showing that β and (α+θ)/β were related to alertness. Finally, θ burst activity, which did not result significant in the mean power analysis, was instead significantly different between driving sessions.

According to what learnt from the literature, the following features have been considered in this work:

- the ratio of alpha on beta activity,
- the ratio between alpha and theta activity on beta activity [2, 5, 7],
- the percentage power in each frequency band [1, 7, 8, 38],
- $log\ (\frac{P\%}{1-P\%})$, for each frequency band [38],
- dominant peak and dominant frequency [37] .

In this work the capacity of each extracted feature to distinguish different vigilance states, method by method, has been investigated by means of non-parametric statistical tests (Kruskal-Wallis test). It emerged from literature that when there is no assumption of any probability distributions, it is opportune to use a non-parametric statistical test. In addition, since in the current dataset the size of the groups to classify was different, a Kruskal-Wallis test has been chosen, according to the literature.

Differently from Mervyn et all. [37] that have employed an SVM, this work aims at classifying three different classes therefore it is more appropriate to use an Artificial Neural Network (ANN) that is able to classify more than two classes. k-Cohen coefficient is usually known to provide a measurement of the degree of accuracy and reliability of a classification [56]. Therefore, it is employed to compare performances of each method.

In conclusion, this work combines features from other studies that resulted to be significant, with new ones here developed. In particular, these new ones will regard smoother AR spectra: features conceptually similar to dominant peak and frequency (above-commented) but more suitable for AR spectra are computed, as it will be discussed in the next chapters. A statistics-based features selection follows. Then a comparison among different spectral approaches is performed in order to state which one can lead to a suitable set of features to classify wakefulness, transitional state and drowsiness, in reaction time tests.

2. Objectives of the work

This thesis aims to detect drowsiness in subjects that have performed three reaction time tests, by extracting appropriate features from electroencephalographic (EEG) signals through three different approaches.

The second purpose is to compare performances of the three developed methods in order to state which one is more able to provide good features.

Finally, the third goal is to evaluate if the employed protocol is suitable or not to detect drowsiness and, in particular, if the collected data are adherent to the aim of this work.

As regards the first objective, it was thought to investigate the response of a tester to a stimulus appearing on the screen of a computer and lasting 400 msec. During these tests, some data (per minute of test) like mean reaction time, number of lapses, number of no reactions and others have been recorded in order to label each minute of test. In the meanwhile, polysomnographic signals (EEG, ECG, EOG, EMG) have been acquired and among them electroencephalographic signals (EEG) have been considered to perform drowsiness detection.

In order to detect drowsiness, it was thought to develop more methods and then to compare their performance in terms of features discriminant capability. More specifically, three methods have been implemented: non parametric analysis (Fourier Transform-based), parametric analysis (AutoRegressive modelling) and singular spectrum analysis (SSA), characterized by different advantages and disadvantages, and from each of them some features have been extracted.

We then used a statistical test to evaluate how each extracted feature allowed to correctly classify a minute of test among the three considered classes. This test has been employed for all the features extracted by each method.

Once the best features have been individuated, they were pre-processed in order to make them suitable as inputs to a classifier, which should automatically recognize to which class each minute belongs.

Then, according to the second aim declared, K-Cohen coefficient has been used to compare performances and select one method.

Finally, the features, identified as the best ones and belonging to the best resulted method, have been evaluated from a physiological point of view in order to verify if they explained

a certain behavior of the current tester, in a coherent way with the associated labels. This evaluation, carried out for all the subjects, has allowed to answer to some questions about the goodness of the chosen and employed protocol: did the idea of performing three different reaction time tests, under different wakefulness/drowsiness conditions, lead to a real discrimination among these different states? Did all the subjects answer in a way that allows to correctly distinguish among the three different conditions of test or the distribution of labels, according to reaction time data, and the features are not so coherent with what expected?

Results from this last survey made possible to individuate which subjects have well mirror the aim of the protocol and so the aim of the work.

3. Materials and methods

In this chapter the protocol through which it has been possible to collect data, the processing chain of the available data and finally all the employed, chosen and implemented methods are described. For any details, it is suggested to consult the correspondent appendix section, if it is present.

3.1 Experimental protocol

All the experimental data used in this work have been collected in the Laboratory "INTELSIG" of the Department of Electrical Engineering and Computer Science (Institute Montefiore), of the Faculty of Applied Science of the University of Liège, in Belgium.
Experiments have been performed on 21 subjects, 9 males and 12 females, in an age range between 19-32 years (mean age 23.9) and in good health. For the selection of the participants, the following exclusion criteria have been fixed: alcohol or drugs addicted, regular smokers, recently medicated people or medical drugs consumers during the 2 weeks before the test, changing schedule workers, people with sleep disorders, with jet lag in the 2 weeks before the test, with the requirement of wearing glasses for driving (wearing contact lenses was allowed), with skin allergies related to cosmetics or lotions.
Before describing the protocol, it must be said that it was asked to participants to not take any stimulants (coffee and tea) from 6:00 pm of the first day until the end of the last reaction-time test on the second day.
Subjects were supposed to perform three visual reaction-time (RT) tests, each lasting 15 minutes, over two days.
After a normal night of sleep, each subject realized the first reaction time test (RT1) between 8,00 am and 10,00 am on the first day.
Then, the subject wore an actimetry sensor, in order to monitor her/his sleep/awake cycle but was free to carry out daily activities, until 11,00 pm when the subject came back to the laboratory. During that night, the subject was not allowed to sleep and she/he no longer wore the actimeter. On the second day, the subject performed the second RT test (RT2) between 2,00 and 4,00 am and, after having breakfast, she/he performed the third and last RT test (RT3) between 11,00 am and 1,00 pm.

As regards the execution of each test, the participant sat in front of a computer. Throughout the whole test, a large number of stimuli was randomly presented to the volunteer on the screen of the computer. Each stimulus lasted 400 msec and the subject was supposed to react to each stimulus by clicking on the mouse of the computer as quickly as possible after having detected the onset of the stimulus.

During each test, images of the eye, reaction time data and polysomnographic signals (ECG, EEG, EOG, EMG) have been recorded. These last ones have been collected through EMBLA titanium™ (Figure 3.1), a wireless PSG diagnostic amplifier with an integrated LCD screen for signal display, impedance checking and patient data entry.

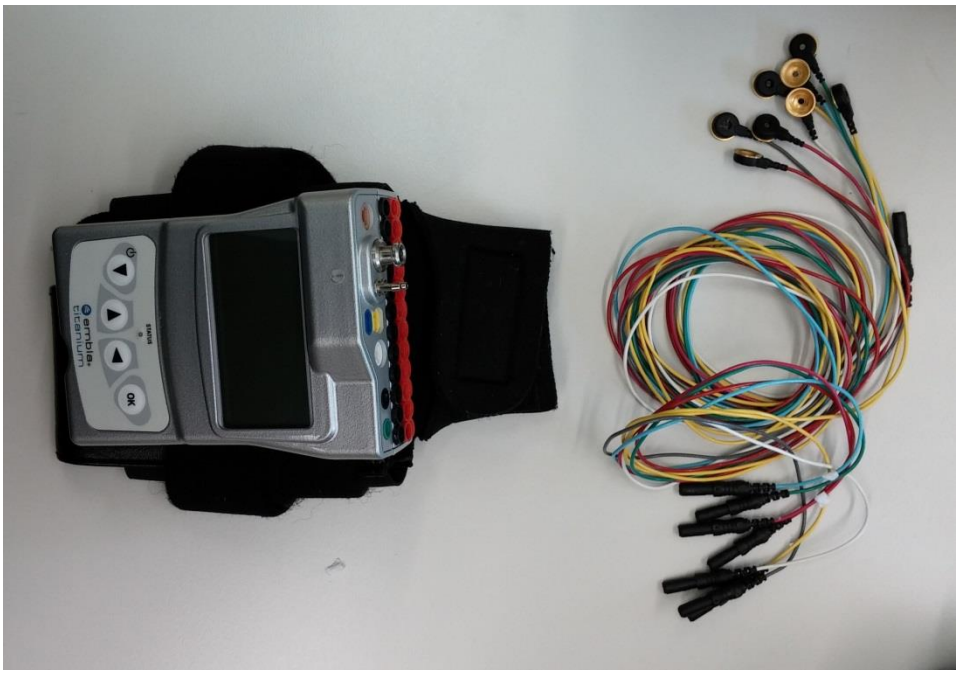

Figure 3.1: EMBLA titanium™ device allows to get signals (EOG, EMG, ECG, EEG) from 9 different channels.

The electroencephalographic (EEG) signals have been acquired with a sampling frequency of 512 Hz through electrodes Ag/AgCl disposed on central, frontal and parietal regions, C3, C4, Cz, Fz, Pz respectively, plus an electrode at the earlobe as reference and a ground electrode, placed according to the standard traditional 10/20 system as it is indicated in the Figure 3.2 below.

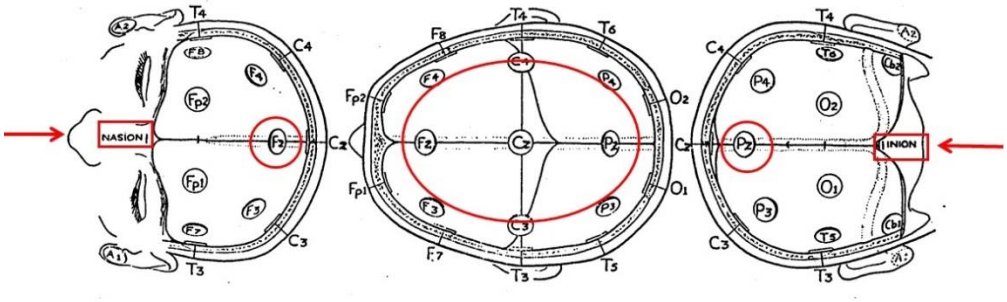

Figure 3.2: standard traditional 10-20 system scheme. The red circular frames indicate which channels (C3,C4,Cz,Fz,Pz) have been considered in this work and red arrows specify the point of view of the piece of the image. The letter "z" is referred to electrodes on the midline, odd numbers to left side of the scalp and even numbers to right side of the scalp.

According to the number of stimuli per minute, reaction time data were computed:

- Mean reaction time = $\sum_i reaction\ time(i) \Big/ number\ of\ stimuli$
- Number of "lapses" (lapse: 500 msec ≤reaction in a time ≤ 2 sec or totally absent)
- Mean number of "lapses" = $\sum_i number\ lapses(i) \Big/ number\ of\ stimuli$
- Number of "no reactions" (no reaction: reaction totally absent)
- Mean "no reaction" = $\sum_i number\_NoReaction(i) \Big/ number\ of\ stimuli$

Finally, each minute of test has been labeled as "DROWSY", "TRANSITION" or "ALERT", exploiting information coming from reaction time data. In particular, the number of lapses and the mean reaction time have been used to assign one of the three labels to each minute of test as follows:

- if a lapse was detected in a minute of test, that minute was labeled as "drowsy";
- if no lapse occurred, two cases were possible:
    - the mean reaction time was greater than 400 msec and smaller than 500 msec then the minute of test was considered "transition";
    - otherwise, if the mean reaction time was equal or smaller than 400 msec, the minute was fixed as "alert".

The whole dataset, got by merging all the data from the three reaction time tests of the 21 subjects, is composed of 812 examples (that is [(21subjects *3 RTs)-5excluded tests]*14 minutes of tests). Five tests, indeed, have been excluded because there were some problems to access to their contents while working in MATLAB®.
According to the above-mentioned way of data labeling, the following repartition of dataset into the three categories has come up: 60 cases of "drowsy", 404 cases of "transition" and 348 cases of "alert".

3.2 Signal processing chain

A block scheme of the general strategy developed to extract information from the EEG signals is represented in Figure 3.3. It aims to discriminate drowsiness from the other two states of mind (alertness and transition) through features extraction and to verify if the protocol employed is suitable or not for this purpose.
The below-mentioned "raw" electroencephalographic signals, that are the signals acquired during a single reaction time test, have been loaded in MATLAB® using the SPM toolbox, well suited to manage multichannel acquisition. Each box that appears in the scheme will be more detailed in the next paragraphs. For each channel (C3, C4, Cz, Fz, Pz), the following processing chain has been run.

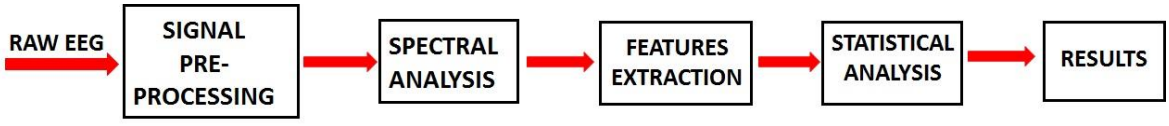

Figure 3.3: signal processing chain of the work

3.2.1 Signal pre-processing

The original signal has been firstly pre-processed before starting with the true and proper analysis in the frequency domain. The pre-processing phase includes the following operations:

- signal mean value removal
- signal pass-band filtering in the range of [0.5,35] Hz in order to eliminate the DC contribute (already drastically reduced through mean value removal) and very low

frequency contribute not of interest for this work, noise due network interference. It has been performed through a band-pass Butterworth filter of 5th order so that it is possible to get the flattest frequency response amplitude in the passing band and monotonicity in the passing and stopping bands as showed in Figure 3.4.

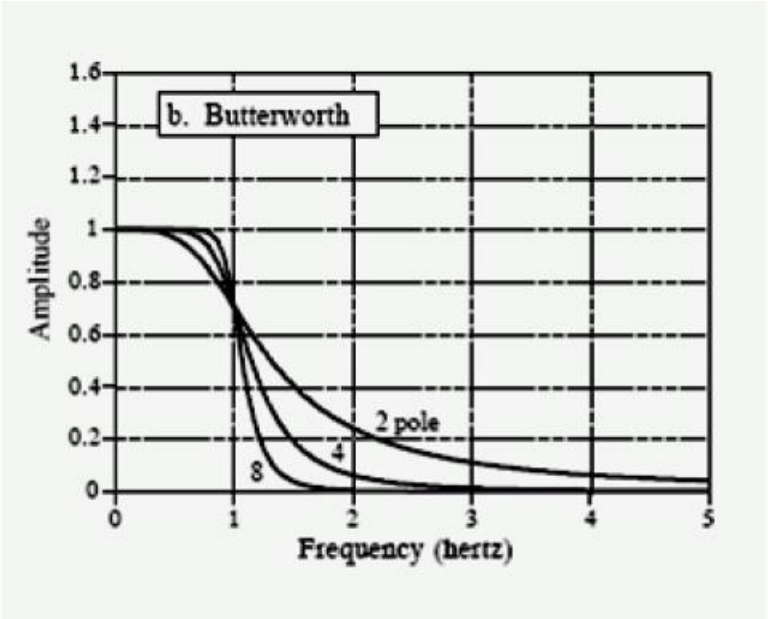

Figure 3.4: an example of frequency response amplitude in passing and stopping band

- zero-phase filter obtained by processing data in both the forward and reverse directions, in order to eliminate problems related to the phase distortion (caused by Butterworth filter): after filtering the signal in the forward direction, this filter reverses the filtered sequence and runs it back through the filter, leading to zero-phase distortion and a filter order that is double the order of the previous filter
- signal resampling from the original sampling frequency of 512 Hz to a more appropriate frequency of 80 Hz because, according to Shannon's theorem, this is a little greater value than the double value of the maximum frequency content of the signal.

The Figures 3.5 and 3.6 show results from the above-said pre-processing operations. In particular, since it is more difficult to individuate the frequency components by looking at the signal in the time domain, it is better to focus on the Figure 3.6. It shows, at the top of the image, the spectrum of the original signal and its filtered version and the bottom graphic contains the resampled signal. One can easily see, on the top, a resetting in the

power value outside the range of interest and, at the bottom, how the frequency content changes after resampling with respect to the over standing graphic.

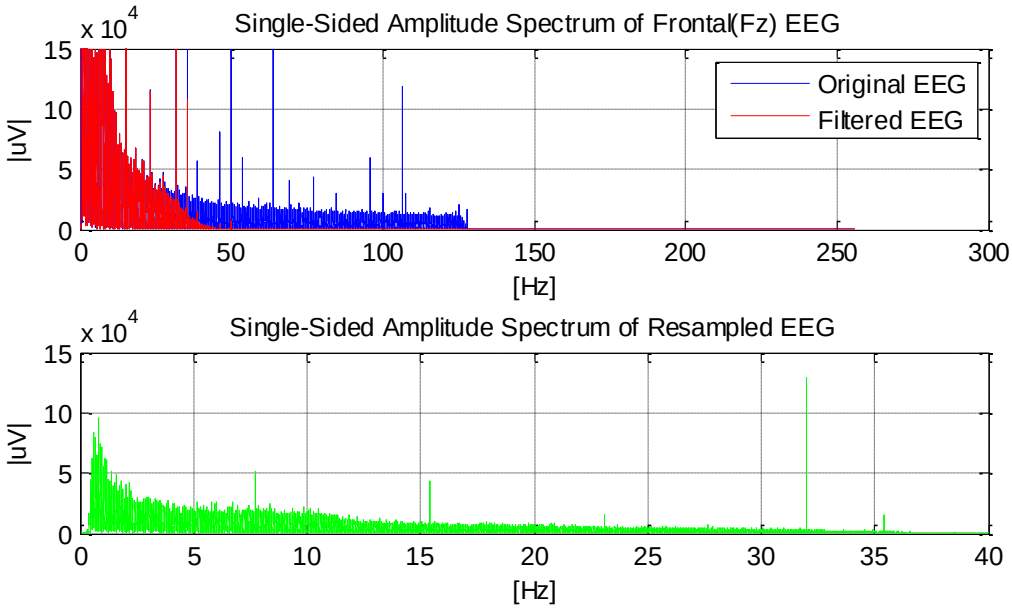

Figure 3.5: a piece of an EEG signal (channel Fz) in frequency domain, for a duration of 60 sec. The plot on the top of the figure represents the original signal in blue and the filtered one in red; at the bottom of the figure, the green trace is the resampled signal. The signal belongs to subject 14 in RT3.

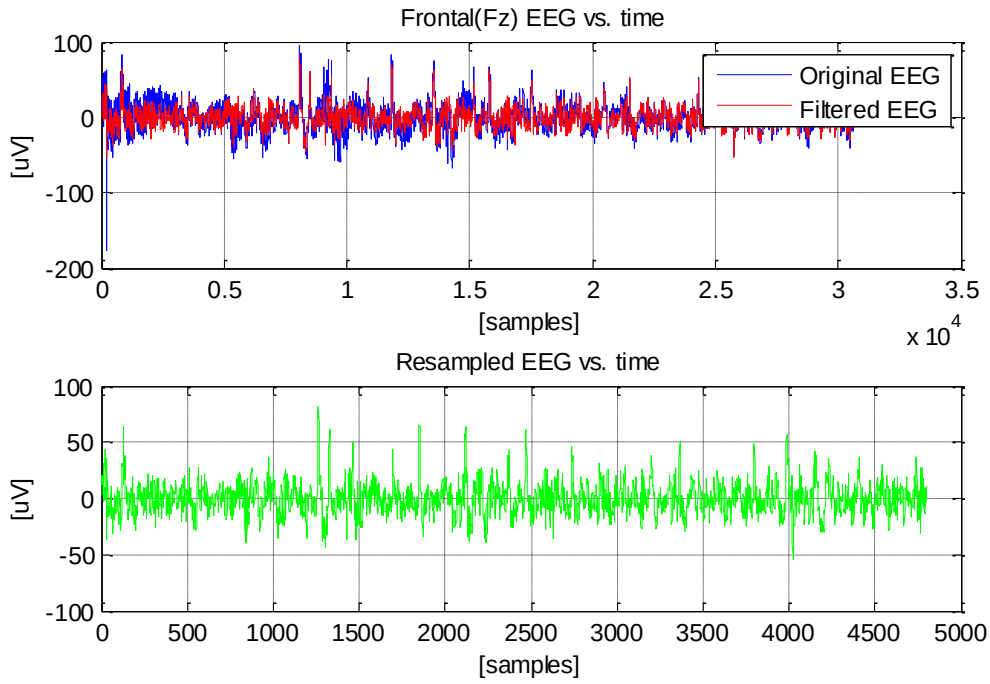

Figure 3.6: a piece of an EEG signal (channel Fz) in time domain, for a duration of 60 sec. The plot on the top of the figure represents the original signal in blue and the filtered one in red; at the bottom of the figure, the green traces is the resampled signal. The signal belongs to subject 14 in RT3.

3.2.2 Spectral analysis

The spectral analysis (Appendix B) is used to estimate the power spectral density (PSD). It can be executed using several approaches and different methods per approach.

The spectral analysis provides a trustable estimation if the property of stationarity of the signal itself is guaranteed. Consequently, once the pre-processing phase has been completed, the signal has been divided into 14 epochs of 1 minute in order to favor the stationarity, to make the signal more suitable for the subsequent processing steps and to have a correspondence between labels per minute of test and epochs of signal.

Three different approaches have been considered and developed to perform the analysis in the frequency domain and to compute power spectral density (PSD) of the EEG signals: non parametric, parametric and singular spectrum analysis.

Non parametric spectral analysis

The non-parametric analysis is based on the usage of the Fourier Transform. It leads to an estimation of the Covariance of the process under analysis, or equivalently its spectrum, according to the theorem of Wiener-Khinchin.

First of all the signal has been converted from the time domain into the frequency domain using the Fast Fourier Transform (FFT) algorithm.

In order to determine the number of points to use to compute FFT, the next power of 2 greater than the length of the signal (80Hz * 900 sec) has been selected. The traditional way of computing the spectrum estimator is the periodogram, that is the squared module of the FFT of the signal normalized for the number of points, as below:

$$\hat{S}_y(f) = \frac{1}{NT}|Y(f)|^2$$

As well-known, the big limits of the periodogram are due to the large variance of the estimator: it is not statistically consistent, that is it doesn't converge to the real spectrum for growing N to infinity.

The Welch method has been chosen to perform non parametric spectral analysis. It is an improvement of the traditional periodogram spectral estimation because it overcomes problems due to imperfect and finite data. It consists in dividing the signal into K smaller segments of M samples per segment. K periodograms (one per segment), mutually independent, are computed and a triangular Bartlett window is applied to each subsequence so as K modified periodograms are obtained as follows:

$$S_M^{(i)}(f) = \frac{1}{MU}\left|\sum_{n=0}^{M-1} x^{(i)}(n) * w(n) * e^{-\left(\frac{j2\pi kn}{M}\right)}\right|^2, \qquad 1 \le i \le K$$

where $x^{(i)}(n)$ is the signal, *w(n)* is the window and *U* is a normalization factor so that the final spectrum estimator P_{xx} , that is then defined, results asymptotically unbiased. The factor *U* is so defined:

$$U = \frac{1}{M}\sum_{n=0}^{M-1} w^2(n)$$

Finally, the spectrum estimator is obtained by averaging on the K modified periodograms as below-indicated:

$$P_{xx}(f) = \frac{1}{K}\sum_{i=1}^{K} S_M^i(f)$$

The problems related to spectral leakage, because of lateral lobs in the spectrum that modify the frequency content, and frequency resolution, limited by the number of point used for the FFT, are partially overcome applying a triangular Bartlett window long 1/4 of the length of the signal. In addition, an overlapping percentage of 50% between adjacent sections of signal has been set. Finally, the Power spectral density (PSD) of the signal and a vector of frequencies as long as the PSD were available.

As emerged from literature, the frequency content of interest in the EEG, in order to discriminate alert-transition-drowsy from a physiological point of view, goes from 0.5 Hz to 35 Hz. The range 4-30 Hz has been preferred and it corresponds to three different frequency bands that are respectively theta (4-8) Hz, alpha (8-13) Hz and beta bands (13-30) Hz. This last band can be further divided into two sub-bands called slow beta (13-18.5) Hz and fast beta band (18.5-30) Hz.

Delta band (frequency < 4Hz), that is the rhythm of 3rd stage of sleep and is characterized by a tension voltage of 150 μV, has been excluded from this analysis. We observed that the voltage value, much larger than the ones related to the other frequency bands, could risk to mask the information from the other three bands, more interesting for the aim of this work.

Coherently with the literature, it has been assumed that the beta band is associated to alertness and vigilance because the beta rhythm is generally predominant when a subject is performing whatever cerebral activity with wide open eyes. This state of mind is normally referred as "arousal" as well. From the point of view of the signal frequency content, it means a faster rhythm in the trend of the signal that corresponds to a frequency range of [13-30] Hz and a mean value, in terms of voltage, around 8-19 μV.

As regards alpha and theta bands, they are supposed to be related respectively to wakefulness but with closed eyes and to the first minutes of falling asleep, deep relaxation, problem solving. Both of them are characterized by a greater mean voltage tension (30 and 75 μV respectively) than in beta band, due to the synchronization level of neurons. Consequently, these two frequency bands are assumed to be related to drowsiness.

So said, the PSD related to each frequency band (theta, alpha, beta) has been extracted from the total PSD as it is visible in Figure 3.8. They will be used then for features extraction that will be explained in next paragraph.

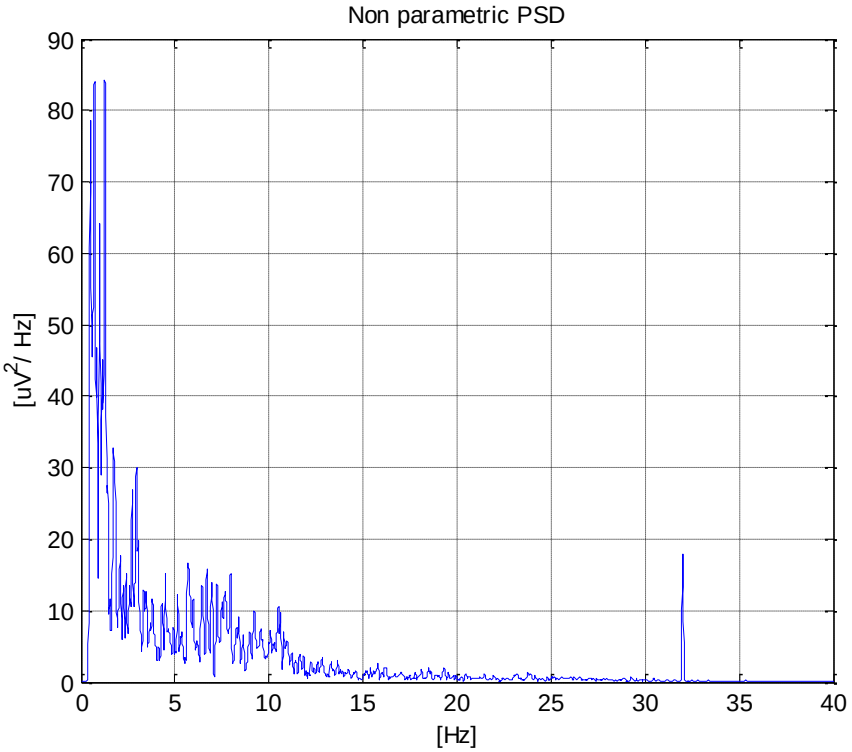

Figure 3.7: non parametric PSD belonging to subject 14 in RT3, at the 7th minute of test, from Fz channel.

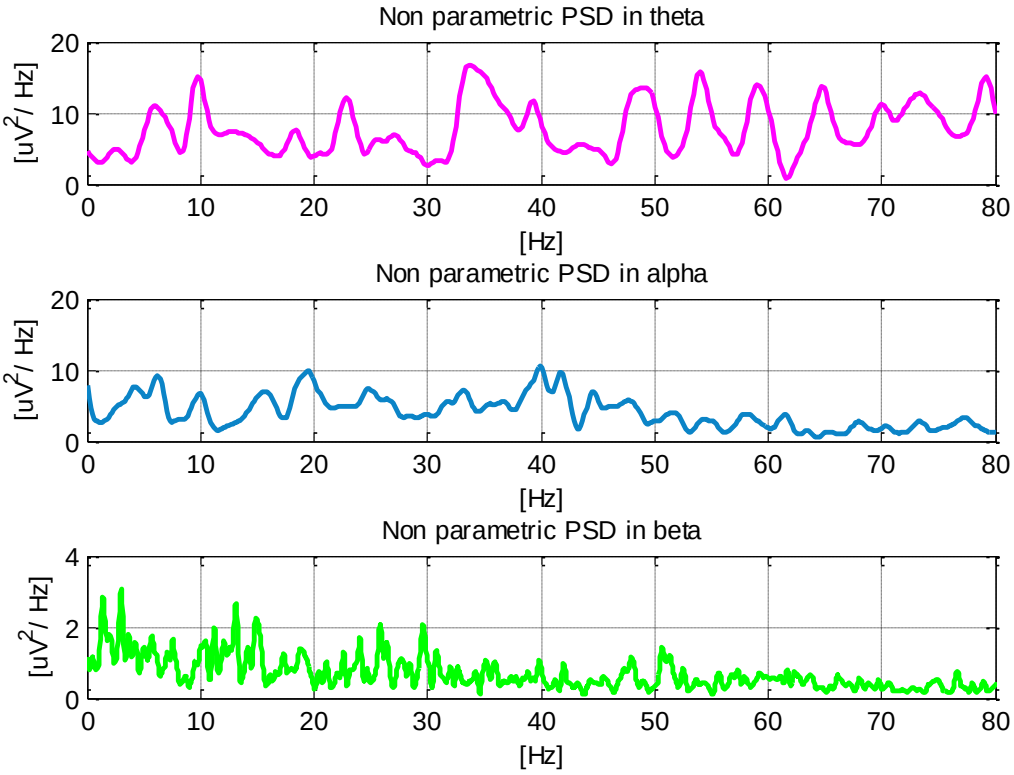

Figure 3.8: PSD related to theta, alpha, beta bands respectively from the top towards the bottom. The signal belongs to subject 14 in RT3 at the 7th minute of test, from Fz channel.

The whole algorithm just explained has been applied to the 14 epochs of signal, subject per subject and test per test. At the end, the non-parametric spectral analysis on the whole dataset has been run.

Parametric spectral analysis

The parametric analysis has been considered as a second alternative approach, in order to be able to compare the performance of different methods, in terms of extracted features, and to verify which one leads to the best features for a good discrimination among alertness, transition and drowsiness.

It differs from the non-parametric one because it solves the above-mentioned limits but with a heavier computational cost. Parametric approach comes from the concept that a certain process generates the time series under analysis. More specifically, its power spectrum can be computed as the power spectrum of the output signal of a LTI system that receives in input a white noise process (Figure 3.9). That is because the power spectrum of

a white noise (the variance of the process) is unitary and so the power spectrum of the output is the squared module of the frequency answer of a system that should be able to represent the signal of interest, if correctly implemented.

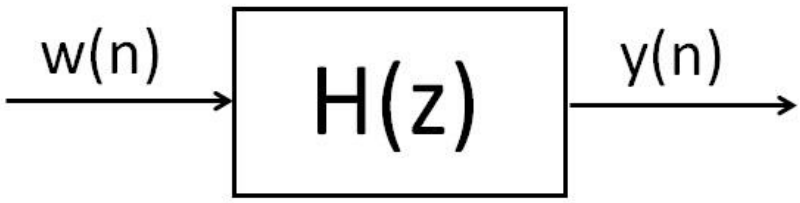

Figure 3.9: model of a signal generated by a system receiving in input a stationary white noise WN(0,σ2), with null mean value and standard deviation σ2. The system is completely described by its transfer function.

It is preferable to take into account the properties of the signal when the family model is chosen. For instance, an Auto-Regressive (AR) model is appropriate for a signal containing sudden peaks in frequency spectrum. On the contrary, Moving Average (MA) model is used for signals that have no sharp peaks. If the information about the signal is not available to take a decision, the Autoregressive Moving Average (ARMA) model can be used for both cases.

As regards EEG signals, AR and ARMA models are preferred because their structure consists of peaks at discrete frequency intervals. In this study, AR model has been employed because it has more advantages than ARMA in terms of computational costs.

According to the AR model, the amplitude of a signal at a given instant can be obtained by summing up the different amplitudes of previous samples. The relationship between the input and the output of the above-mentioned system, shown in Figure 3.9, can be written with the formula below:

$$y(n) = \sum_{k=1}^{p} a_k y(n-k) + w(n)$$

where *w(n)* is a white noise of variance σ^2 and null mean value. The optimum order *p* of the AR model has been individuated according to the Akaike information criterion (AIC):

$$AIC(p) = Nln(\sigma_e^2) + 2p$$

Then, the Anderson's whiteness test was also realized on prediction error. This test involves to check if the prediction error results to be white and so if its autocorrelation function (ACF) is maximum at *lag=0* and around zero elsewhere. If the order suggested by

AIC does not satisfy the condition of the Anderson's test, the order needs to be incremented until the residual error becomes white.

It is necessary to pay attention not to increment too much the order to avoid the problem of overfitting. In this case, indeed, even if the model seems to replicate perfectly the signal, it risks to lose its capacity of generalization and the model comes up to be inadequate.

By summing up all the squared values of the prediction errors on the N samples of the signal, a "cost function" called J can be obtained:

$$J = \sum_{n=1}^{N} e(n)^2$$

This figure of merit is a function of the coefficients of the model so that the coefficients are determined through Yule Walker's equations that are based on the minimization of the function *J* using Levinson-Durbin recursion.

Once the estimated coefficients $\hat{a}_k$ of the model have been determined, that are as many as the order of the model, it is possible to compute the power spectrum (Figure 3.10) of the signal, as in the following formula:

$$\hat{S}_y\left(e^{j\omega T}\right) = \sigma^2 T \left|H\left(e^{j\omega T}\right)\right|^2 = \frac{\sigma^2 T}{\left|1 + \sum_{k=1}^{p} a_k e^{-j\omega T k}\right|^2}$$

where σ^2 must be substituted with *J* and a_k with the above-mentioned estimated coefficients $\hat{a}_k$; *T* is the sampling period of the signal.

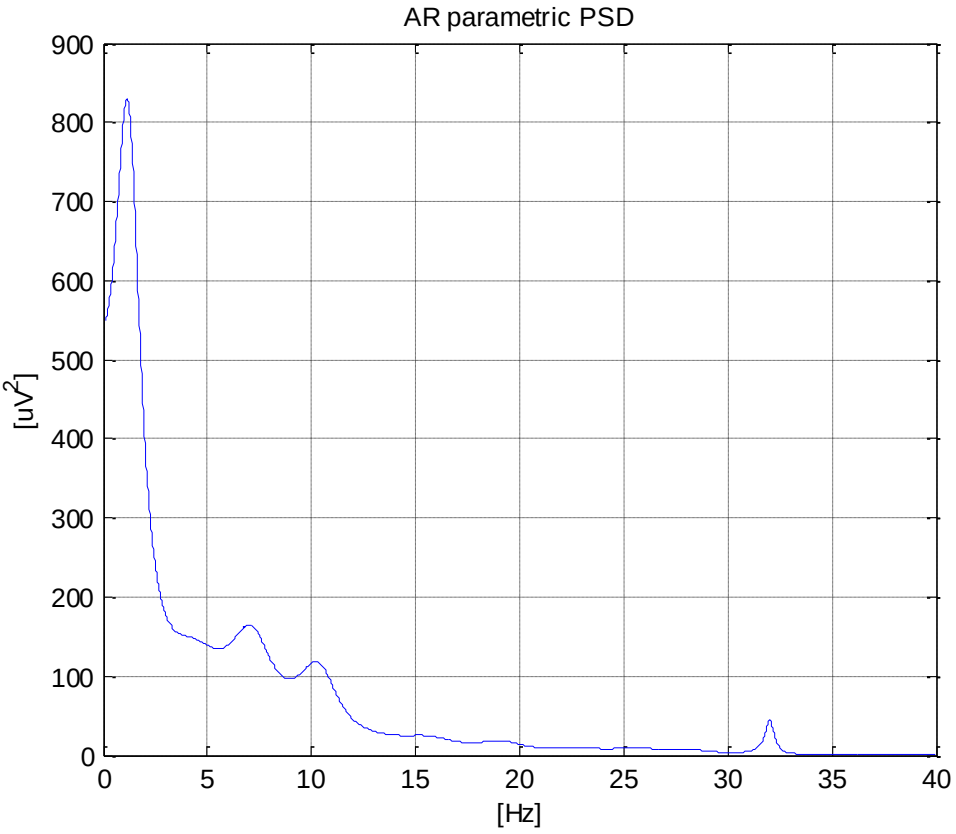

Figure 3.10: AR parametric power spectrum belonging to subject 14 in RT3, at the 7th minute of test, from Fz channel.

It is also possible to perform a so-said "spectral decomposition" of the spectrum of the process by exploiting the poles of the model and their phases.

In particular, the module and the phase of each pole of the spectrum of the process represent the information of the spectrum at a certain frequency. Therefore, it is possible to exploit the phases associated to poles in order to individuate the frequency range related to each frequency band and the module in order to get the amplitude of the spectrum at that frequency. This strategy has been used, as explained later, for features extraction.

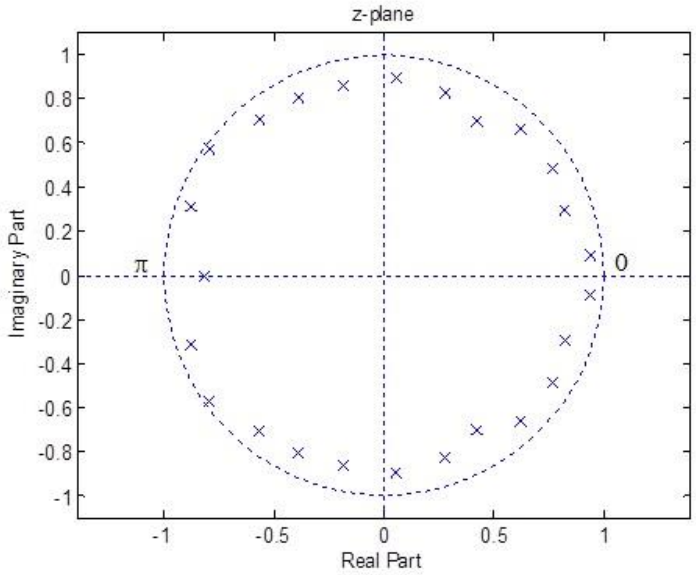

Figure 3.11: an example of z-plane with poles represented in the circle with unitary ray from the power spectrum of subject 14 in RT3 at the 7th minute (EEG from channel Fz).

After the complete identification of the model (involving the choice of the model family, its order and the computation of its coefficients), the spectrum of each frequency band (Figure 3.12) has been defined just as for the non-parametric analysis.

All the operations described until now have been run for all the 14 epochs of the signal considered, subject per subject and test per test, with the final goal of analyzing the whole signal and better detecting its dynamics.

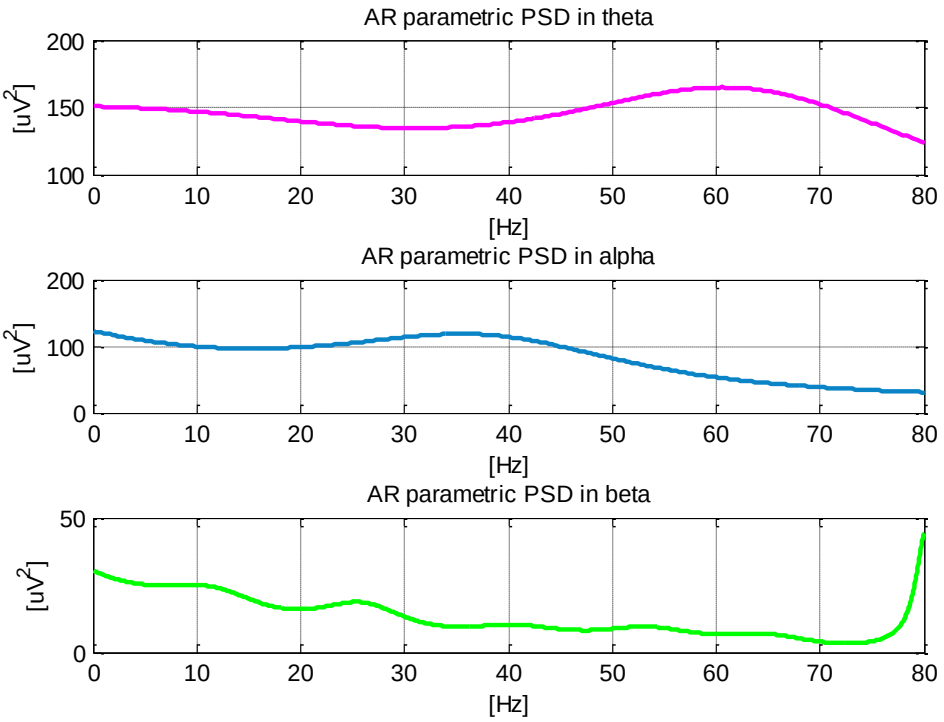

Figure 3.12: power spectrum related to theta, alpha, beta band respectively from the top to the bottom. The signal belongs to subject 14 in RT3 at the 7th minute of test, from Fz channel.

Singular spectrum analysis

The third method implemented to perform spectral analysis is called "Singular spectrum analysis" (SSA). This is a technique used for time series analysis and forecasting and it results from a combination of classical time series analysis, multivariate statistics, multivariate geometry, dynamical systems and signal processing.

It aims at decomposing the original series into a sum of a few components that represent the main content of the signal such as a slowly varying trend, oscillatory components and the background noise. It exploits the advantages of both singular value decomposition (SVD) and principal component analysis (PCA). SSA is characterized by the fact that neither a parametric model or stationarity hypothesis are assumed for the time series so it is a model-free technique.

The reason why SSA has been employed is to extract monocomponent signals, each of whom should be related to a certain frequency band according to the frequency content of the several epochs of signal. In this way, it is possible to detect changes in the power

spectrum for each frequency band more easily. For example, for a subject that was really drowsy during a certain minute of test, a decrease or even null value of the amplitude of the power spectrum in beta band is expected; on the other side, power spectrum in alpha or theta band should have increased.

The SSA algorithm can be summarized in 2 principal operations that are the "decomposition stage" and the "reconstruction stage", each of whom consists of other two sub-steps for a total of 4 main passages:

1) Decomposition stage

1.1 Embedding step

The one-dimensional series is embedded into a multidimensional series (lagged vectors) whose dimension is called "*window length*" L. The multidimensional time series, which has become a sequence of vectors as long as the window length, forms the so-called "trajectory matrix" D. The only parameter to determine at this step is the window length L which is really important for the frequency resolution. In fact, L is linked to the frequency by the relationship:

$$\Delta f = \frac{F_s}{L}$$

Since the sampling frequency F_s is 80Hz, L has been chosen equal to 20 in order to have a frequency resolution of 4Hz.

If 1 < L < N, where N is the length of the signal, the embedding step creates K=N – L+1 lagged vectors:

$$X_i = (f_{i-1}, \dots, f_{i+L-2})^T, \qquad 1 \le i \le K$$

where X_i have dimension equal to L and it is L-lagged. The trajectory matrix is obtained from the sequence of the X_i vectors:

$$D = \begin{pmatrix} f_0 & f_1 & f_2 & \cdots & f_{K-1} \\ f_1 & f_2 & f_3 & \cdots & f_K \\ f_2 & f_3 & f_4 & \cdots & f_{K+1} \\ \vdots & \vdots & \vdots & \ddots & \vdots \\ f_{L-1} & f_L & f_{L+1} & \cdots & f_{N-1} \end{pmatrix}$$

The trajectory matrix is characterized by having equal elements on the diagonals i+j = const. and so it is a *Hankel matrix*.

Then, the real and proper trajectory matrix has been computed and the corresponding covariance matrix C has been obtained as: $C = D * D^T$.

1.2 Singular value decomposition (SVD)

The result of this step is the SVD of the trajectory matrix D, but as we have fixed C as the covariance matrix, it is easier to compute its eigenvalues and eigenvectors. $\lambda_1, \dots\dots\dots, \lambda_L$ is the notation of the eigenvalues considered in a decreasing order of magnitude so as $\lambda_1 \geq \cdots \geq \lambda_L \geq 0$ and $U_1, \dots\dots\dots, U_L$ the notation of the orthonormal system of the eigenvectors corresponding to the eigenvalues of the matrix C.

By computing the percentage of the norm of the trajectory matrix retained as the ratio $\frac{\lambda_i}{\sum \lambda_i} * 100$, it is possible to visualize the number of eigenvalues that are able to explain the variance of the process for less than 5%, or more.

The graphic in Figure 3.13 shows the plots of the singular spectra as a function of k =1..L, computed for L = 20 at C3 for subject no. 14. The end of the step decay has been considered as "*statistical dimension*" S and it could be seen that the flat floor part is reached for $k \leq 6$ and varies with the window length L [27]. After the step decay, it is assumed there is the background noise so, by considering just the first 6 components, the significant part of the signal can be distinguished by the noise [27].

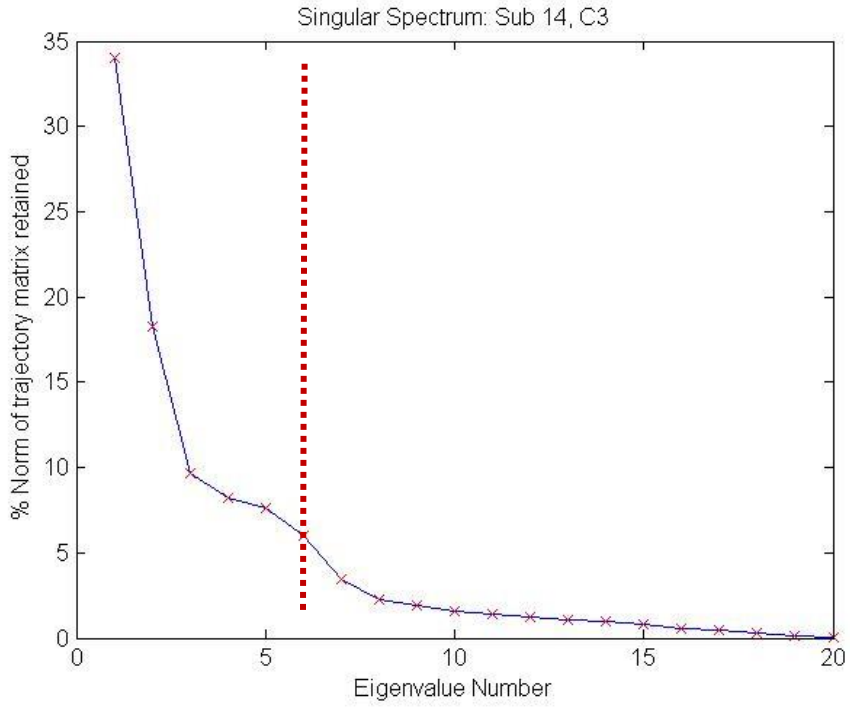

Figure 3.13: percentage of the norm of the retained trajectory matrix (y axes) in function of the number of eigenvalues k (x axes). For k = 6 (signalized by the dotted red line), it can be possible to explain a variance≥5%.

2) Reconstruction stage

2.1 Grouping step

Once the number of eigenvalues, k, is determined and starting from the eigenvectors, it is possible to compute the principal components of the signal by projecting the signal on the eigenvectors system as $V_i = X^T U_i$, with $1 \leq i \leq k$.

The power spectrum of each principal component has been computed by using a non-parametric approach (Welch method). Initially a parametric AR spectrum had been also considered but it was actually excluded as it was a redundant approach: both SSA and AR analysis allow to perform a sort of spectral decomposition with the final goal of extracting single components from the spectrum of the process.

Also in this case, a Bartlett window and a percentage of 50% have been applied to compare methods performances under the same conditions and choices.

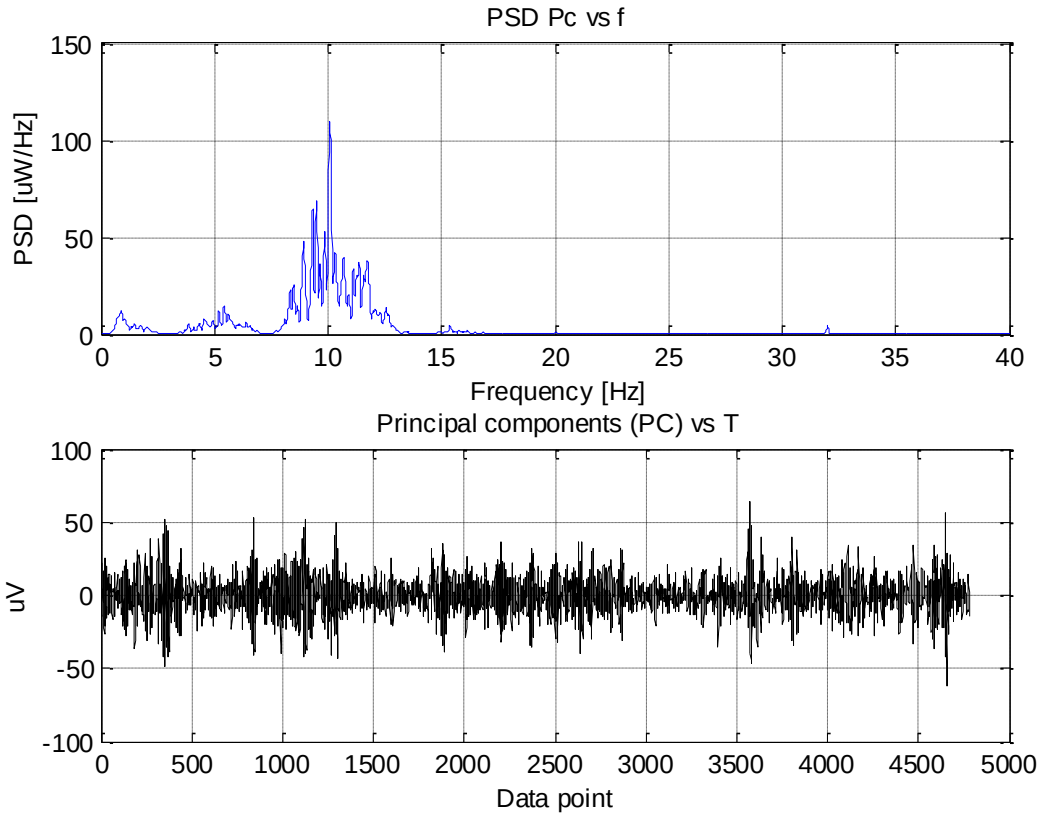

Figure 3.14: example of PSD with Welch method on the top of the image and time domain signal on the bottom for a principal component (PC). Both the two signal are related to an EEG signal from subject nb. 14, in RT3.

Then, the indexes of the principal components related to each frequency band have been searched by checking if the dominant frequency in the spectrum of each principal component belonged to one of the frequency ranges (4,8)Hz or (8,13) Hz or (13,30)Hz respectively for θ,α, β band.

2.2 Reconstruction step

According to the indexes found with this method, a new signal composed of all 6 principal components and a signal for each frequency band, which is the sum of the k components individuated, have been computed (Figure 3.15) as follows:

$$g_k = \begin{cases} \frac{1}{k+1} \sum_{m=1}^{k+1} y^*_{m,k-m+2} & \text{for } 0 \le k < L^* - 1, \\ \frac{1}{L^*} \sum_{m=1}^{L^*} y^*_{m,k-m+2} & \text{for } L^* - 1 \le k < K^*, \\ \frac{1}{N-k} \sum_{m=k-K^*+2}^{N-K^*+1} y^*_{m,k-m+2} & \text{for } K^* \le k < N. \end{cases}$$

Golyandina, N., Nekrutkin, V., & Zhigljavsky, A. A. (2010). *Analysis of time series structure: SSA and related techniques*. CRC Press. [20]

The procedure above is necessary in order to bring back the neo-computed signals (Figure 3.15 and 3.16) to the real time-scale. Indeed, before that, the signals are not of the length of the original signal but as K (=N-L+1). As regards the new signal, it represents a filtered version of the original one that should be cleaned of the noise as much as possible.

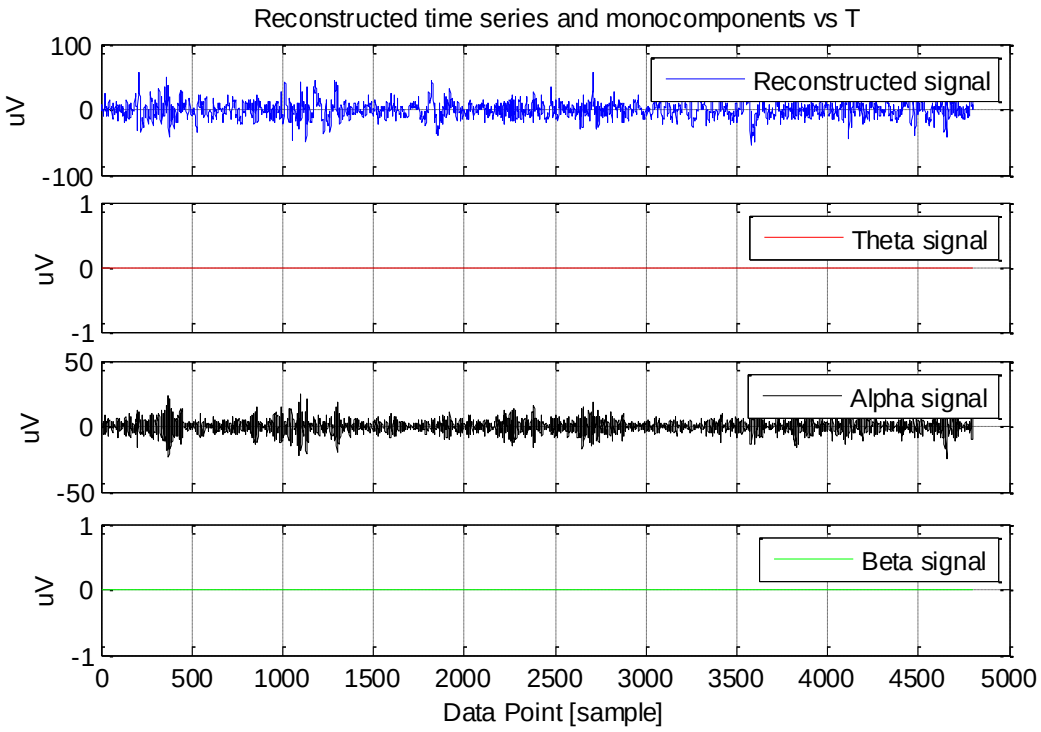

Figure 3.15: reconstructed time series and monocomponent signals respectively for θ, α, β band in a particularly drowsy epoch for the subject no. 14, RT3. It is clearly visible how the signal in the alpha band is detectable while it is absent in beta band.

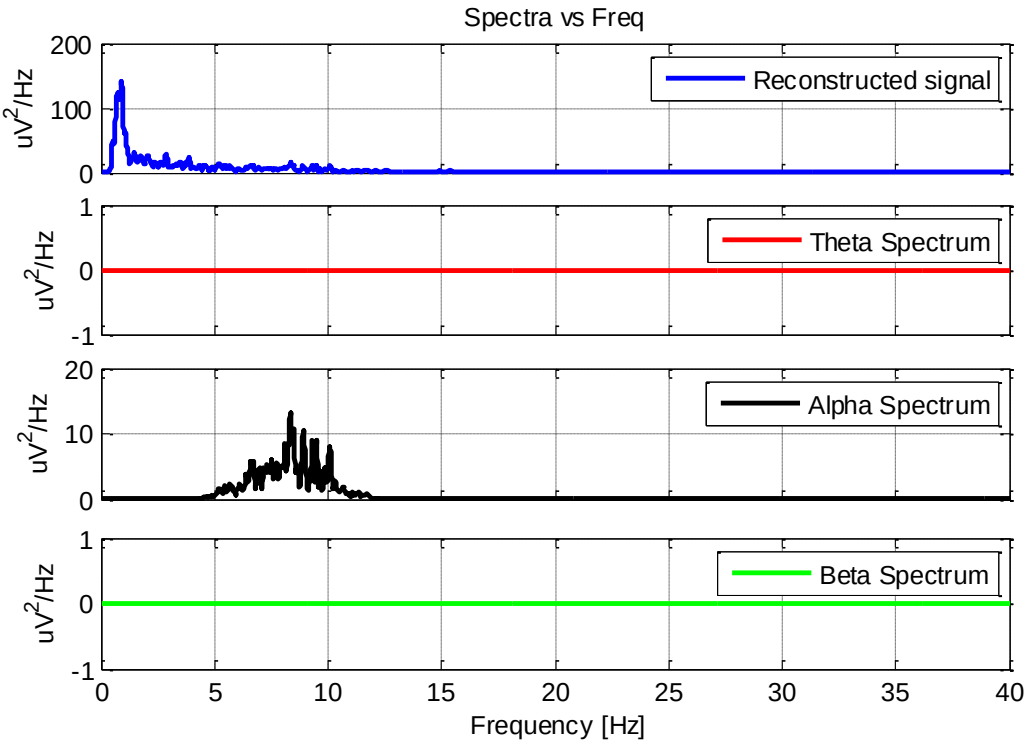

Figure 3.16: PSD of the reconstructed signals (the new filtered signal, and θ, α, β band signals) for a particularly drowsy epoch for the subject nbr. 14, RT3. It is even more visible how the frequency content in the alpha band is detectable while it is absent in beta band.

3.2.3 Features extraction

The features chosen to be extracted from EEG to detect drowsiness are:

- percentage power (P%) in each frequency band computed as:
  $P_i\% = \frac{PSD_i}{PSD_{EEG}}, \qquad i = \theta, \alpha, \beta$
- $\log(\frac{P_i\%}{1-P_i\%})$
- the ratio between alpha PSD and beta PSD: $\frac{P_\alpha}{P_\beta}$
- the ratio between PSD in low frequency (LF) band and high frequency (HF) band: $\frac{P_\theta + P_\alpha}{P_\beta}$
- dominant frequency and dominant peak for each frequency band and for the whole range.

All those features, above defined, have been extracted for all the five EEG electrodes, so a total of 80 features (16 features per channel) are available.
While the features related to the PSD in the band have been computed in the same way for all the methods, the last two ones (dominant frequency and dominant peak) have been extracted essentially in two different ways depending on whether a non-parametric method or a parametric approach was used.
As regards the non-parametric approach, the following reasoning has been developed:

1. peaks have been searched in the PSD of the whole range and of each band and their PSD is referred as "P_{peak}"
2. full width half maximum (FWHM) band of the peak have been defined by a minimum and a maximum value, found through the two frequencies associated to the corresponding value P_i on the ordinate axes according to the following disequation: $P_i < 0.5\ P_{peak}$, on the rising slope and the falling slope
3. the average among all the P_i included in the so-individuated FWHM has been computed for each peak
4. among all the peaks, the peak with the largest average power in its FWHM band is the dominant peak
5. the corresponding frequency is the dominant frequency

Some observations must be done: at the beginning (the end) of the spectrum, this algorithm is not able to find a peak, as usually defined, so the peak has been forced to be the first (the last) value of the spectrum.
In addition, it can happen that no peak is detected:

- in this case, if the signal was flat, that is the minimum and the maximum value of the spectrum coincided, no dominant peak and dominant frequency have been defined (signed as NaN);
- otherwise, the dominant peak has been forced to be the maximum value of the spectrum and the corresponding frequency is the dominant frequency.

The algorithm described until now has been used for both the non-parametric analysis and the SSA with non-parametric spectra. In particular, for this last case, another check must

be done because it can happen that no signal, in a certain frequency band, was detected and so it was consequently impossible to define dominant peak and frequency.
For what concerns the AR spectra, dominant peak and dominant frequency have been extracted exploiting poles and their phases as said before, in the previous paragraph. For the sake of simplicity, the following dotted list summarizes what has been done:

1. poles and the corresponding phases (the angles) have been computed starting from the AR model identified from time to time
2. each frequency band has been defined using the angles associated to the poles, like small slices on the unitary circle
3. the pole with the largest module has been defined as the dominant peak
4. the corresponding frequency has been fixed as the dominant frequency

Also in this case, an observation must be done: if no poles were detected, no dominant peak and dominant frequency have been defined (signed as NaN).
Generally, the case when dominant peak and dominant frequency could not be defined is really delicate, especially for the dominant frequency. Indeed, if you think to indicate with a zero value, for example, the absence of dominant frequency for a certain epoch, that is not possible and the reason is clear: in the frequency domain, the null value has a precious sense, it is indeed related to the DC (direct current) contribute.
As concerns the next statistical analysis, the features values exactly as they are (included the NaN values) have been used while for the employment of those features in a classifier, the absent values have been substituted with the median value of the feature for each set of 14 epochs of signal, as it will be explained then.

3.2.4 Statistical analysis

A preliminary analysis of the content of the 80 features has been run through ROC curves. Features have been normalized by subtracting their minimum value and dividing by the maximum value in order to make each feature belonging to a more manageable range [0,1]. In addition, ROC curves have been constructed by defining cut-off step according to the size of each feature per class, because it strongly depended on which feature was being analyzed. Finally the significance level has been set to 95%.

The test has been run in two ways depending on whether it is used to compare one class against another one or one class against the combination of the remaining two classes.
When a class was compared to another one, the three following combinations have been obtained:

1. class 0 = transition epochs, class 1 = alert epochs
2. class 0 = transition epochs, class 1 = drowsy epochs
3. class 0 = alert epochs, class 1 = drowsy epochs.

Obviously, for this case, the part of values in the dataset related to the excluded class has been eliminated.
In the second case, these are these other three possible combinations:

1. class 0 = transition epochs, class 1 = (alert epochs) + (drowsy epochs)
2. class 0 = alert epochs, class 1 = (transition epochs) + (drowsy epochs)
3. class 0 = drowsy epochs, class 1 = (transition epochs) + (alert epochs).

For each combination tested and for each feature, the AUC (area under curve) has been used as parameter; more precisely, an AUC greater than 0.7 has been chosen as threshold to evaluate if a feature was good or not.
A second statistic test has been run in order to check the capacity of classes discrimination of each feature. For this purpose, Kruskal-Wallis test, that allows to check if different groups come from the same probability distribution, has been employed. It has been chosen because it is a non-parametric statistic test and so it allows not to assume any specific probability distribution like for example the correspondent parametric test ANOVA. In addition, it is also able to manage groups with different sizes like in this case where the number of drowsy, transition and alert cases are totally different.
The test has been run on the following six combinations. In particular firstly the test has been performed in order to verify if features discriminated a class from another one like in the following list:

- class 0 = transition epochs , class 1 = alert epochs
- class 0 = transition epochs, class 1 = drowsy epochs
- class 0 = alert epochs, class 1 = drowsy epochs

Secondly, the test has been carried out in order to verify the capability of each feature to discriminate a class from the combination of the other two ones, like below:

- class 0 = transition epochs, class 1 = (alert epochs) + (drowsy epochs)
- class 0 = alert epochs, class 1 = (transition epochs) + (drowsy epochs)
- class 0 = drowsy epochs, class 1 = (alert epochs) + (transition epochs)

This second approach has been thought because it could happen that a class could be not able to discriminate two different states because of the numerosity of that class, but if combined with another one, its behavior could change. This strategy has been considered in particular in favor of drowsy cases that are less than the other two classes.
As significance value, p-values of 1%, 5% and 10% have been firstly considered. Thanks to these two tests, with a particular attention for the last one, decisive for the individuation of the best features, it has been possible to individuate the features that are efficient to discriminate both the first and the second set of combinations. The selected features have been used for the subsequent classifier.

3.2.5 The classifier

The last step implies the use of a classifier in order to classify data according to the three classes. The classifier chosen is a feed-forward neural network, which will be more detailed then.
Generally, in order to perform a good classification, three steps are necessary: pre-process, main process and post-process.
In the pre-processing phase, data are prepared in a suitable way to be managed for the main process. A matrix of labels has been created putting in order alert, transition and drowsy cases: each column will contain binary decoding, assigning 1 to the current class and 0 to the others. Instead, for the matrix of features, it was created by putting aside the vectors associated to each feature, selected through the before-said statistical analysis, column by column.
As concerns the main process, it consists of running the classifier itself. A feed-forward neural network, with a number of input neurons as long as the number of selected features, has been chosen. In addition, it was decided to employ one hidden layer composed of the same number of neurons as in the input layer. As activation function in this layer, a

sigmoid function was used and the algorithm for the training is the Levenberg-Marquardt method. Finally, the output layer consisted of three neurons, one for each class.
The whole structure of the so-defined neural network can be seen in Figure 3.17.

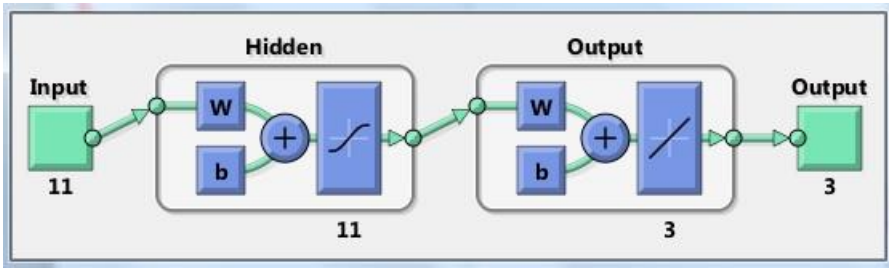

Figure 3.17: structure of the neural network with 11 neurons for the input layer and the hidden layer, 3 neurons in the output layer, sigmoid function in hidden layer as activation function.

Besides, it was thought to perform a *5-fold cross-validation* in order to avoid problems due to the random initial conditions.
This technique consists in dividing the dataset into a base of 5 subsets that are exchanged five times just as the number of times that the neural network is run.
The whole dataset has been rearranged for a *5-fold cross-validation* in order to have, more or less, the same distribution of drowsy, transition and alert cases in each subset. Going into more details, at each time that the neural network has been run, 80% of the dataset was employed for training and the resting 20% for testing. Each times, the repartition of subsets that contribute to the training set and the testing set changed until each 20% of the dataset is used one time in the training set and the other times in the testing set. As evaluation parameter, the mean squared error, committed by the classifier, was chosen.
Finally, the entire algorithm has been run 10 times more in order to moderate the effect of the random distribution of the dataset.
Since the outputs of the neural network represent the probability of the value of each feature to fall into a class, they have been managed in order to express these values in terms of "0, 1, 2" (coding transition, alert, drowsy respectively) and compare them with the real labels. This procedure is necessary to produce a confusion matrix.
The confusion matrix investigates the capability of the classifier in terms of specificity, sensitivity and accuracy; these parameters are obtained by computing the number of true positives rate and false positives rate.

True positives are data belonging to a certain class and correctly classified for that class; false positives are data belonging to a certain class but classified as belonging to another class.

In addition, it is possible to get the misclassification rate of the classifier and plot the confusion matrix, for a faster panorama (Figure 3.18).

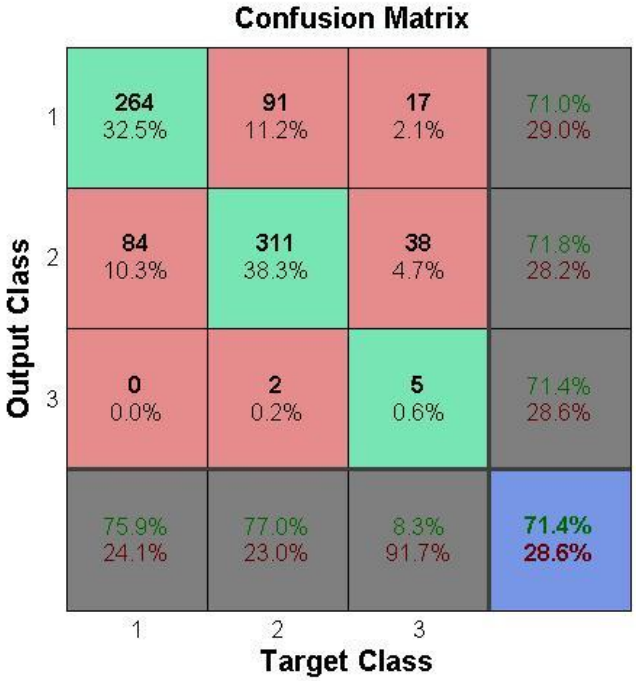

Figure 3.18: an example of confusion matrix obtained through the so-explained procedure; numbers 1, 2, 3 which appear on the matrix are associated in order to alert, transition and drowsy targets.

It can be read in the following way:

- each square represents the relationship between an output class and a target class: 1 stands for alert, 2 for transition, 3 for drowsy
- the numbers that appear inside each green frame on the main diagonal are the percentage of having correctly classified a class and the number itself of data for each class
- outside the main diagonal there are the misclassified cases
- the grey boxes are the precision and the recall: the precision is the percentage of data to belong to a certain class and correctly classified for that class; the recall is

essentially the TP (true positives) rate and that is the percentage of correctly classified;

- the blue box is the whole accuracy computed as the sum of true positives and true negatives out of the total number N of cases.

Once the confusion matrix was available, the K-Cohen coefficient has been used in order to compare features coming from the three developed methods (non-parametric, parametric and singular spectrum analysis).

The K-Cohen coefficient is a statistic coefficient that evaluates the degree of accuracy and reliability of the classifier employed in this work. It exploits the confusion matrix because it is so defined:

$$k = \frac{\Pr(a) - \Pr(e)}{a - \Pr(e)}$$

where *Pr(a)* represents the proportion of agreement and it is obtained by the ratio between the sum of the elements on the first diagonal and the total number of cases; *Pr(e)* is the "agreement expected just by chance" and it results from product between the sum of all the positive cases and the sum of the negative cases.

Doing a 5-fold cross-validation repeated for 10 times, a vectors of 50 K-Cohen has been obtained; the mean value of such vector has been computed for each method (features for non-parametric, parametric, singular spectrum analysis) and this has been the final parameter used to realize a comparison among their performances.

According to what k-Cohen has stated, a further analysis about which of the selected features has been run, subject per subject. In particular, 3 subjects have been taken into account because they were the most significant ones, inside the available dataset: they well adhere to the thought protocol and the aims of this work. However, all these aspects will be better commented in the next chapters.

4. Results

In this chapter, results coming from the methods just explained in the previous chapter are presented. In particular, as declared in the section about the objectives of the work, this thesis aims to three specific goals: extracting features from EEG signals, comparing methods performances, validating the employed protocol and the physiological correlation of the selected features.

4.1 Results from features extraction

In this paragraph, results regarding features extracted through the three above-described different methods are presented. In particular, for each method, results obtained from spectral analysis will be firstly reported in order to make clear how features have been extracted. Secondly, results from statistical tests, performed in order to select the best features, will be shown and, consequently, the features chosen for each method will be declared.

4.1.1 Spectral analysis

Non-parametric spectral analysis

The results reported in this paragraph have been obtained using Welch method. Taking into account that the sampling frequency is 80Hz, one epoch of signal lasts one minute, or equivalently it consists of 4800 samples. The signal, related to each of the 14 epochs, has been divided into 4 segments and each segment has been multiplied with a Bartlett window as long as such segment (1200 samples), in order to moderate the effects of spectral leakage due to the rectangular windowing with the FFT computation. For each epoch a PSD of the whole range of frequency [0.5,35]Hz and a PSD for each frequency band (θ, α, β) have been computed and the following features have been extracted from them:

- percentage power (P%) in each frequency band computed as:
  $P_i\% = \frac{PSD_i}{PSD_{EEG}}, \qquad i = \theta, \alpha, \beta$
- $\log(\frac{P_i\%}{1-P_i\%})$

- the ratio between alpha PSD and beta PSD: $\frac{P_\alpha}{P_\beta}$
- the ratio between PSD in low frequency (LF) band and high frequency (HF) band: $\frac{P_\theta + P_\alpha}{P_\beta}$
- dominant frequency and dominant peak for each frequency band and for the whole range.

These features in the dotted list are related to a single acquisition channel. Therefore, since EEG has been acquired though 5 different electrodes, overall 80 (16 x 5) features are available.

The Kruskal-Wallis test allowed to examine all these features and to individuate which features better discriminated drowsiness, transition and alertness (Table 4.1). Indeed, as already said in the previous chapter, this is a non-parametric test that enables to compare the median value of different groups and to verify if they belong to the same probability distribution or to a probability distribution with the same median value.

LEGEND

p-value = 1%
p-value = 5%
p-value = 10%
other

Nr.	Features	TRANS vs. ALERT	TRANS vs. DROWSY	ALERT vs. DROWSY	TRANS vs. (ALERT+ DROWSY)	ALERT vs. (TRANS+ DROWSY)	DROWSY vs. (ALERT+ TRANS)
1	PZ_(Pa/Pb)	0.170497	0.944885	0.399331	0.230851	0.148235	0.656334
2	PZ_(Pa+Pt)/Pb	0.808986	0.711840	0.808919	0.747463	0.876503	0.747879
3	PZ_Pt%	0.023134	0.014183	0.148126	0.006333	0.094774	0.039656
4	PZ_transf(Pt%)	0.031262	0.016817	0.148126	0.009118	0.117532	0.043073
5	PZ_Pa%	0.145451	0.527737	0.100146	0.266658	0.084227	0.252899
6	PZ_transf(Pa%)	0.094703	0.656158	0.115714	0.175045	0.057188	0.314521
7	PZ_Pb%	0.908598	0.351481	0.355786	0.709700	0.894648	0.336037
8	PZ_transf(Pb%)	0.737884	0.533824	0.394047	0.906857	0.604521	0.449576
9	PZ_freq_dominant	0.069169	0.106051	0.009766	0.251428	0.021955	0.032178
10	PZ_APDP	0.000018	0.235395	0.209357	0.000033	0.000030	0.958491
11	PZ_freq_dominantTHETA	0.288069	0.948161	0.531316	0.354757	0.265412	0.735306
12	PZ_APDP_THETA	0.000000	0.047932	0.000000	0.000000	0.000000	0.000123
13	PZ_freq_dominantALPHA	0.002222	0.260246	0.002373	0.016747	0.000428	0.036583
14	PZ_APDP_ALPHA	0.000025	0.611700	0.004076	0.000322	0.000006	0.095466
15	PZ_freq_dominantBETA	0.799509	0.321037	0.375195	0.607538	0.998180	0.328406
16	PZ_APDP_BETA	0.000009	0.130374	0.310249	0.000012	0.000022	0.727171
17	FZ_(Pa/Pb)	0.348947	0.369912	0.619414	0.274597	0.474961	0.461319
18	FZ_(Pa+Pt)/Pb	0.024513	0.542680	0.542330	0.029593	0.029627	0.965328
19	FZ_Pt%	0.000000	0.000013	0.000000	0.000647	0.000000	0.000000
20	FZ_transf(Pt%)	0.000000	0.000013	0.000000	0.000647	0.000000	0.000000
21	FZ_Pa%	0.156758	0.000135	0.000003	0.879411	0.013461	0.000012
22	FZ_transf(Pa%)	0.147275	0.000136	0.000002	0.855982	0.012129	0.000011
23	FZ_Pb%	0.088270	0.000021	0.000001	0.778489	0.005159	0.000002
24	FZ_transf(Pb%)	0.087831	0.000139	0.000007	0.680297	0.007343	0.000018
25	FZ_freq_dominant	0.000587	0.000694	0.000000	0.038175	0.000012	0.000015
26	FZ_APDP	0.000000	0.000295	0.000000	0.000008	0.000000	0.000000
27	FZ_freq_dominantTHETA	0.661823	0.493534	0.619775	0.556977	0.790051	0.535962
28	FZ_APDP_THETA	0.000019	0.663256	0.006684	0.000241	0.000006	0.121143
29	FZ_freq_dominantALPHA	0.555684	0.841326	0.642957	0.641442	0.517375	0.737899
30	FZ_APDP_ALPHA	0.000000	0.826850	0.000815	0.000002	0.000000	0.082484
31	FZ_freq_dominantBETA	0.709883	0.716898	0.934249	0.662970	0.754260	0.809695
32	FZ_APDP_BETA	0.000000	0.815615	0.002915	0.000000	0.000000	0.117480
33	CZ_(Pa/Pb)	0.450756	0.094415	0.024083	0.853047	0.210352	0.043846
34	CZ_(Pa+Pt)/Pb	0.162250	0.040044	0.214565	0.066113	0.348005	0.082383
35	CZ_Pt%	0.000000	0.148301	0.000057	0.000028	0.000000	0.006076
36	CZ_transf(Pt%)	0.000000	0.148301	0.000057	0.000028	0.000000	0.006076
37	CZ_Pa%	0.768820	0.098761	0.068462	0.827780	0.466221	0.072778
38	CZ_transf(Pa%)	0.667120	0.098761	0.058347	0.923119	0.384804	0.067469
39	CZ_Pb%	0.101929	0.016675	0.001034	0.447566	0.021130	0.003613
40	CZ_transf(Pb%)	0.126888	0.011240	0.000791	0.534252	0.025965	0.002491
41	CZ_freq_dominant	0.001725	0.038938	0.000285	0.028725	0.000184	0.003789
42	CZ_APDP	0.000000	0.089441	0.000003	0.000000	0.000000	0.001407

Nr.	Features	TRANS vs. ALERT	TRANS vs. DROWSY	ALERT vs. DROWSY	TRANS vs. (ALERT+ DROWSY)	ALERT vs. (TRANS+ DROWSY)	DROWSY vs. (ALERT+ TRANS)
43	CZ_freq_dominantTHETA	0.865769	0.367367	0.376135	0.680585	0.941064	0.354087
44	CZ_APDP_THETA	0.000000	0.019437	0.000000	0.000018	0.000000	0.000144
45	CZ_freq_dominantALPHA	0.008970	0.688116	0.062864	0.027367	0.004786	0.262716
46	CZ_APDP_ALPHA	0.000000	0.699574	0.001105	0.000012	0.000000	0.073788
47	CZ_freq_dominantBETA	0.222118	0.786793	0.683510	0.244546	0.229967	0.962732
48	CZ_APDP_BETA	0.000000	0.214890	0.097482	0.000000	0.000000	0.910742
49	C3_(Pa/Pb)	0.912869	0.034237	0.021333	0.605300	0.493087	0.022349
50	C3_(Pa+Pt)/Pb	0.017251	0.012562	0.328685	0.004505	0.058848	0.063618
51	C3_Pt%	0.000000	0.002042	0.000000	0.000089	0.000000	0.000004
52	C3_transf(Pt%)	0.000000	0.002042	0.000000	0.000089	0.000000	0.000004
53	C3_Pa%	0.270633	0.001145	0.000098	0.971355	0.047395	0.000231
54	C3_transf(Pa%)	0.215918	0.001147	0.000073	0.875400	0.033763	0.000202
55	C3_Pb%	0.160036	0.000038	0.000002	0.957521	0.012848	0.000004
56	C3_transf(Pb%)	0.156314	0.000020	0.000001	0.981498	0.010920	0.000002
57	C3_freq_dominant	0.000562	0.025504	0.000042	0.015595	0.000034	0.001310
58	C3_APDP	0.000000	0.003409	0.000000	0.000006	0.000000	0.000007
59	C3_freq_dominantTHETA	0.897384	0.565759	0.487956	0.958587	0.769744	0.513767
60	C3_APDP_THETA	0.000000	0.196062	0.000001	0.000001	0.000000	0.001774
61	C3_freq_dominantALPHA	0.058048	0.346132	0.029771	0.158138	0.024054	0.116246
62	C3_APDP_ALPHA	0.000000	0.919458	0.001124	0.000000	0.000000	0.129601
63	C3_freq_dominantBETA	0.623850	0.091547	0.105093	0.354343	0.976690	0.086346
64	C3_APDP_BETA	0.000000	0.577408	0.000027	0.000000	0.000000	0.085978
65	C4_(Pa/Pb)	0.059060	0.307512	0.024532	0.167001	0.023283	0.098808
66	C4_(Pa+Pt)/Pb	0.875065	0.284627	0.313653	0.652666	0.907814	0.280465
67	C4_Pt%	0.002858	0.852660	0.135280	0.006833	0.002218	0.536767
68	C4_transf(Pt%)	0.002861	0.852660	0.135280	0.006839	0.002220	0.536767
69	C4_Pa%	0.600838	0.802024	0.983922	0.590756	0.634803	0.897151
70	C4_transf(Pa%)	0.693895	0.802024	0.959348	0.672637	0.733528	0.870063
71	C4_Pb%	0.298343	0.437189	0.170958	0.484532	0.199445	0.275146
72	C4_transf(Pb%)	0.388840	0.323934	0.138408	0.631343	0.249417	0.207046
73	C4_freq_dominant	0.009295	0.295234	0.014614	0.044561	0.003087	0.078724
74	C4_APDP	0.000000	0.598018	0.000235	0.000000	0.000000	0.038730
75	C4_freq_dominantTHETA	0.038793	0.430440	0.786001	0.038897	0.054245	0.759569
76	C4_APDP_THETA	0.000000	0.209597	0.000000	0.000000	0.000000	0.000717
77	C4_freq_dominantALPHA	0.084810	0.989297	0.309065	0.126532	0.070747	0.618332
78	C4_APDP_ALPHA	0.000000	0.527737	0.000300	0.000002	0.000000	0.036216
79	C4_freq_dominantBETA	0.590204	0.018010	0.034763	0.244182	0.956299	0.019827
80	C4_APDP_BETA	0.000000	0.007439	0.637925	0.000000	0.000000	0.208905

Table 4.1: results from Kruskal-Wallis test for all the 80 features from a non-parametric spectral estimation; as the legend suggests, green boxes indicate Kruskal-Wallis results less than a p-value of 1%, the yellow boxes for a p-value $\leq$ 5% and the red ones are related to p-value $\leq$ 10%.

As it could be seen in the Table 4.1, results have been differentiated based on whether they were able to discriminate with a p-value of 1%, 5% or 10%.

Generally, results that have p-values ≤ 1% are considered the best ones because it means that features can discriminate almost perfectly the classes; if they have a p-value ≤ 5% , they discriminate average well and finally for p-value ≤ 10%, features are weakly separated and so their discriminant power is poor.

In this case, enough features resulted with a p-value of 5% so that significance value has been chosen as threshold to select good features. It came up that 11 features, extracted with a non-parametric spectral estimation, were able to correctly distinguish drowsy cases, transition cases and alert cases. They are listed below and their name (as in Table 4.1) is reported in brackets:

1. dominant peak in θ band ("Pz_APDP_theta"), from parietal area (Pz channel)
2. percentage power in θ band ("Fz_Pt%"), from frontal area (Fz channel)
3. a transformed version of percentage power ("Fz_transf(Pt%)"), just to remember it is $\log(\frac{P_i\%}{1-P_i\%})$, in θ band, from frontal area (Fz channel)
4. dominant frequency in the whole range ("Fz_freq_dominant"), from frontal area (Fz channel)
5. dominant peak in the whole range ("Fz_APDP"), from frontal area (Fz channel)
6. dominant frequency in the whole range ("Cz_freq_dominant"), from central area (Cz channel)
7. dominant peak in θ band ("Cz_APDP_theta"), from central area (Cz channel)
8. percentage power in θ band ("C3_Pt%"), from left central area (C3 channel)
9. $\log(\frac{P_i\%}{1-P_i\%})$, in θ band ("C3_transf(Pt%)"), from left central area (C3 channel)
10. dominant frequency in the whole range ("C3_freq_dominant"), from left central area (C3 channel)
11. dominant peak in the whole range ("C3_APDP"), from left central area (C3 channel)

Once features have been selected, for each of them a "box plot" has been evaluated in order to visualize their statistical distribution and how much the distribution of the feature for a class was separated from the distribution of another one. The rectangular frame in the boxplot represents the 25^{th} and the 75^{th} percentiles, the line inside is the median value,

some whiskers spread until the most distant value not considered as outlier (5^{th} and 95^{th}) and the red crosses are the outliers.

In the figures below the boxplots of the eleven selected features are presented.

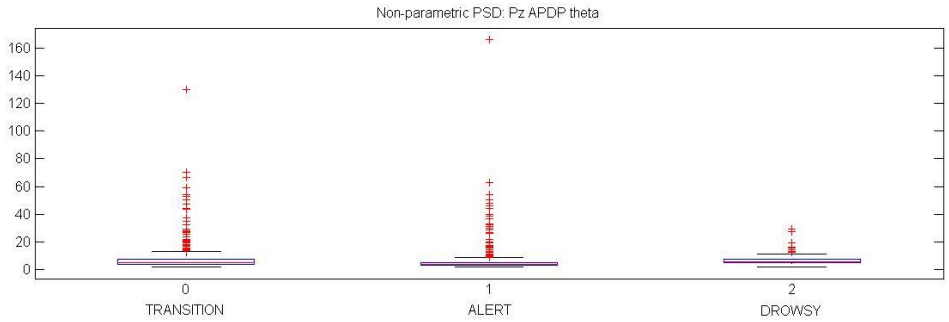

Figure 4.1: dominant peak in θ band, parietal area (Pz). It is characterized by many outliers but not so large variance; alert and drowsy cases are well-separated while transition and drowsy cases not so well.

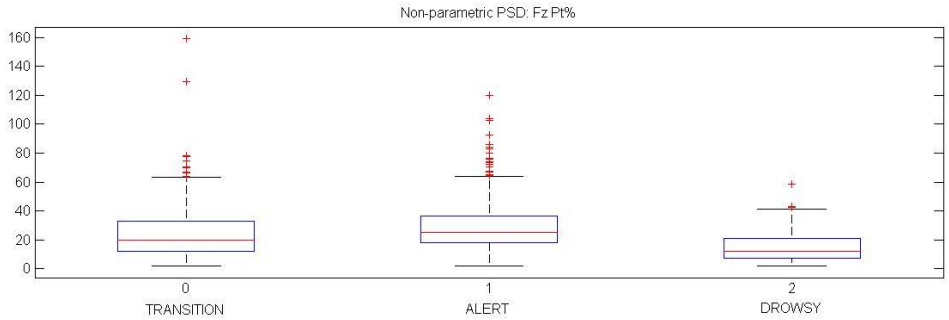

Figure 4.2: percentage power in θ band, frontal area. The statistical distributions for the three classes are almost well-separated.

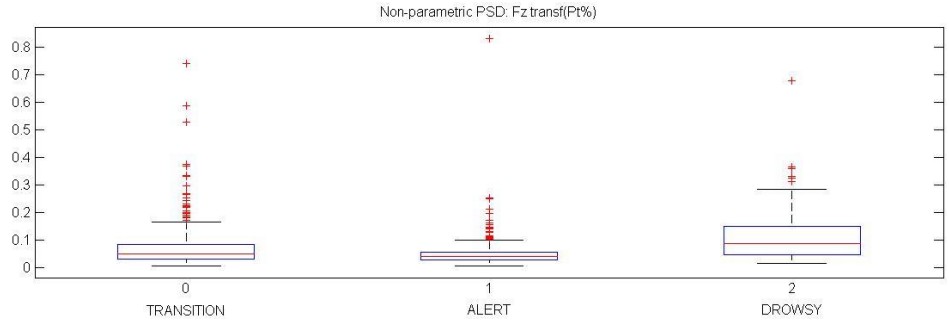

Figure 4.3: a transformed version of percentage power in θ band, frontal area. Alert and drowsy are really well-separated and the statistical distribution is generally good thanks to a not so large variance.

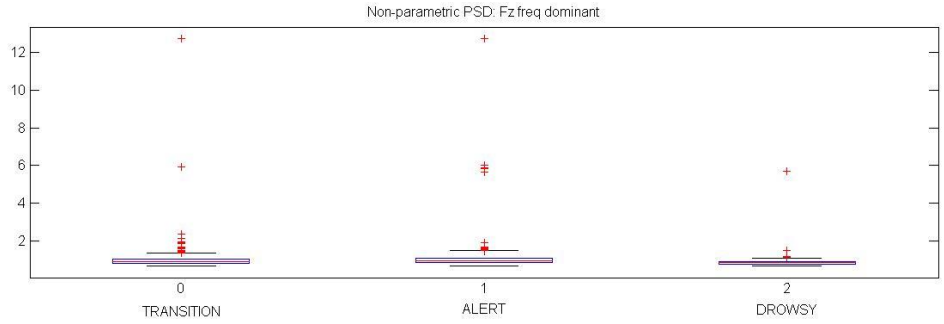

Figure 4.4: dominant frequency in the whole range, frontal area. The statistical distribution is in this case not so interesting, even if its p-value was good.

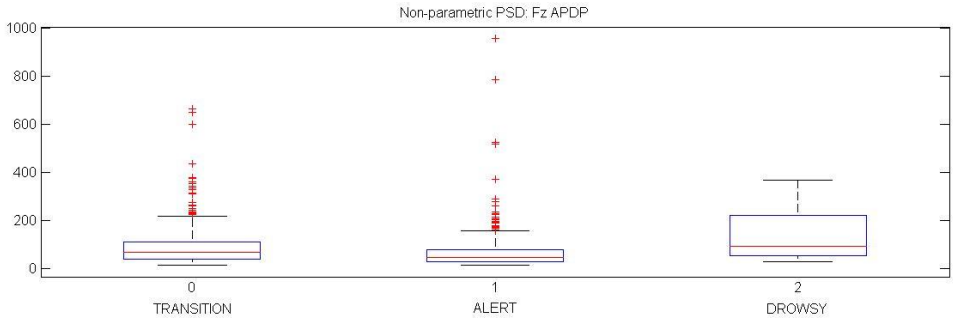

Figure 4.5: dominant peak in the whole range, frontal area. The three classes are really well-separated.

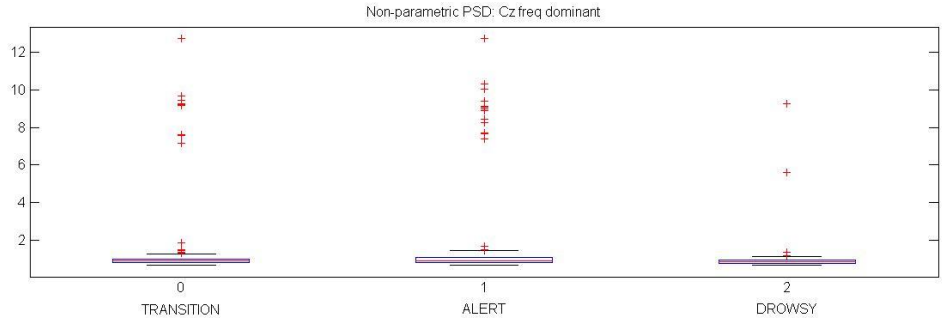

Figure 4.6: dominant frequency in the whole range, central area. Alert and drowsy classes are almost discriminated and alert and transition classes as well; it is not the same for the distinction between transition and drowsy cases.

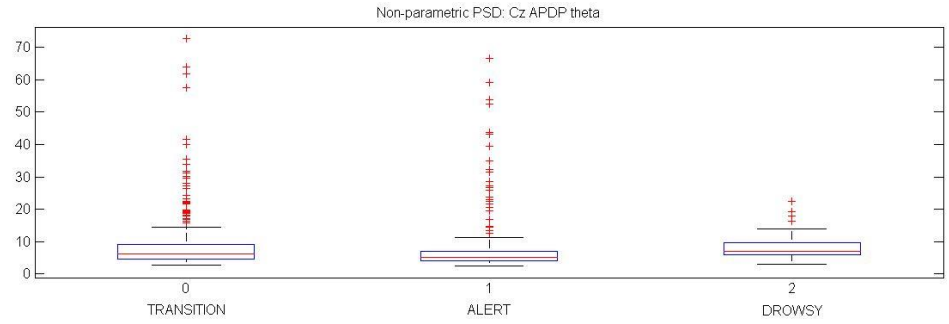

Figure 4.7: dominant peak in θ band, central area. Alert class is well-distinguished from transition class and from drowsy class but transition and drowsy classes have almost the same distribution.

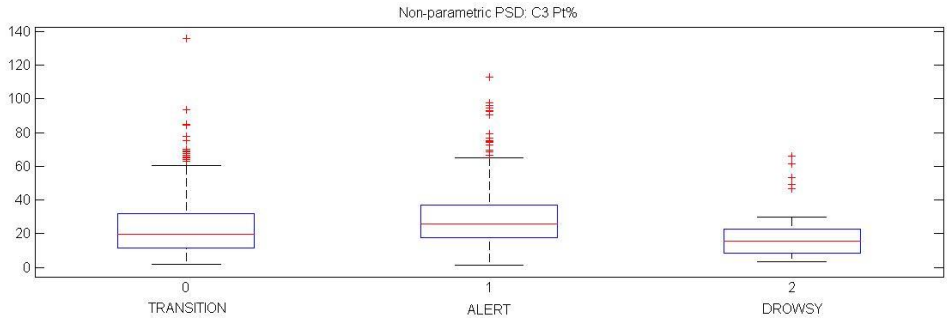

Figure 4.8: percentage power in θ band, left central area. Alert and drowsy classes are really well-separated as well as transition class from drowsy class; a less distinction emerges instead between transition and alert classes.

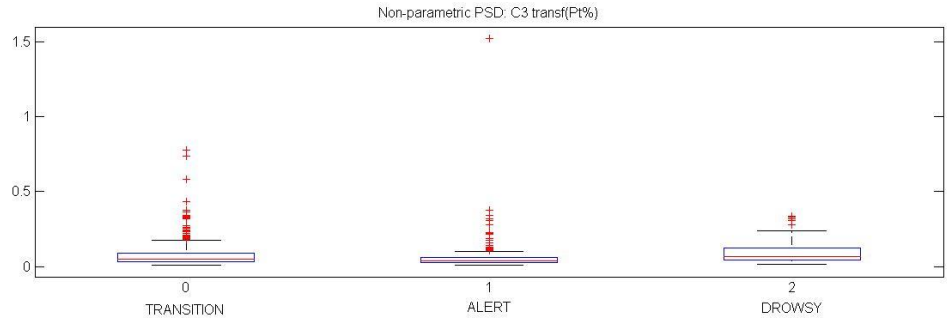

Figure 4.9: a transformed version of percentage power in θ band, left central area. The three classes are well-separated.

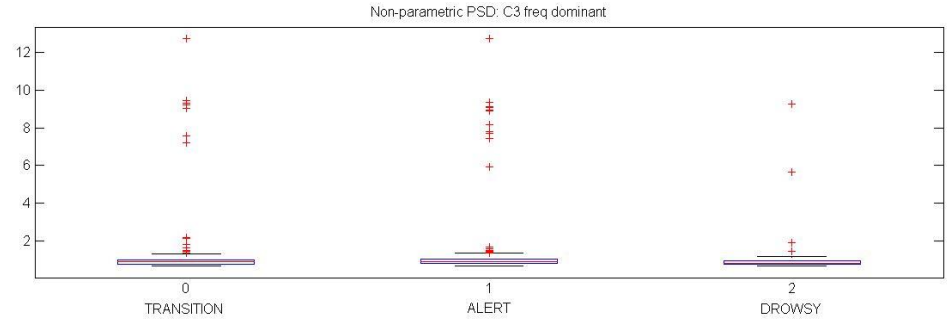

Figure 4.10: dominant frequency in the whole range, left central area. Transition and drowsy classes have almost the same distribution while alert class is well-separated from the other two ones.

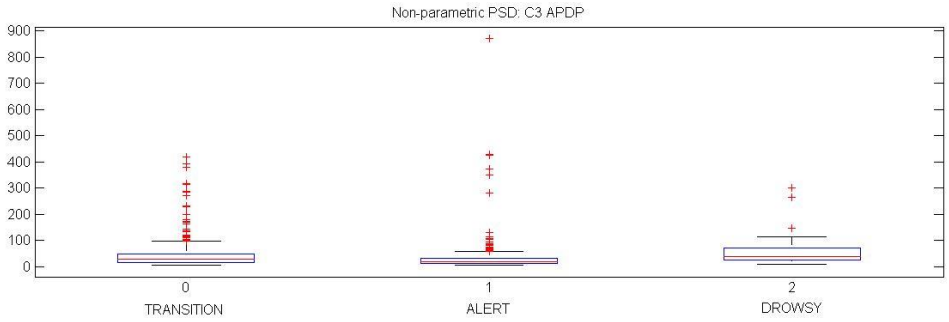

Figure 4.11: dominant peak in the whole range, left central area. All the three cases are well-discriminated.

Even if it was said that some selected features don't result so meaningful by boxplot, they weren't excluded because a classifier, that receives a combination of almost good features, can still provide good results, in terms of classification.

So said, all the eleven features have been given as input to the classifier who has run a 5-fold cross-validation for 10 times. Since there are eleven features, the neural network had, in this case, eleven neurons in the input layer and in the hidden layer; the output layer was always composed of 3 neurons because it aimed to distinguish data into three classes.

The choice of performing a 5-fold cross-validation is motivated by the fact that, each time, the neural network is randomly initialized so outputs would be strongly related to initial conditions. The cross-validation tempers this aspect. In addition, repeating ten times the algorithm allows to mitigate the effect due the random distribution of examples into 5 subsets. However, for more details, like how data were distributed in order to keep a certain balance among classes and so on, it is suggested to come back to the chapter 3, paragraph 3.2.5.

Parametric spectral analysis

Parametric spectral analysis has been performed by developing an auto-regressive model of the spectrum of the signal. The order of the model has been fixed by combining Akaike information criterion (AIC) and whiteness Anderson's test. Such a model has been created for each epoch of signal. Therefore, epoch by epoch, the order of the model and the correspondent set of coefficients have been computed.

In addition, poles, angles of the poles and the variance of the prediction error of the model have been computed. This last parameter, the variance of the prediction error (VPE), is included in the formula to compute the power spectrum, as already detailed in the previous chapter, where σ^2 must be substituted by VPE and the coefficients by the estimated coefficients:

$$\hat{S}_y(e^{j\omega T}) = \sigma^2 T \left|H(e^{j\omega T})\right|^2 = \frac{\sigma^2 T}{\left|1 + \sum_{k=1}^{p} a_k e^{-j\omega T k}\right|^2}$$

For each epoch, a power spectrum of the whole range of frequency [0.5,35]Hz and for each frequency band (θ, α, β) have been computed.

Poles with maximum module and their corresponding angles have been used in order to extract dominant peak and dominant frequency.

In conclusion, sixteen features per channel have been computed with this method and therefore 80 features were globally available, as for the non-parametric method, and they are listed as follows:

- percentage power (P%) in each frequency band computed as:
  $P_i\% = \frac{PSD_i}{PSD_{EEG}}, \qquad i = \theta, \alpha, \beta$
- $\log(\frac{P_i\%}{1-P_i\%})$
- the ratio between alpha power spectrum and beta power spectrum: $\frac{P_\alpha}{P_\beta}$
- the ratio between power spectrum in low frequency (LF) band and high frequency (HF) band : $\frac{P_\theta + P_\alpha}{P_\beta}$
- dominant frequency and dominant peak for each frequency band and for the whole range.

They have been tested by using Kruskal-Wallis test in order to evaluate the degree of separation among the three classes. The following table (Table 4.2) shows results from each features against one among the six possible combinations.

LEGEND

- p-value = 1%
- p-value = 5%
- p-value = 10%
- other
- NaN

Nr.	FEATURES	Nr.	TRANS vs. ALERT	TRANS vs. DROWSY	ALERT vs. DROWSY	TRANS vs. (ALERT+ DROWSY)	ALERT vs. (TRANS+ DROWSY)	DROWSY vs. (ALERT+ TRANS)
1	PZ_(Pa/Pb)	1	0.056835	0.939138	0.271311	0.094786	0.046490	0.566579
2	PZ_(Pa+Pt)/Pb	2	0.745007	0.742825	0.650677	0.846247	0.683600	0.688886
3	PZ_Pt%	3	0.113717	0.034677	0.227535	0.043550	0.265874	0.079596
4	PZ_transf(Pt%)	4	0.112263	0.034501	0.226623	0.042900	0.263672	0.079204
5	PZ_Pa%	5	0.036309	0.901460	0.147793	0.068033	0.024505	0.443088
6	PZ_transf(Pa%)	6	0.014912	0.777396	0.088490	0.037357	0.008775	0.327771
7	PZ_Pb%	7	0.880640	0.480983	0.517485	0.735479	0.975880	0.482099
8	PZ_transf(Pb%)	8	0.878781	0.481625	0.519021	0.734127	0.978051	0.483169
9	PZ_freq_dominant	9	0.000333	0.000517	0.167648	0.000027	0.004099	0.009587
10	PZ_peak_dominant	10	0.014272	0.000202	0.005000	0.001131	0.137678	0.000639
11	PZ_freq_dominantTHETA	11	0.036548	0.467599	0.642979	0.038557	0.045976	0.857291
12	PZ_peak_dominantTHETA	12	0.000107	0.184030	0.335384	0.000129	0.000195	0.784721
13	PZ_freq_dominantALPHA	13	0.022490	0.834897	0.250701	0.036733	0.019169	0.660887
14	PZ_peak_dominantALPHA	14	0.160437	0.977775	0.572182	0.215173	0.160163	0.773363
15	PZ_freq_dominantBETA	15	0.888083	0.669257	0.673890	0.803384	0.984803	0.660059
16	PZ_peak_dominantBETA	16	0.978244	0.675280	0.583116	0.922525	0.869358	0.619170
17	FZ_(Pa/Pb)	17	0.275940	0.643163	0.933869	0.270152	0.338461	0.766586
18	FZ_(Pa+Pt)/Pb	18	0.019393	0.843769	0.272345	0.032753	0.017340	0.674204
19	FZ_Pt%	19	0.000000	0.000009	0.000000	0.000044	0.000000	0.000000
20	FZ_transf(Pt%)	20	0.000000	0.000009	0.000000	0.000048	0.000000	0.000000
21	FZ_Pa%	21	0.214858	0.000660	0.000046	0.908635	0.031286	0.000116
22	FZ_transf(Pa%)	22	0.215357	0.000662	0.000046	0.909466	0.031392	0.000116
23	FZ_Pb%	23	0.265686	0.000173	0.000045	0.920505	0.041361	0.000051
24	FZ_transf(Pb%)	24	0.265541	0.000174	0.000045	0.920861	0.041331	0.000051
25	FZ_freq_dominant	25	0.000000	0.622598	0.000742	0.000000	0.000000	0.057354
26	FZ_peak_dominant	26	0.000000	0.603043	0.022919	0.000007	0.000000	0.165795
27	FZ_freq_dominantTHETA	27	0.064163	0.272711	0.937038	0.049535	0.099949	0.518400
28	FZ_peak_dominantTHETA	28	0.243787	0.744401	0.330528	0.345141	0.195424	0.515786
29	FZ_freq_dominantALPHA	29	0.155872	0.121196	0.605273	0.087123	0.253227	0.267669
30	FZ_peak_dominantALPHA	30	0.560150	0.216804	0.454827	0.381011	0.739455	0.295910
31	FZ_freq_dominantBETA	31	0.451767	0.079950	0.211949	0.239345	0.720817	0.115748
32	FZ_peak_dominantBETA	32	0.460313	0.077320	0.180409	0.242587	0.747916	0.104058
33	CZ_(Pa/Pb)	33	0.189283	0.130112	0.015802	0.466761	0.072751	0.045118
34	CZ_(Pa+Pt)/Pb	34	0.295070	0.033201	0.181181	0.121554	0.549013	0.067899
35	CZ_Pt%	35	0.000003	0.315902	0.000595	0.000105	0.000000	0.026905
36	CZ_transf(Pt%)	36	0.000003	0.316899	0.000618	0.000109	0.000000	0.027342
37	CZ_Pa%	37	0.700869	0.182163	0.283900	0.466394	0.942877	0.208905
38	CZ_transf(Pa%)	38	0.579463	0.174837	0.293598	0.375585	0.818264	0.208077
39	CZ_Pb%	39	0.274607	0.026599	0.004927	0.742934	0.089461	0.009715
40	CZ_transf(Pb%)	40	0.274755	0.026599	0.004927	0.743160	0.089518	0.009715
41	CZ_freq_dominant	41	0.000009	0.761623	0.070280	0.000054	0.000008	0.480674
42	CZ_peak_dominant	42	0.000314	0.894112	0.231671	0.001189	0.000398	0.614740

Nr.	FEATURES	Nr.	TRANS vs. ALERT	TRANS vs. DROWSY	ALERT vs. DROWSY	TRANS vs. (ALERT+ DROWSY)	ALERT vs. (TRANS+ DROWSY)	DROWSY vs. (ALERT+ TRANS)
43	CZ_freq_dominantTHETA	43	0.028723	0.003599	0.134687	0.005326	0.112026	0.019518
44	CZ_peak_dominantTHETA	44	0.001573	0.639259	0.019811	0.007392	0.000598	0.166975
45	CZ_freq_dominantALPHA	45	0.350682	0.232961	0.694788	0.239823	0.460506	0.395050
46	CZ_peak_dominantALPHA	46	0.951676	0.245521	0.310249	0.777227	0.754110	0.257077
47	CZ_freq_dominantBETA	47	0.274311	0.135431	0.400658	0.160126	0.442879	0.217527
48	CZ_peak_dominantBETA	48	0.423256	0.147146	0.299080	0.257556	0.649637	0.192020
49	C3_(Pa/Pb)	49	0.815515	0.022166	0.008150	0.648356	0.376509	0.010940
50	C3_(Pa+Pt)/Pb	50	0.028010	0.004402	0.137464	0.005456	0.110882	0.021719
51	C3_Pt%	51	0.000000	0.020706	0.000000	0.000052	0.000000	0.000155
52	C3_transf(Pt%)	52	0.000000	0.020706	0.000000	0.000049	0.000000	0.000155
53	C3_Pa%	53	0.577391	0.006951	0.002871	0.773674	0.207395	0.003339
54	C3_transf(Pa%)	54	0.638595	0.007485	0.003348	0.720198	0.241977	0.003754
55	C3_Pb%	55	0.384316	0.000050	0.000007	0.686669	0.053495	0.000010
56	C3_transf(Pb%)	56	0.385052	0.000050	0.000007	0.685788	0.053664	0.000010
57	C3_freq_dominant	57	0.000717	0.968724	0.086079	0.002741	0.000510	0.395368
58	C3_peak_dominant	58	0.017016	0.661011	0.819039	0.024562	0.027712	0.894436
59	C3_freq_dominantTHETA	59	0.171330	0.492618	0.864681	0.157085	0.203471	0.764691
60	C3_peak_dominantTHETA	60	0.023414	0.141474	0.002314	0.112843	0.004933	0.022426
61	C3_freq_dominantALPHA	61	0.568911	0.311935	0.591278	0.423955	0.707958	0.412439
62	C3_peak_dominantALPHA	62	0.783137	0.206614	0.184296	0.903182	0.558020	0.180031
63	C3_freq_dominantBETA	63	0.213245	0.834897	0.376531	0.295628	0.179175	0.587672
64	C3_peak_dominantBETA	64	0.265830	0.903095	0.509083	0.340241	0.242952	0.699446
65	C4_(Pa/Pb)	65	0.026784	0.294019	0.018622	0.096094	0.009627	0.085978
66	C4_(Pa+Pt)/Pb	66	0.992478	0.294019	0.269251	0.754501	0.784610	0.264963
67	C4_Pt%	67	0.000973	0.877002	0.048553	0.003894	0.000530	0.299492
68	C4_transf(Pt%)	68	0.000994	0.877816	0.049096	0.003955	0.000543	0.300826
69	C4_Pa%	69	0.547413	0.618956	0.943299	0.497148	0.601571	0.756562
70	C4_transf(Pa%)	70	0.476004	0.615323	0.964071	0.435844	0.529633	0.763967
71	C4_Pb%	71	0.259305	0.299032	0.111654	0.483037	0.155977	0.179197
72	C4_transf(Pb%)	72	0.259376	0.299512	0.112189	0.482944	0.156197	0.179753
73	C4_freq_dominant	73	0.001222	0.439017	0.264654	0.001944	0.001430	0.913010
74	C4_peak_dominant	74	0.003472	0.194283	0.808000	0.002939	0.010392	0.402723
75	C4_freq_dominantTHETA	75	0.002821	0.007745	0.447561	0.000612	0.012935	0.065648
76	C4_peak_dominantTHETA	76	0.000015	0.645313	0.023489	0.000071	0.000008	0.400306
77	C4_freq_dominantALPHA	77	0.508247	0.089831	0.270795	0.280156	0.754110	0.141119
78	C4_peak_dominantALPHA	78	0.870689	0.100245	0.170958	0.534350	0.839118	0.116014
79	C4_freq_dominantBETA	79	0.771394	0.018492	0.012713	0.670891	0.370018	0.012141
80	C4_peak_dominantBETA	80	0.718161	0.015582	0.007178	0.703472	0.312582	0.008343

Table 4.2: results from Kruskal-Wallis test for all the 80 features from an AR spectral estimation; the meaning of the colors is written in the legend upon the table.

As previously explained, according to results from Kruskal-Wallis, just the following four features resulted to be the best ones:

1. percentage power in θ band (Fz_Pt%), from frontal area (Fz channel)

2. a transformed version of the percentage power in θ band (Fz_transf(Pt%)), from frontal area (Fz channel)
3. percentage power in θ band (C3_Pt%), from left central area (C3 channel)
4. a transformed version of the percentage power in θ band (C3_transf(Pt%)), from left central area (C3 channel).

For each feature, a boxplot (see Figures below) has been evaluated in order to quickly visualize the statistical distribution.

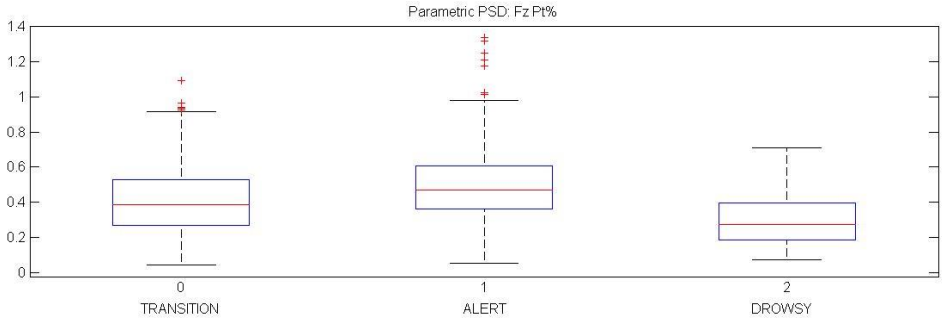

Figure 4.12: percentage power in θ band, frontal area. All the three classes are well separated.

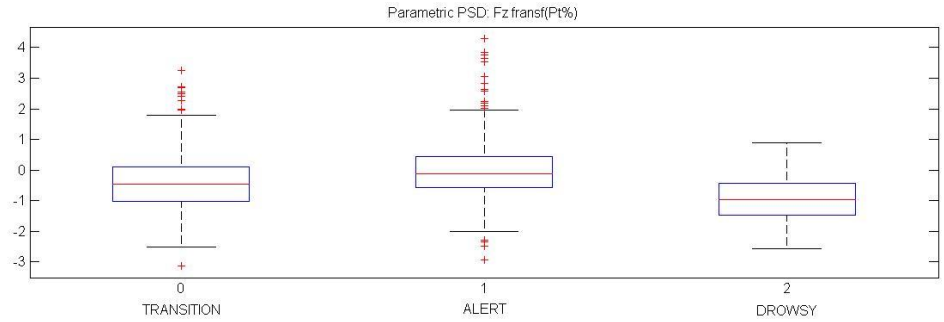

Figure 4.13: a transformed version of the percentage power in θ band, frontal area. The three classes are better and better separated than by the previous feature, as clearly visible.

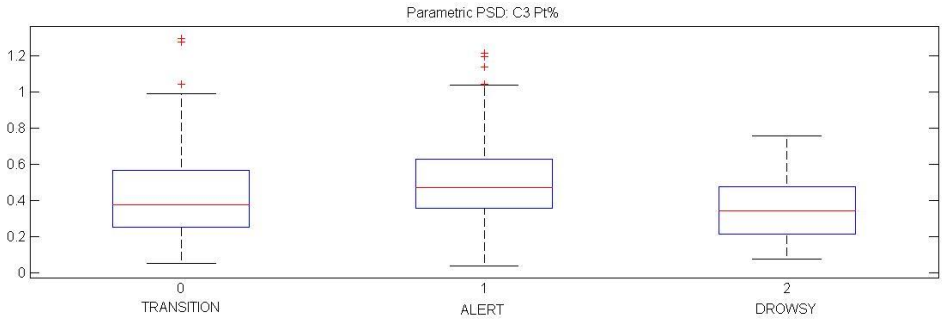

Figure 4.14: percentage power in θ band, left central area. Alert and drowsy cases are better distinguished than the other two combinations.

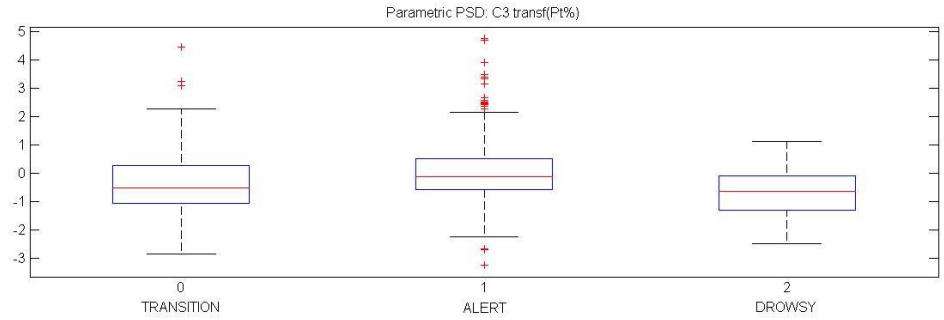

Figure 4.15: a transformed version of the percentage power in θ band, left central area. Alert and drowsy cases are better and better separated than the previous feature. The distinction between transition and drowsy classes is improved.

It must be observed that in this case just four features resulted to well behave with respect to the distinction into three classes. This could represent a problem for the employment of a neural network because there are not as many significant parameters as the previous method.

Generally, if a neural network is well trained, it should correctly classify data into desired classes and it should have high accuracy. When the dataset is too small, it risks to not allow the neural network to appropriately learn and so to not correctly classify.

By the way, these four features have been given as input to the classifier that gave in output the probability that each value of each feature was related to a certain class.

As regards the classifier, in this case, since the number of significant features changed, the number of neurons in the input layer and in the hidden layer changed as well. Indeed, 4 neurons for both the input layer and the hidden layer are present; as regards the output layer, three neurons have been always used.

Starting from the outputs of the classifier, a confusion matrix has been obtained and used in order to compute k-Cohen coefficients. Since a 5-fold cross-validation, repeated 10 times, has been performed, overall 50 values of k-Cohen coefficients have been computed.

Singular spectrum analysis

The algorithm of the SSA, already explained in the previous chapter, has been applied on each epoch of signal. As regards the embedding dimension, also previously referred as "window length", several values have been tested and it has been actually preferred to use L=20 because the frequency resolution obtained was 4Hz. Such a value was considered appropriate because each frequency band is wide 4Hz, at least.
In addition, it was observed that the "statistical dimension S" improved as decreasing the window length and this choice resulted to be the best one, as visible in figures below.

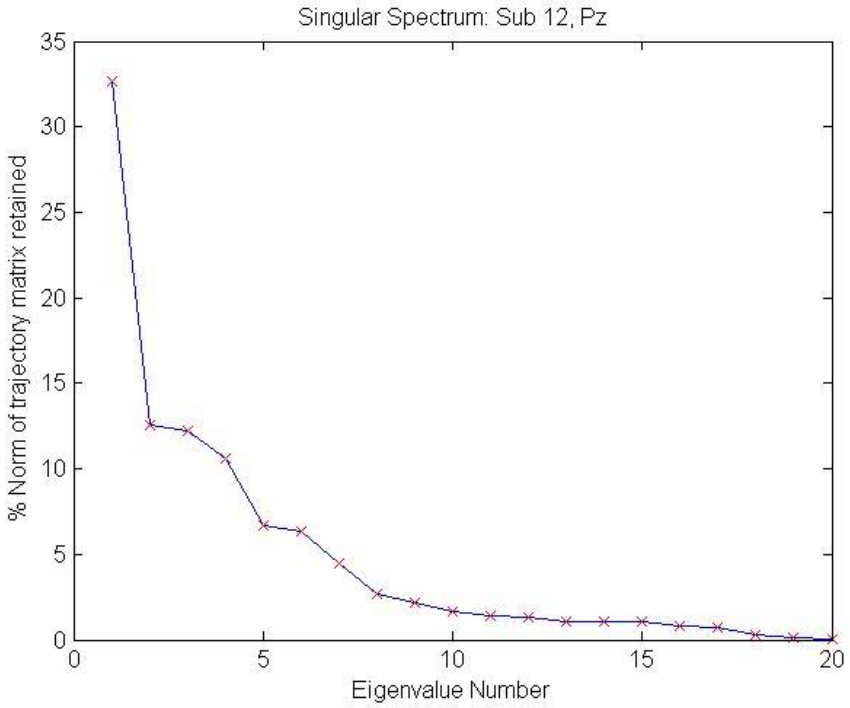

Figure 4.16: L = 20 for an EEG coming from parietal area, subject 12 at 9th minute of RT3.

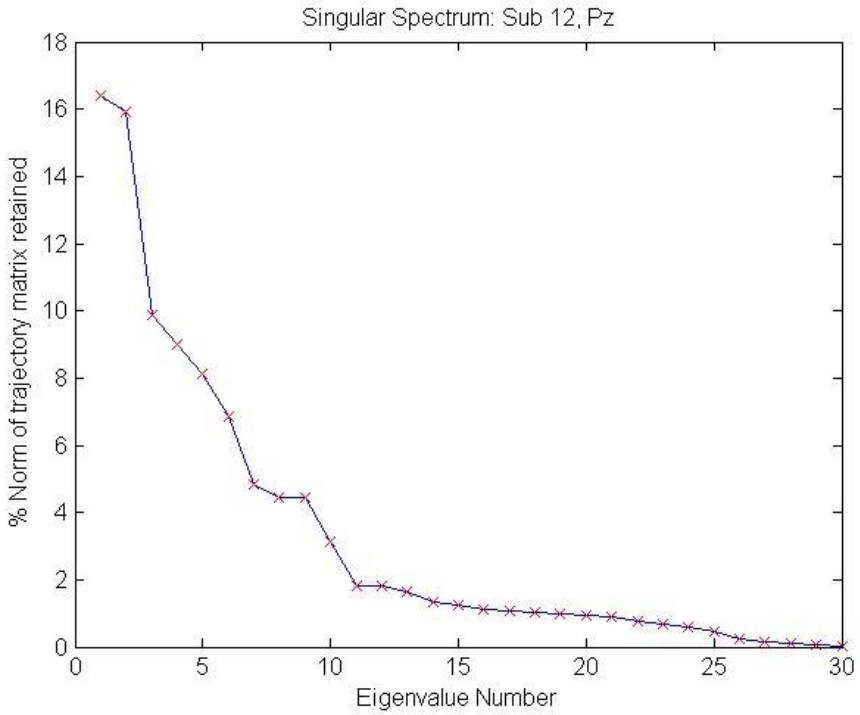

Figure 4.17: L=30, for an EEG coming from parietal area, subject 12 at 9th minute of RT3.

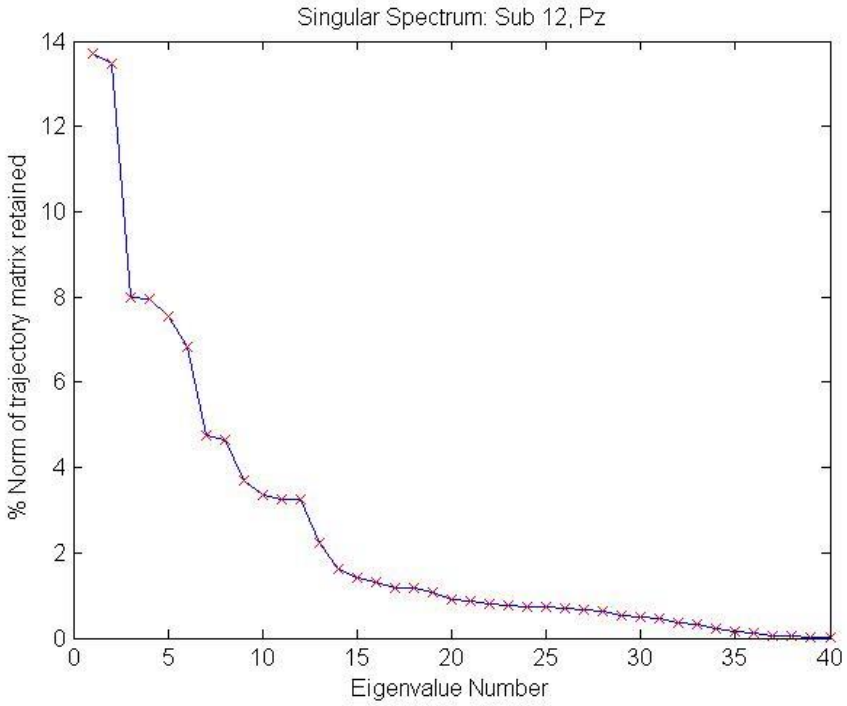

Figure 4.18: L =40, for an EEG coming from parietal area, subject 12 at 9th minute of RT3.

As it can be observed by the figures from 4.16 to 4.18, as L increases the maximum percentage of variance explained by the first k components decreases and also the number k of significant eigenvalues decreases.

In conclusion, L=20 is thus the most suitable choice as it allows to obtain a greater explained maximum variance, a better frequency resolution and a more appropriate number of significant eigenvalues. This last parameter has been fixed equal to 6, observing that for L=20 and $k \geq 6$ the trajectory matrix retained was above 5%.

In fact, since the aim of this method is to produce some new filtered signals, for each frequency band, and a cleaned version of the original signal (4 new signals overall), it is better to get a number of eigenvalues ≥ 4, in order to individuate at least a principal component per researched signal.

Once the window length L was fixed, it is possible to compute six principal components by projecting the signal on the six eigenvectors, related to the first six selected eigenvalues. In the figures below from 4.19 to 4.24, non-parametric power spectra of each principal component are reported.

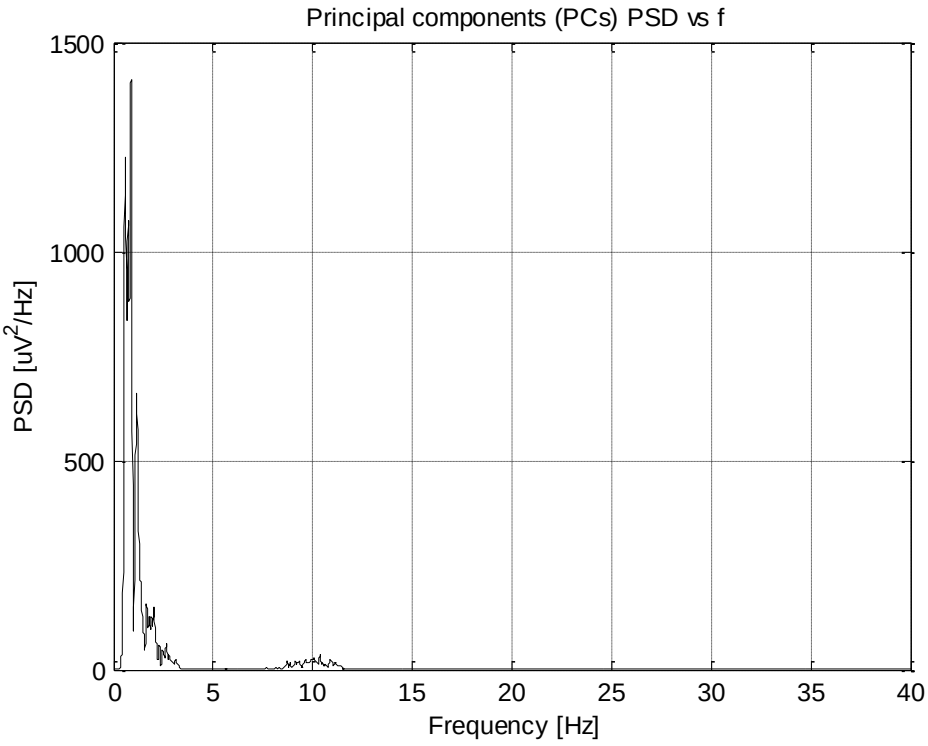

Figure 4.19: PSD of the first principal component of the subject 12 in RT3, parietal area.

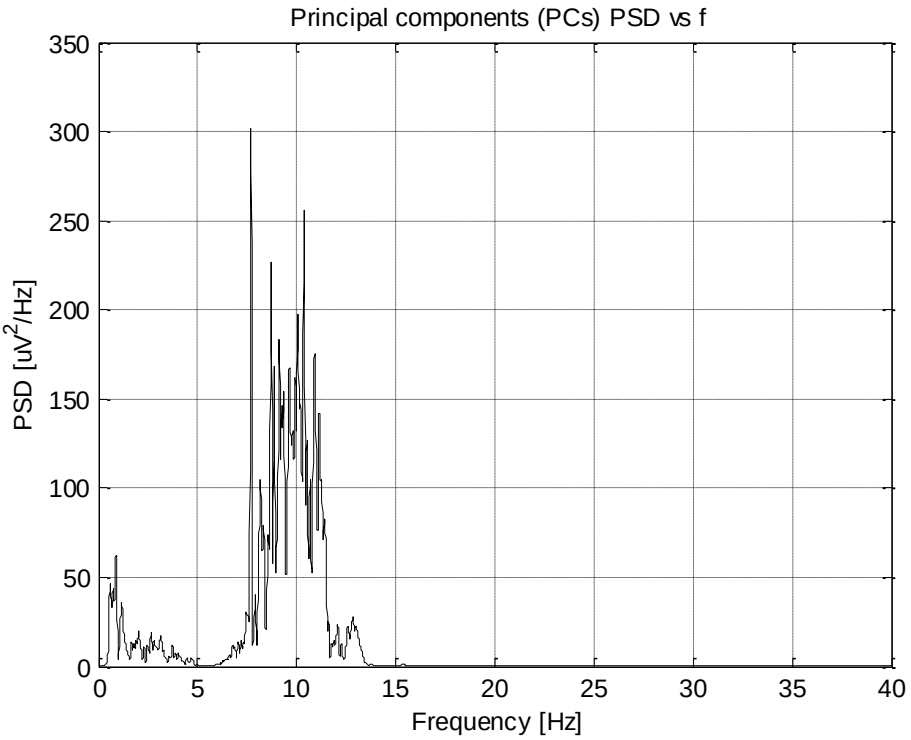

Figure 4.20: PSD of the second principal component of the subject 12 in RT3, parietal area.

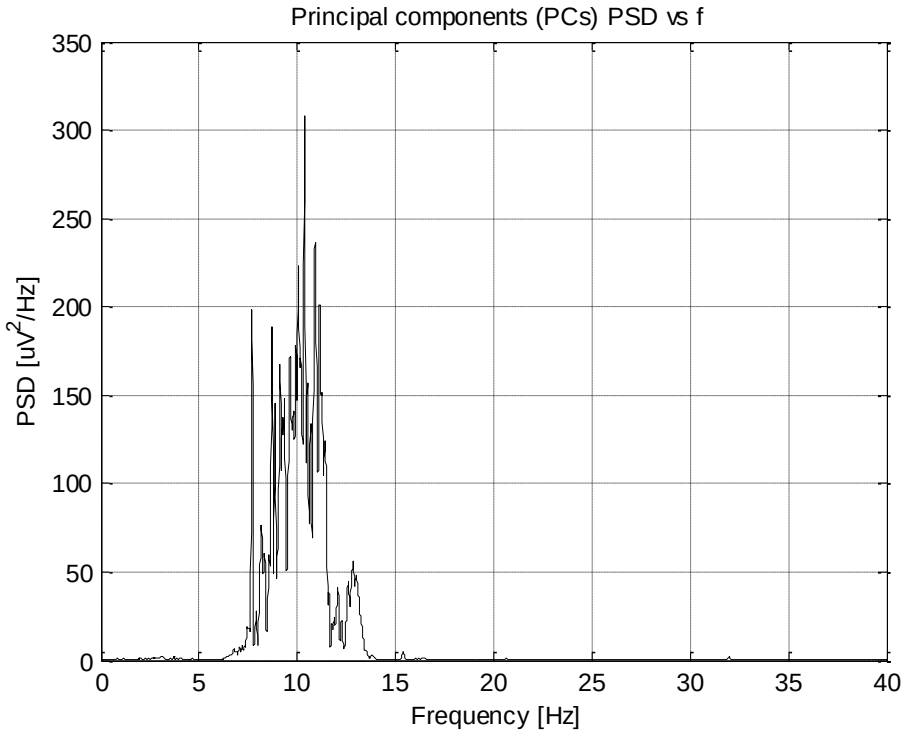

Figure 4.21: PSD of the third principal component of the subject 12 in RT3, parietal area.

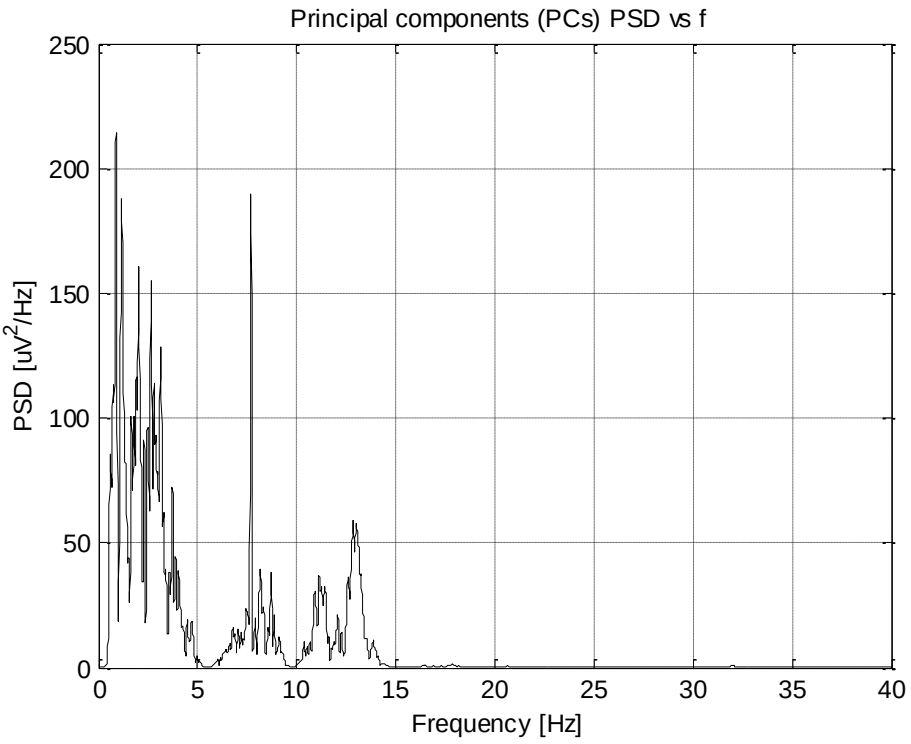

Figure 4.22: PSD of the fourth principal component of the subject 12 in RT3, parietal area.

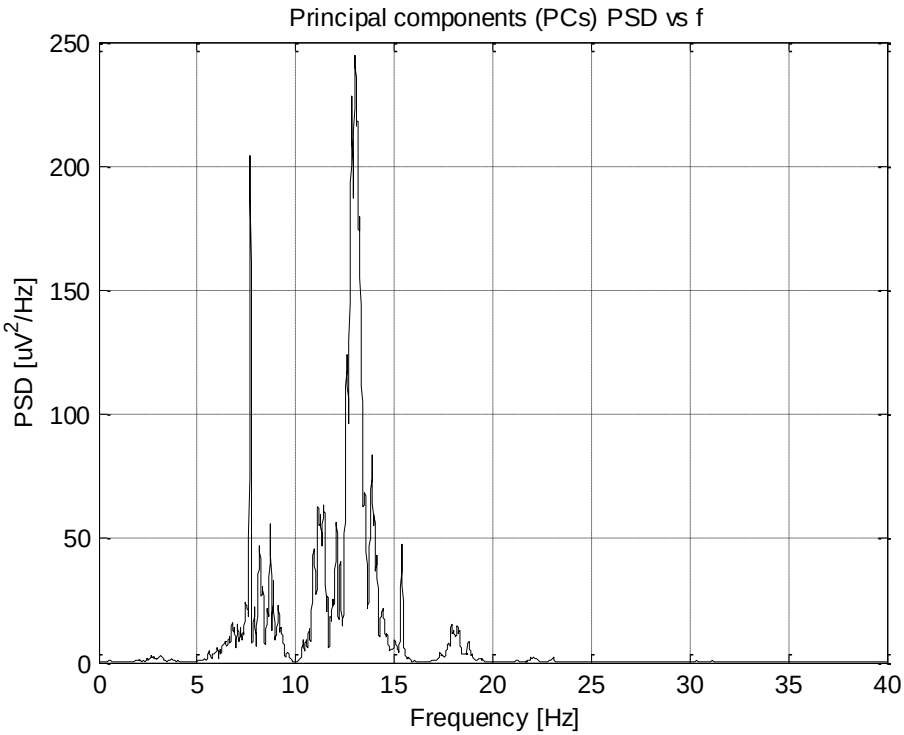

Figure 4.23: PSD of the fifth principal component of the subject 12 in RT3, parietal area.

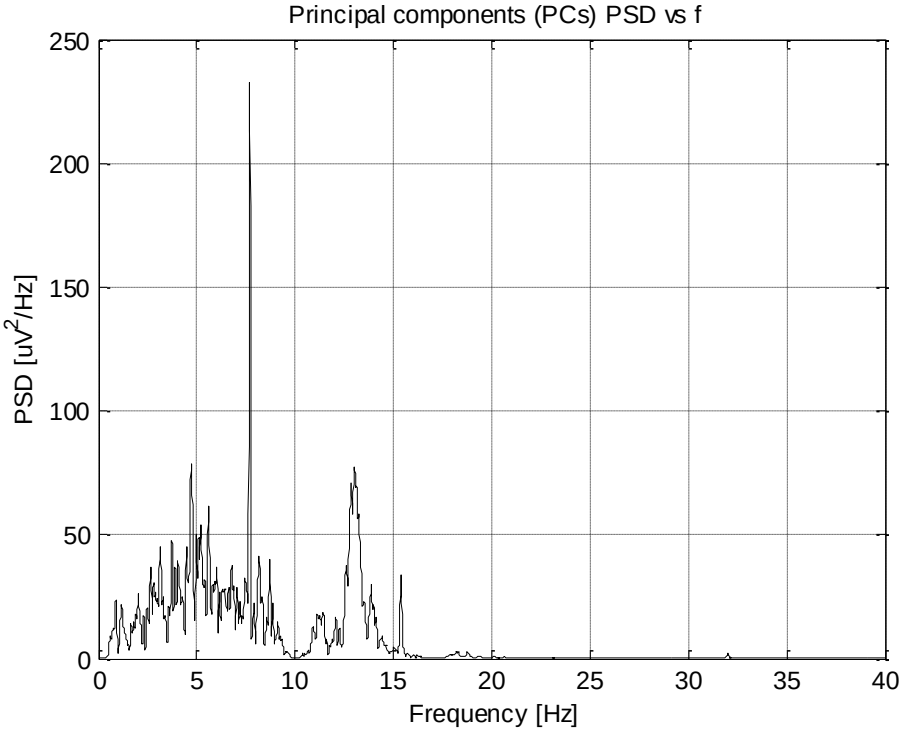

Figure 4.24: PSD of the sixth principal component of the subject 12 in RT3, parietal area.

As explained in the paragraph about the protocol, the third reaction time test was the one when the tester was more tired so it was expected to have a dominant frequency content in theta and alpha bands. From the figures above, it is possible to well-appreciate this fact. Indeed in all the six principal components the most dominant frequencies are in the ranges corresponding to θ and α bands.

Once principal components were computed, it has been possible to reconstruct the signals for the whole range and for each frequency band. Firstly, the relation between the principal components and each frequency band has been investigated. Then, according to these indexes, the signals have been computed and the results are visible in the next Figure 4.25

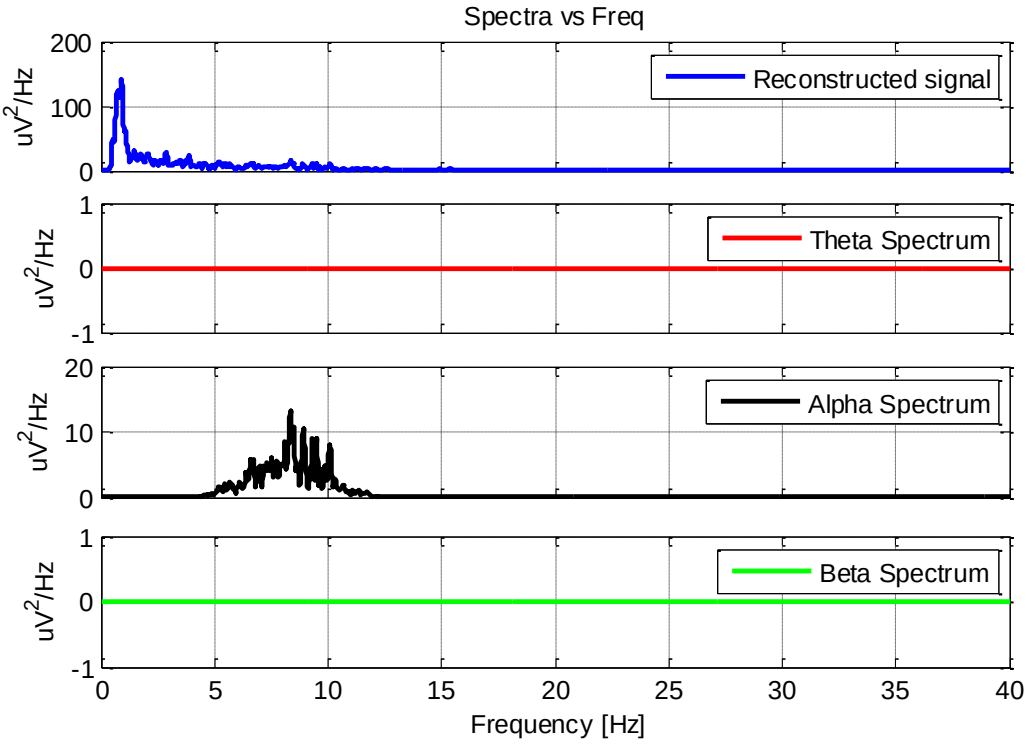

Figure 4.25: power spectral density (PSD) of the whole range and θ, α, β bands signals, subject no. 12 in RT3.

It is easily observable that the signal in beta band is absent: this is exactly what was expected for a really drowsy case.

Also in this case, the same set of features as before has been computed and then tested through a Kruskal-Wallis test. The results from this test are reported below in Table 4.3.

LEGEND

- p-value = 1%
- p-value = 5%
- p-value = 10%
- other
- NaN

Nr.	FEATURES	TRANS vs. ALERT	TRANS vs. DROWSY	ALERT vs. DROWSY	TRANS vs. (ALERT+ DROWSY)	ALERT vs. (TRANS+ DROWSY)	DROWSY vs. (ALERT+ TRANS)
1	PZ_(Pa/Pb)	0.795126	0.259640	0.234764	0.710397	0.971422	0.235236
2	PZ_(Pa+Pt)/Pb	0.035006	0.827259	0.275234	0.064078	0.027891	0.487453
3	PZ_Pt%	0.406684	0.095968	0.037011	0.825791	0.200880	0.053782
4	PZ_transf(Pt%)	0.406897	0.096075	0.037011	0.825919	0.200998	0.053820
5	PZ_Pa%	0.092268	0.765089	0.201798	0.161953	0.066369	0.435837
6	PZ_transf(Pa%)	0.092268	0.765089	0.201560	0.161953	0.066343	0.435647
7	PZ_Pb%	0.345847	0.192103	0.268614	0.267452	0.504269	0.223900
8	PZ_transf(Pb%)	0.345847	0.192103	0.268614	0.267452	0.504269	0.223900
9	PZ_freq_dominant	0.655127	0.003449	0.001036	0.651871	0.215797	0.001356
10	PZ_peak_dominant	0.000002	0.133017	0.241530	0.000003	0.000005	0.788950
11	PZ_freq_dominantTHETA	0.553306	0.823118	0.570441	0.650391	0.499230	0.693480
12	PZ_peak_dominantTHETA	0.001622	0.347763	0.014306	0.012952	0.000569	0.091394
13	PZ_freq_dominantALPHA	0.038425	0.220245	0.997314	0.028175	0.064278	0.492354
14	PZ_peak_dominantALPHA	0.002718	0.756285	0.113782	0.006114	0.002001	0.558441
15	PZ_freq_dominantBETA	0.768280	0.088379	0.030959	0.580157	0.872075	0.045671
16	PZ_peak_dominantBETA	0.774893	0.324015	0.219005	0.907284	0.601545	0.251997
17	FZ_(Pa/Pb)	0.310635	0.884836	0.709815	0.352028	0.301387	0.781511
18	FZ_(Pa+Pt)/Pb	0.807541	0.769698	0.275234	0.769698	0.567709	0.592980
19	FZ_Pt%	0.021312	0.282498	0.026238	0.078161	0.008490	0.095546
20	FZ_transf(Pt%)	0.021312	0.282498	0.026238	0.078161	0.008490	0.095546
21	FZ_Pa%	0.275155	0.807957	0.794912	0.295432	0.293031	0.994067
22	FZ_transf(Pa%)	0.275239	0.807957	0.795988	0.295511	0.293269	0.993527
23	FZ_Pb%	0.552245	0.852644	0.735424	0.573453	0.540627	0.948208
24	FZ_transf(Pb%)	0.548968	0.852644	0.735424	0.570659	0.537878	0.948208
25	FZ_freq_dominant	0.066961	0.040312	0.002742	0.301336	0.015993	0.009827
26	FZ_peak_dominant	0.000000	0.000618	0.000000	0.000009	0.000000	0.000001
27	FZ_freq_dominantTHETA	0.022718	0.007489	0.176596	0.005289	0.084734	0.033345
28	FZ_peak_dominantTHETA	0.019797	0.876925	0.147925	0.040968	0.013707	0.432585
29	FZ_freq_dominantALPHA	0.438955	0.348976	0.636573	0.339917	0.559724	0.457093
30	FZ_peak_dominantALPHA	0.000000	0.444344	0.000734	0.000012	0.000000	0.039606
31	FZ_freq_dominantBETA	0.342672	0.209814	0.103675	0.726714	0.185363	0.129921
32	FZ_peak_dominantBETA	0.127801	0.019025	0.002796	0.657186	0.024598	0.005014
33	CZ_(Pa/Pb)	0.000551	0.801059	0.281466	0.001366	0.000686	0.541542
34	CZ_(Pa+Pt)/Pb	0.368261	0.512691	0.223494	0.522817	0.161429	0.235333
35	CZ_Pt%	0.091412	0.464003	0.093208	0.198228	0.051971	0.224446
36	CZ_transf(Pt%)	0.091342	0.464343	0.093208	0.198058	0.051931	0.224564
37	CZ_Pa%	0.169275	0.989042	0.420527	0.224032	0.150750	0.705162
38	CZ_transf(Pa%)	0.169032	0.989042	0.420913	0.223770	0.150601	0.705400

Nr.	FEATURES	TRANS vs. ALERT	TRANS vs. DROWSY	ALERT vs. DROWSY	TRANS vs. (ALERT+ DROWSY)	ALERT vs. (TRANS+ DROWSY)	DROWSY vs. (ALERT+ TRANS)
39	CZ_Pb%	0.673963	0.093190	0.054829	0.476249	0.943392	0.062521
40	CZ_transf(Pb%)	0.673963	0.093190	0.054829	0.476249	0.943392	0.062521
41	CZ_freq_dominant	0.045469	0.126806	0.010659	0.181844	0.014380	0.037666
42	CZ_peak_dominant	0.000000	0.145712	0.000005	0.000000	0.000000	0.002567
43	CZ_freq_dominantTHETA	0.905983	0.601393	0.532172	0.962502	0.790842	0.554588
44	CZ_peak_dominantTHETA	0.015707	0.632802	0.442302	0.022303	0.018035	0.916951
45	CZ_freq_dominantALPHA	0.004159	0.142899	0.935532	0.003002	0.009919	0.434566
46	CZ_peak_dominantALPHA	0.000087	0.982650	0.016889	0.000529	0.000037	0.257280
47	CZ_freq_dominantBETA	0.282354	0.505844	0.374841	0.376895	0.225891	0.417332
48	CZ_peak_dominantBETA	0.059181	0.703866	0.675573	0.065223	0.064011	0.943325
49	C3_(Pa/Pb)	0.235842	0.165684	0.102470	0.390231	0.187003	0.135017
50	C3_(Pa+Pt)/Pb	0.709131	0.105193	0.126630	0.412770	0.915792	0.097918
51	C3_Pt%	0.602148	0.416866	0.301761	0.830845	0.456521	0.340006
52	C3_transf(Pt%)	0.602148	0.416866	0.301761	0.830845	0.456521	0.340006
53	C3_Pa%	0.556946	0.196848	0.538143	0.367904	0.708671	0.308862
54	C3_transf(Pa%)	0.556946	0.196848	0.538773	0.367904	0.708493	0.309078
55	C3_Pb%	0.271973	0.001763	0.008891	0.065362	0.696949	0.002811
56	C3_transf(Pb%)	0.271974	0.001763	0.009087	0.065362	0.695658	0.002843
57	C3_freq_dominant	0.053850	0.013240	0.000616	0.319612	0.009192	0.002483
58	C3_peak_dominant	0.000000	0.018441	0.000000	0.000002	0.000000	0.000080
59	C3_freq_dominantTHETA	0.286990	0.107718	0.036195	0.648543	0.128959	0.056294
60	C3_peak_dominantTHETA	0.000712	0.002353	0.000001	0.039619	0.000015	0.000046
61	C3_freq_dominantALPHA	0.162075	0.709398	0.242311	0.257470	0.120922	0.444453
62	C3_peak_dominantALPHA	0.008514	0.279758	0.566866	0.007957	0.012080	0.737303
63	C3_freq_dominantBETA	0.000073	0.485969	0.461943	0.000161	0.000149	0.968859
64	C3_peak_dominantBETA	0.000202	0.158180	0.994053	0.000183	0.000700	0.429324
65	C4_(Pa/Pb)	0.003616	0.198033	0.607066	0.002621	0.007878	0.342940
66	C4_(Pa+Pt)/Pb	1.000.000	0.310635	0.354539	0.855858	0.836996	0.317311
67	C4_Pt%	0.741392	0.932043	0.891304	0.751994	0.741587	0.986120
68	C4_transf(Pt%)	0.741699	0.932043	0.890761	0.752265	0.741724	0.985858
69	C4_Pa%	0.602300	0.450547	0.300895	0.809754	0.463858	0.358866
70	C4_transf(Pa%)	0.602450	0.450547	0.300895	0.809902	0.463976	0.358866
71	C4_Pb%	0.723720	0.044609	0.034532	0.906366	0.430096	0.034465
72	C4_transf(Pb%)	0.722631	0.044610	0.034532	0.907437	0.429306	0.034465
73	C4_freq_dominant	0.082175	0.056430	0.006893	0.321338	0.024443	0.018219
74	C4_peak_dominant	0.000000	0.989298	0.001344	0.000000	0.000000	0.120049
75	C4_freq_dominantTHETA	0.061246	0.125648	0.567203	0.034753	0.129706	0.257422
76	C4_peak_dominantTHETA	0.000004	0.656273	0.001075	0.000089	0.000001	0.069800
77	C4_freq_dominantALPHA	0.312066	0.316279	0.664793	0.233882	0.426500	0.443641
78	C4_peak_dominantALPHA	0.001195	0.645358	0.024611	0.006179	0.000499	0.181111
79	C4_freq_dominantBETA	0.110554	0.297724	0.601143	0.086457	0.170450	0.420549
80	C4_peak_dominantBETA	0.090960	0.157977	0.433422	0.059473	0.160882	0.258526

Table 4.3: results from Kruskal-Wallis test for all the 80 features from SSA; the legend upon the table explains what the meaning of the colored features is .

From the table above, it could be seen that just three features resulted to have a p-value≤5% and, as for the other two methods, this p-value has been chosen as threshold to select features. The selected features are:

1. dominant peak in the whole range ("Fz_peak_dominant"), from frontal area (Fz channel)
2. dominant peak in the whole range ("C3_peak_dominant"), from left central area (C3 channel)
3. dominant peak in θ band ("C3_peak_dominantTHETA"), from left central area (C3 channel)

Then, exactly as already done for the previous two approaches, boxplots of the selected features (see figures below) have been considered in order to visualize their statistical properties.

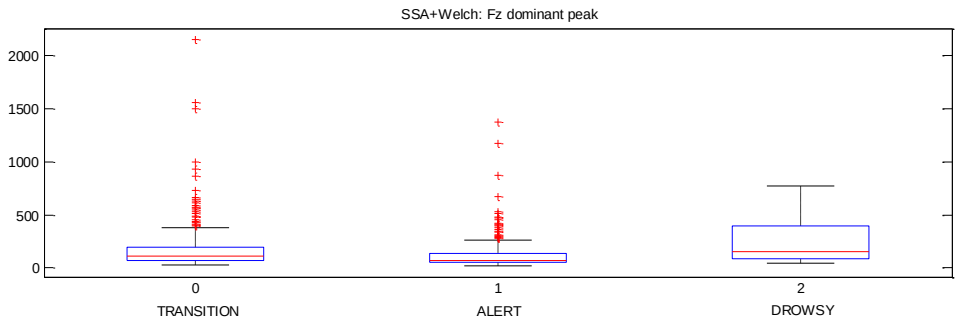

Figure 4.26: dominant peak in the whole range, frontal area. The three classes are well distinguished; drowsy class presents a major variance than the other two ones.

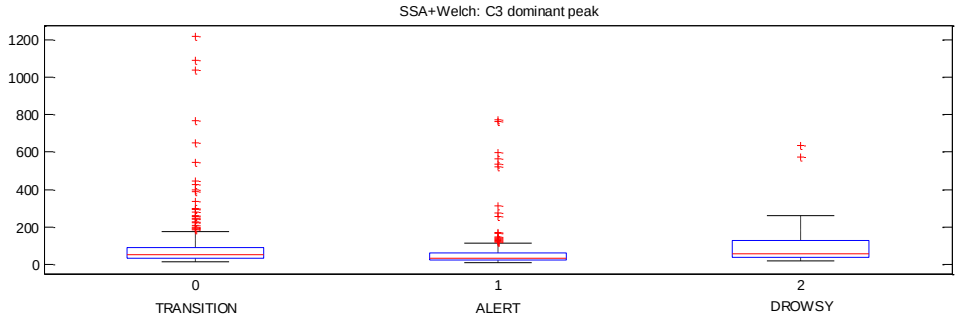

Figure 4.27: dominant peak in the whole range, left central area. The three classes result to be correctly separated one from each other.

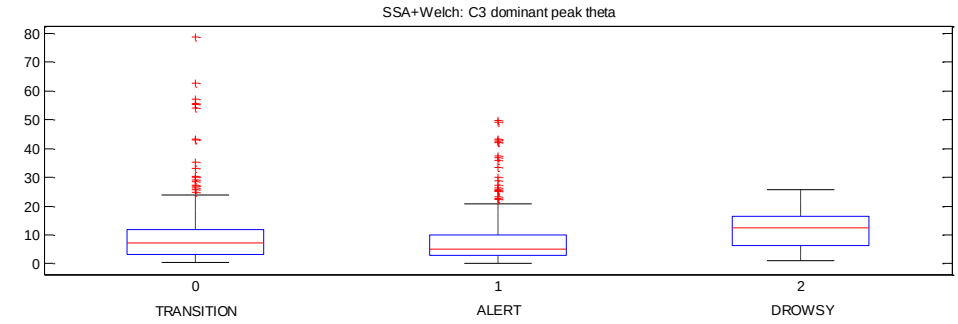

Figure 4.28: dominant peak in θ band, left central area. Drowsy class is better discriminated from alert class and transition class; the separation between transition and alert class is instead less strong.

Since three features resulted to be significant, the input layer and the hidden layer were composed of three neurons and the output layer always consisted of three neurons as well, one per class of interest. The outputs of the neural network have been used to compute the confusion matrix used for the k-Cohen coefficients.

As already said for the parametric case, the fact that only three features presented a good p-value could be a problem to make the classifier to correctly learn.

4.2 Results from methods comparison

As regards the non-parametric method, 11 features resulted to be good and they have been given in input to the classifier.

Starting from the outputs of the neural network, a confusion matrix has been computed as reported in the previous chapter. It contains the correct classification rate on the main diagonal and the misclassification rate outside the main diagonal. The confusion matrix is then employed to compute k-Cohen coefficients. All the 50 values are reported in the

graphic below (Figure 4.29) with a mean value of 0.5087 and a standard deviation of 0.0194.

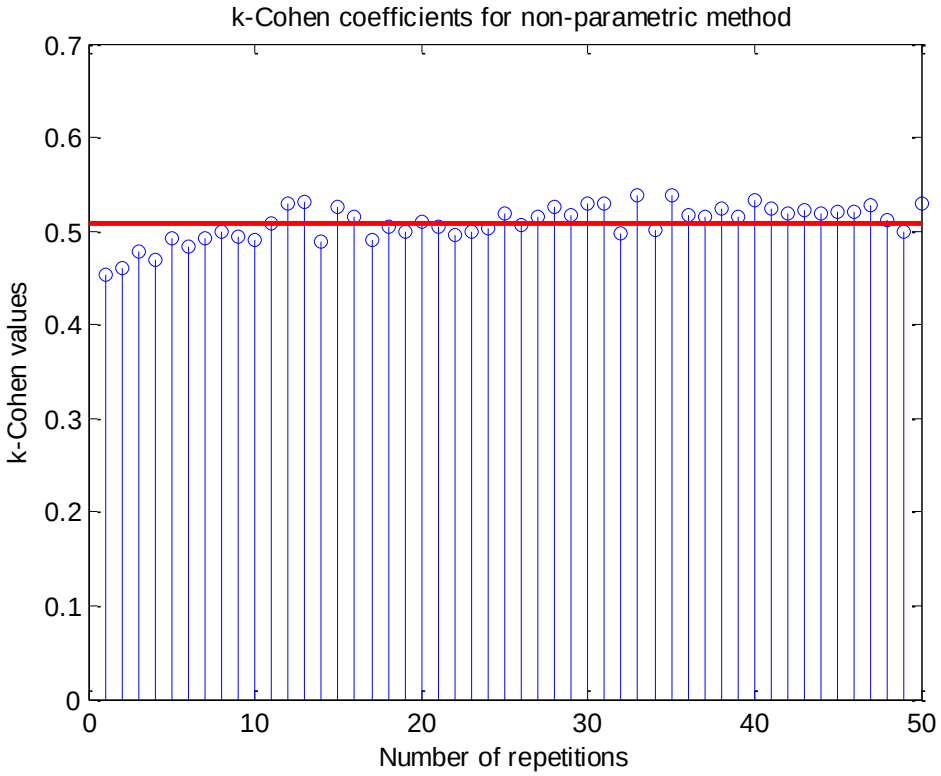

Figure 4.29: plot of the 50 k-coefficients for non-parametric method; they were derived from a 5-fold cross-validation repeated 10 times in order to moderate the effect of the random division of the dataset in training set and testing set, and the division in subsets.

As regards AR method, only four features resulted to be appropriate to correctly discriminate among the three classes so they have been used to construct the neural network. Also in this case, starting from the outputs of the classifier, a confusion matrix has been created and employed to compute k-Cohen coefficients.

The 50 values of the k-Cohen coefficients, the mean value of 0.2227 (Figure 4.30) and a standard deviation of 0.0053 have been computed.

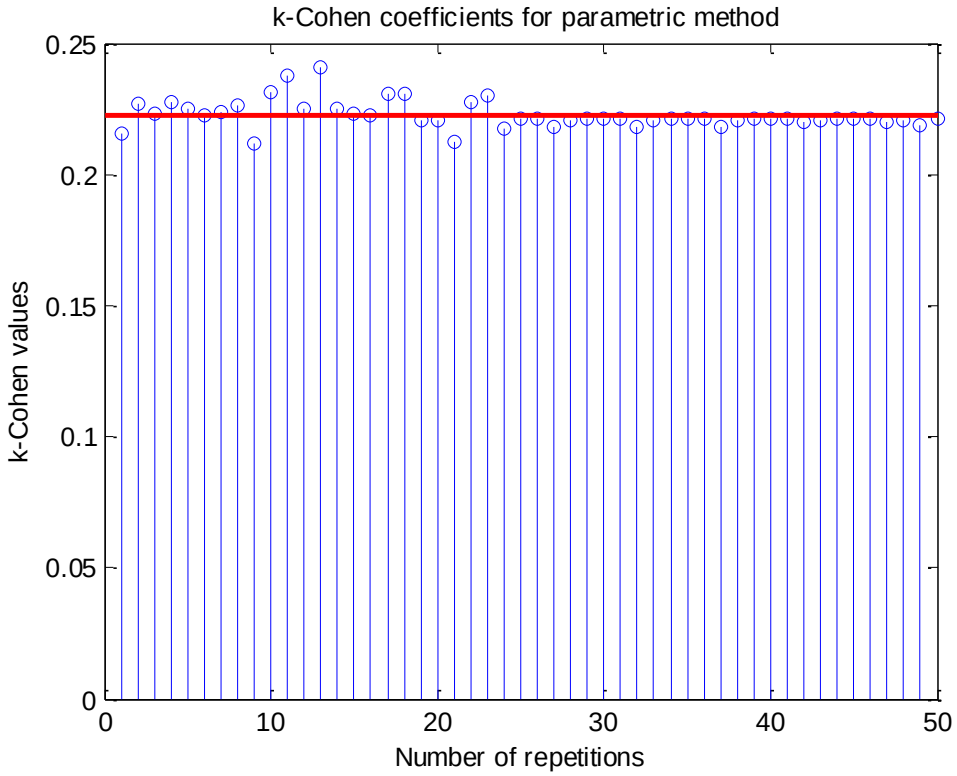

Figure 4.30: plot of the 50 k-coefficients related to AR method; they were derived from a 5-fold cross-validation repeated 10 times in order to moderate the effect of the random division of the dataset in training set and testing set, and the division in subsets.

Finally, for SSA, only three features came up as statistically significant for a correct separation among classes. They have been used as inputs for the neural network, composed this time, of three neurons in the input and hidden layer, as wide as the number of features in input. The outputs of such classifier have been exploited to compute the confusion matrix for k-Cohen coefficients.

50 values of k-Cohen coefficients have been computed also in this case and a mean value of 0.1659 and a standard deviation of 0.0027 resulted. They are shown in the Figure below.

Figure 4.31: plot of the 50 k-coefficients related to SSA method; they were derived from a 5-fold cross-validation repeated 10 times in order to moderate the effect of the random division of the dataset in training set and testing set, and the division in subsets.

k-Cohen is a parameter used to evaluate if and how much a certain classification has been accurate: if $k = 1$, the statistics has been optimal because $-1 \leq k \leq +1$ and generally the following range of k-Cohen values are considered:

- if k is smaller than 0, there is no agreement
- if k belongs to the range [0, 0.4], there is a weak concordance
- if k is in the range [0.4, 0.6], the accordance is reasonable
- if k assumes values in the range [0.6, 0.8], the agreement is good
- if k takes values in the range [0.8, 1], the statistics is optimal.

As it is observable in the graphic in Figure 4.12, k-Cohen for non-parametric method resulted to be in the range [0.4, 0.6] so it is possible to state that this is a statistically consistent method of extracting features and it well-discriminates among the three considered classes. It is not possible to conclude the same for the other two methods: using the features that resulted significant from Kruskal-Wallis test and statistical boxplots, the

number of features is really less than the number of selected features for the first method and this is certainly a factor to take into account because maybe the classifier could not learn enough with just three or four parameters.
In conclusion, from the comparison among methods, it is possible to state that the features, emerged as good and significant from the statistical analysis, have allowed the classifier to correctly classify the classes of interest and non-parametric method has presented consequently the best performance.
Standing on the results obtained until this point, just non-parametric method has been considered for the next step: the validation of the protocol, that will be more detailed in the next paragraph.

4.3 Results from protocol validation

The protocol, more detailed in chapter 3 at paragraph 3.1, aims to detect changes in reaction times and in related EEG signals, passing through a first test when a subject should be normally well-awake, a second test when the participant is more or less awake and finally in the third test the volunteer should be drowsy, after a sleep deprivation night.
According to this goal, labels were assigned to each minute of test in order to detect variations in the signals, by using reaction time data.
In this section, an examination has been performed in order to verify if the protocol, so as it is set for this work, results to be really respected in the reality by the response of the participants.
In addition, once a method has been selected, it has been possible to consider the performance of the selected features, subject per subject, and so to verify the correspondence between what the features suggest and what the labels indicate, so as they have been set. Practically, in this last part, a physiological correlation among signals, more precisely features of signals, and labels that should estimate the state of alertness/drowsiness of each volunteer, test by test , have been also investigated.
Through such analysis, subject per subject and test per test, it resulted that just a few people have mirrored the idea of the protocol, that is a noticeable difference in terms of alertness/transition/drowsiness among the three performed reaction time tests.
So for the analysis that will follow, only the results from the three best subjects will be reported. In particular, an additional reason has been considered: in these three following

cases, a considerable numbers of drowsy epochs is present so it is possible to run a complete evaluation for all the three targets.

Subject nr. 2:

It is possible to appreciate that the distribution of alert, transition and drowsy epochs mirrors well the idea of the protocol.

The first reaction time test was performed when the subject was normally awake and in fact in the first frame, delimitated by 0 and the first red vertical line, there are enough labels for alert or transition; it is visible that as the person gets used to the test, the transition epochs decrease.

The second section between the first and the second red vertical line is dominated by "transition" labels, exactly as it is planned for the second reaction time test, with an exception for the first minutes of test: the subject has passed a sleepless night and in the early morning he/she has been running this test.

The third test occurred after a sleep deprivation night and the subject has just had breakfast: here the most of drowsy labels is concentrated and, as it is expected, at the beginning some transition epochs appear.

In the following figures, all the eleven selected features are reported in comparison with the labeling placed on the top of each image; they have been appropriately distributed in several graphics just for a better visualization.

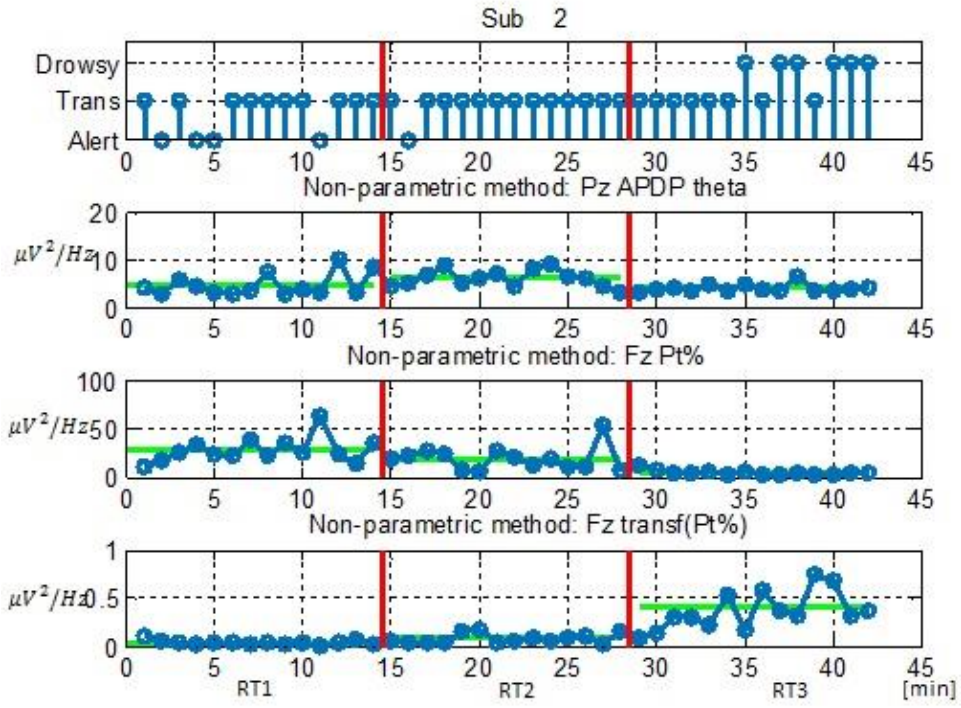

Figure 4.32: starting from the top there are labels per minutes of test, dominant peak in θ band from parietal area, percentage power in θ band and a transformed version of percentage power in θ band.

The most interesting feature among these three ones in the figure above is the last one. Indeed as drowsiness increases, the transformed version of percentage power in θ band increases as well and in addition one can observe a clear difference in the amplitude among the three reaction time tests. Therefore, the last feature is more coherent with the expectations than the simple percentage power.

As regards the first feature in the parietal area, dominant peak in θ band, at the third test, is instead slightly minor than in the previous tests; the interesting thing is that there is a remarkable difference among the various sections, in this case as well.

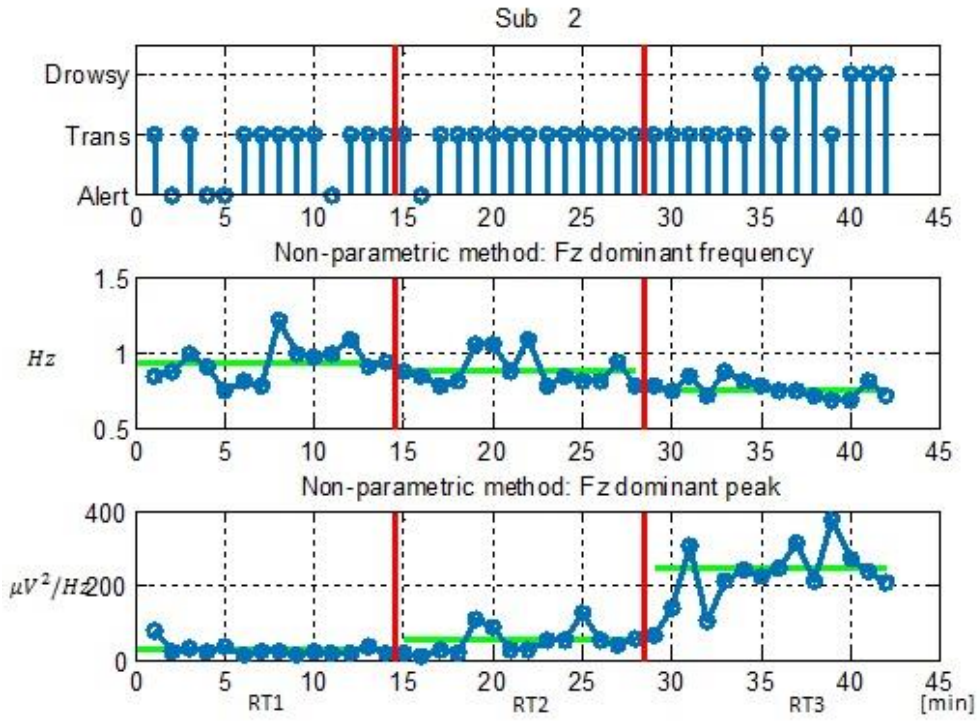

Figure 4.33: starting from the top there are labels per minutes of test, dominant frequency in the whole range from frontal area, dominant peak in the whole range from frontal area.

The features in figure 4.33 perfectly mirror the expectations: a diminution of the dominant frequency in the whole range as drowsiness occurred and a general decreasing trend from the first test to the last one.

A good performance is noticeable for dominant peak as well: a general variation throughout the three tests can be seen.

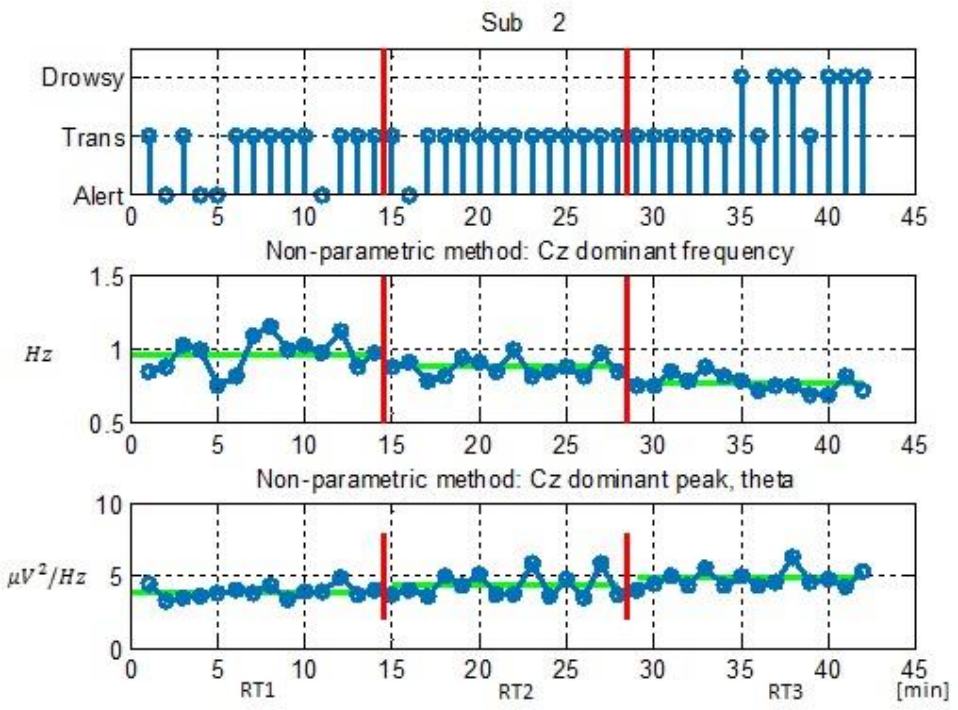

Figure 4.34: starting from the top there are labels per minutes of test, dominant frequency in the whole range from central area, dominant peak in θ band from central area.

The first feature appearing in the figure correctly suits the expectations, dominant frequency is assumed to decrease as drowsiness occurs. In addition, it is possible to detect differences as passing from a test to another.

A slight increase in dominant peak of that band is remarkable in the graphic at the bottom: it is coherent with the meaning of theta band that is generally related to falling asleep so it is normal to detect a little increase of theta dominant peak at the end of the last test.

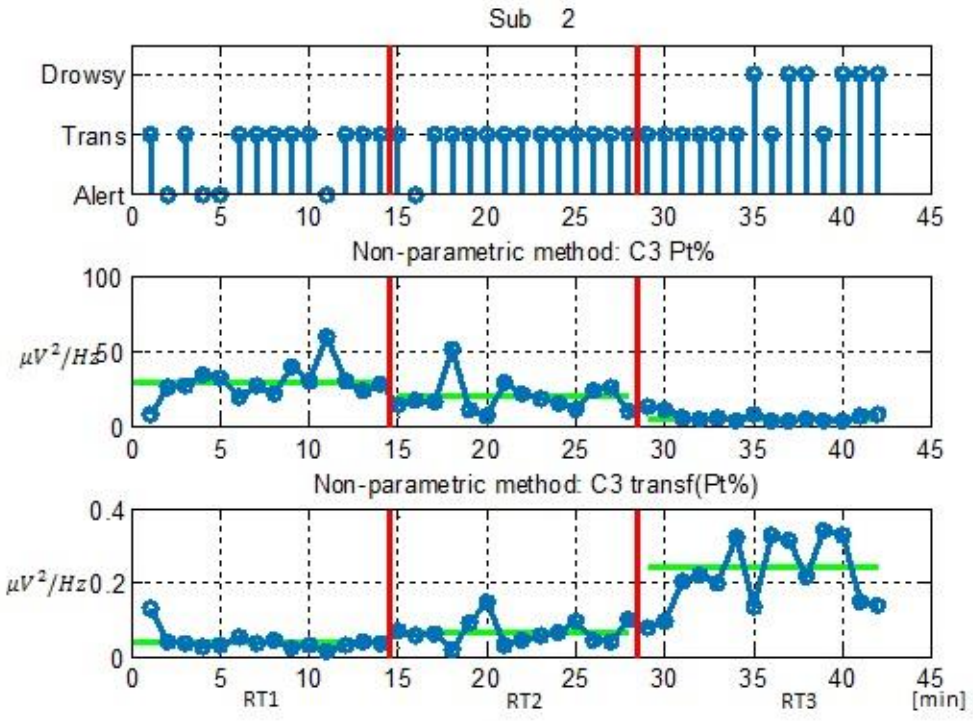

Figure 4.35: starting from the top, there are labels per minutes of test, percentage power in θ band and a transformed version of the percentage power in θ band from left central region.

Once again, comparing the performance of percentage power and a transformed version of it, this last one results to be coherent with expectations: it increases with drowsiness. In both cases, a remarkable difference in the trend can be seen.

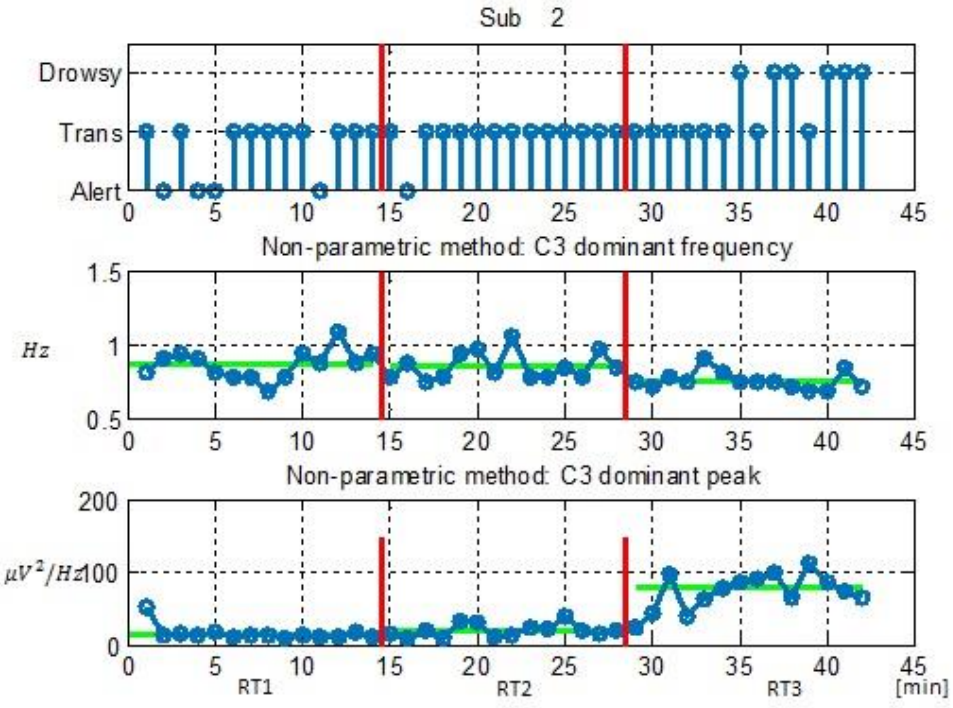

Figure 4.36: starting from the top, there are labels per minutes of test, dominant frequency and dominant peak in the whole range from left central area.

Especially from the mean value, it is clearly visible that dominant frequency decreases from the first test to the last one while dominant peak increases. This fact perfectly confirm what it is believed.

Subject nr. 12:

As regards this subject, the distribution of the epochs results particularly coherent with the protocol for the second and the third reaction time test; in the first one, in fact, the presence of alert cases is less than transition epochs.

Besides, it is interesting to observe that this volunteer results a little drowsy even at the end of the first reaction time test therefore he(she) is maybe particularly drowsy him(her)self.

This observation is confirmed if one looks at the concentration of drowsy labels in the last section that is greater than the previous subject, for example.

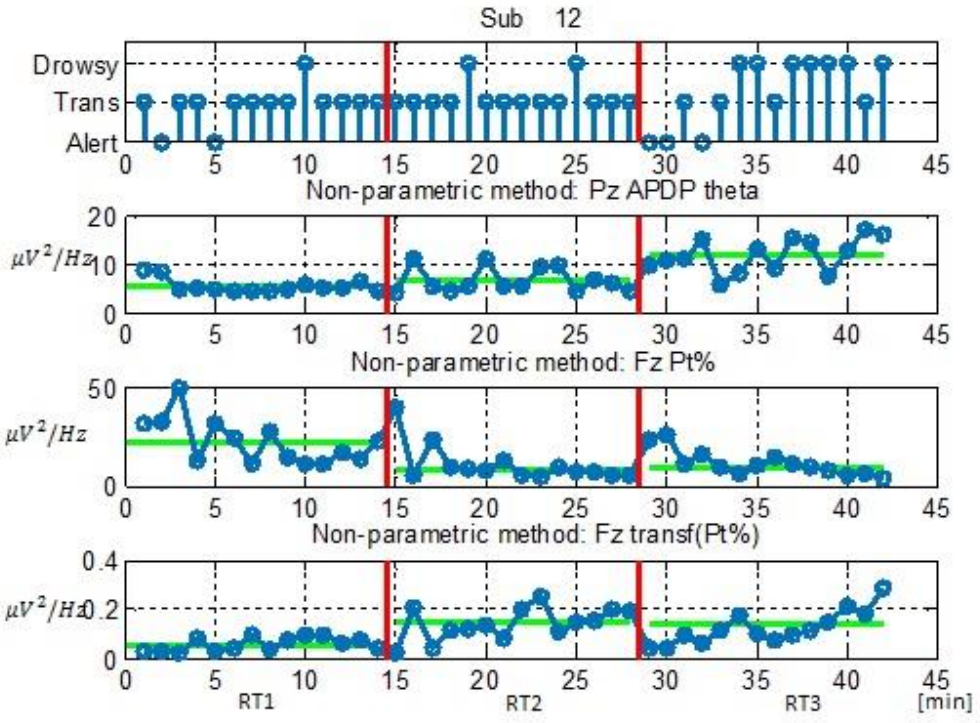

Figure 4.37: : starting from the top, there are labels per minutes of test, dominant peak in θ band from parietal area, percentage power in θ band and the transformed version of percentage power in the band from frontal area.

Here dominant peak in theta band correctly presents the same trend as usual: an increment as drowsiness occurred.

Besides, exactly as emerged from the last two features in the previous figures of the other participant, the third feature is more coherent with expectation than the simple percentage power.

In this case, however, there is no particular distinction in the trend of the two last reaction time tests but the difference is noticeable with the first one.

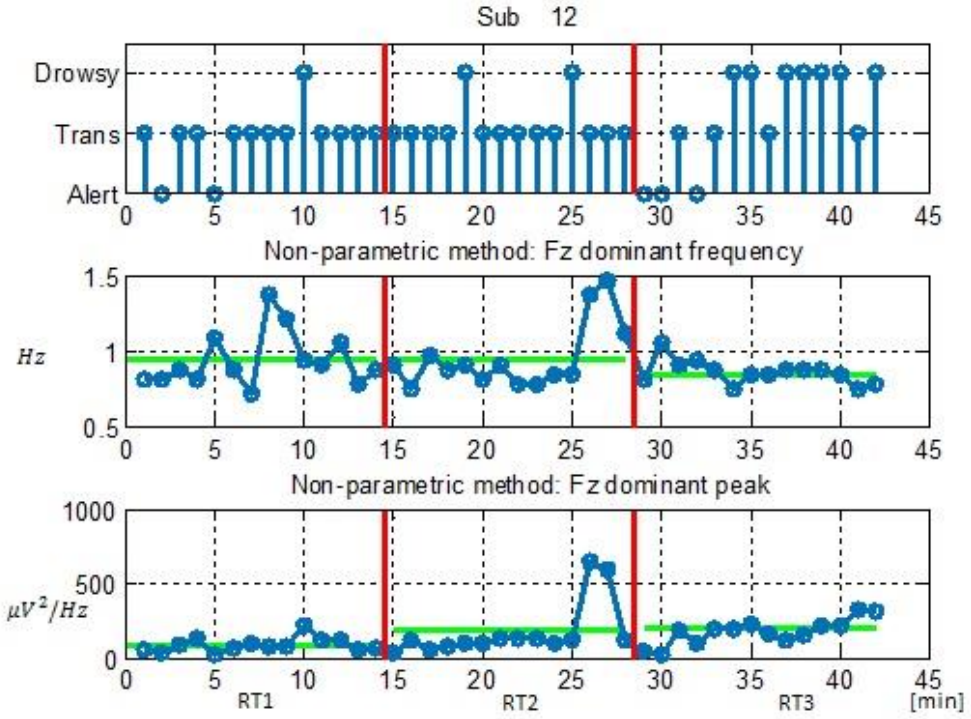

Figure 4.38: starting from the top, there are labels per minutes of test, dominant frequency and dominant peak in the whole range from frontal area.

Observing in particular the mean value, it is possible to detect a decrease of dominant frequency in correspondence of the last test, especially when labels indicate drowsy epochs. The trend for the first two tests is almost similar. This fact is interesting if one combines these trends with what emerged from the previous two features: these last ones showed a similarity between the second and the third test and the features in Figure 4.38 a similarity between the last two tests. Combining all the information, a classifier can detect all the shades contained in a signal.

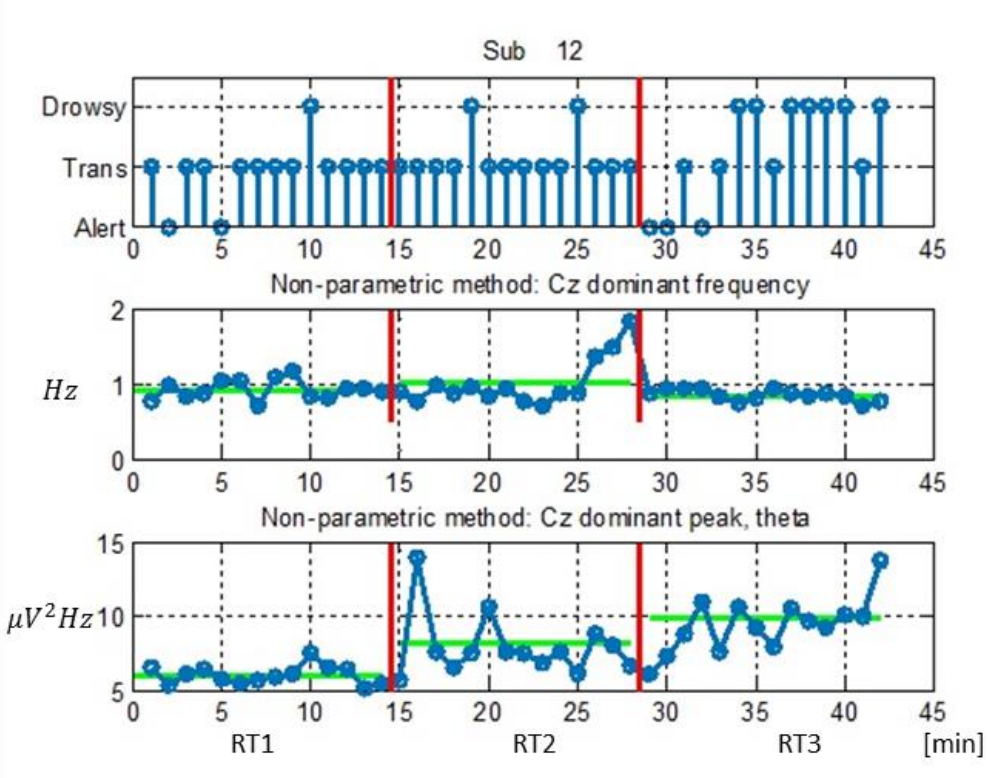

Figure 4.39: starting from the top, there are labels per minutes of test, dominant frequency in the whole range and dominant peak in θ band, both from central area.

In this case a slight increase of dominant frequency in the middle section is visible, especially observing the mean value. This fact is a little bizarre but it is easily explained by observing that there is a peak at the end of the second test that influences that value. Generally a decreasing trend of the dominant frequency is observable here as well. Dominant peak in theta band is still perfectly suitable with expectations.

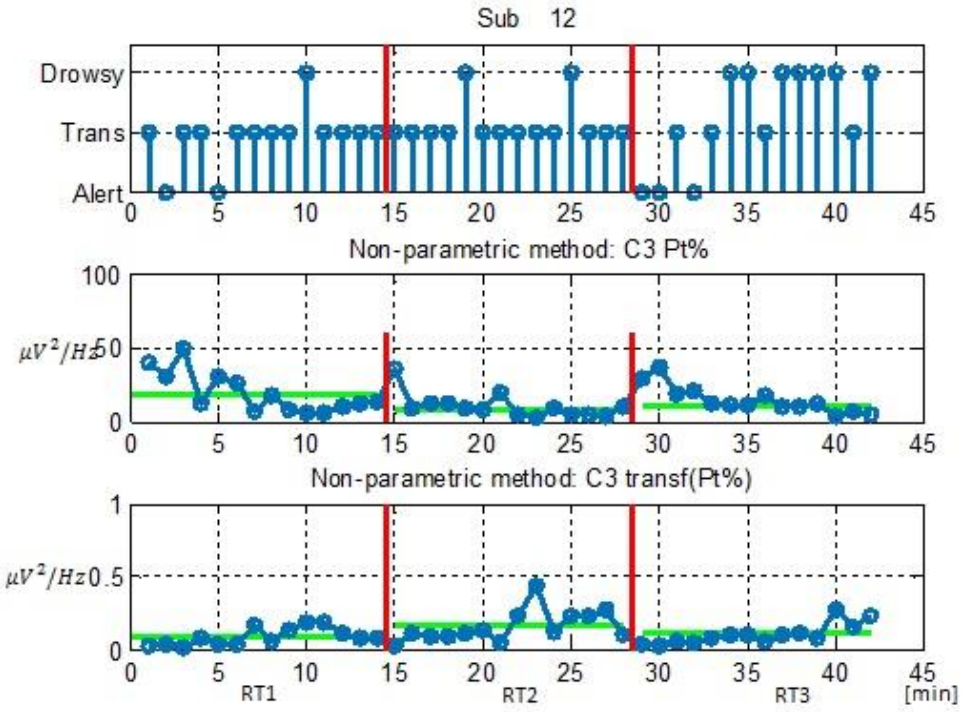

Figure 4.40: starting from the top, there are labels per minutes of test, percentage power in θ band and its transformed version from left central area.

Nothing is remarkable for these two features. Indeed, unlike the other cases where they appeared, here they present a trend that is not interesting.

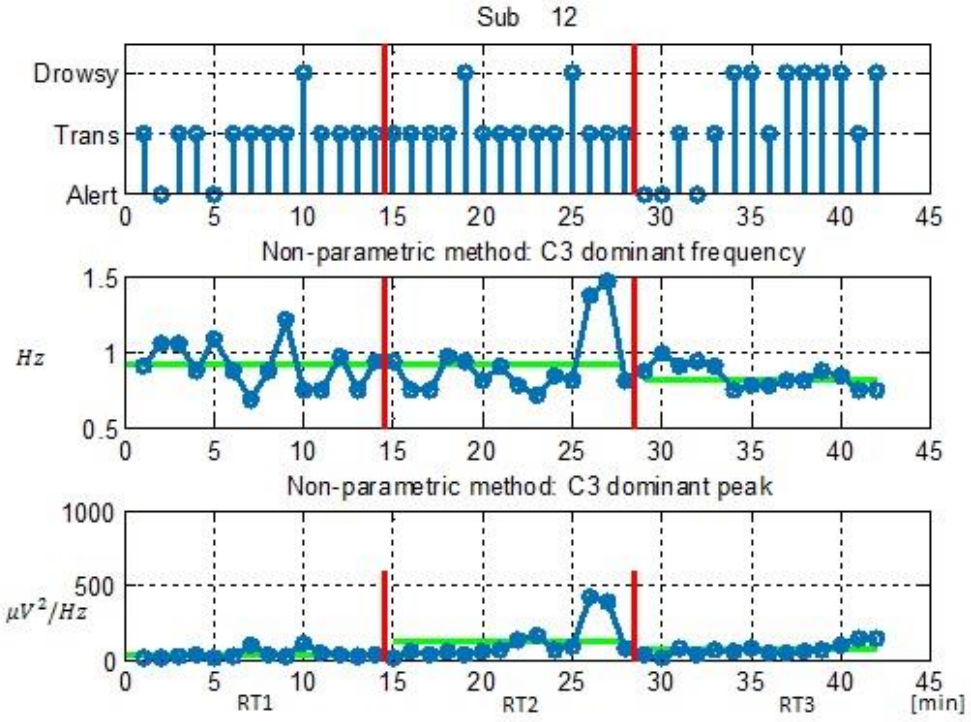

Figure 4.41: starting from the top, there are labels per minutes of test, dominant frequency and dominant peak in the whole range from left central area.

No particular differences between the first two reaction time tests are present, as regard dominant frequency; instead it decreases, coherently, as drowsiness occurs in the third test. Dominant peak shows a strange increment just in the middle section.

Subject nr. 14:

This participant resulted to be the one who perfectly adhered to the protocol: all the minutes in the first test are signed as alert, all drowsy epochs are present in the last test and in the second test a mix of all the three possible states (alert, transition, drowsy) appears, in particular it is interesting to observe transition epochs towards the end of the second test and just one drowsy epoch at the beginning as if the subject had to get used to the test.

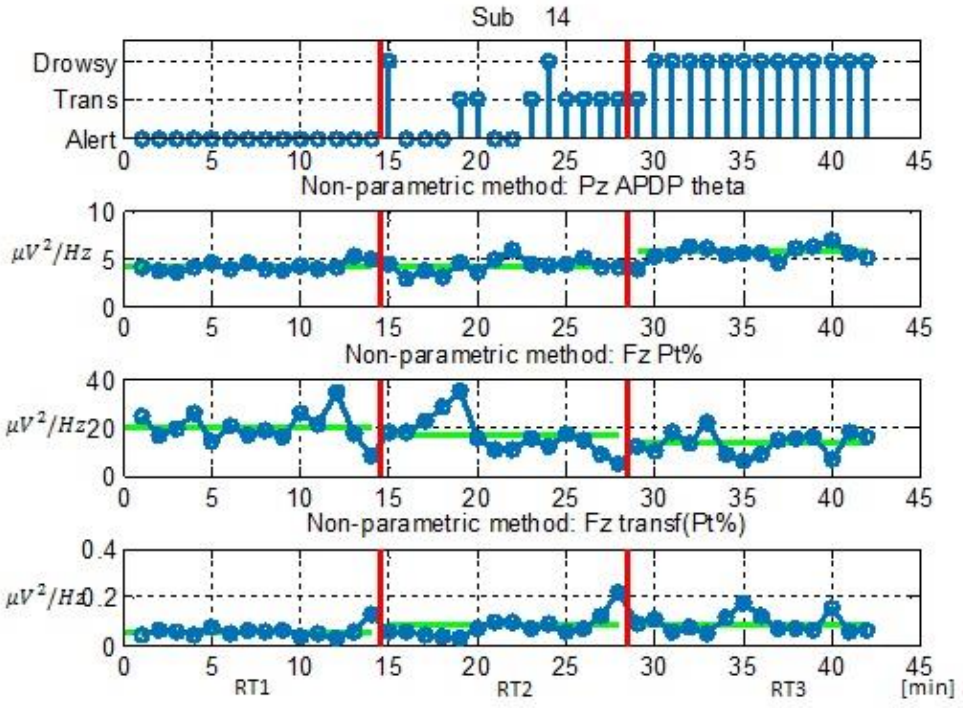

Figure 4.42: starting from the top, there are labels per minutes of test, dominant peak in θ band from parietal area, percentage power in θ band and its transformed version, from frontal area.

Again for this subject, the feature $\log\left(\frac{P_i\%}{1-P_i\%}\right)$ results to be very coherent with expectations when drowsiness occurred.

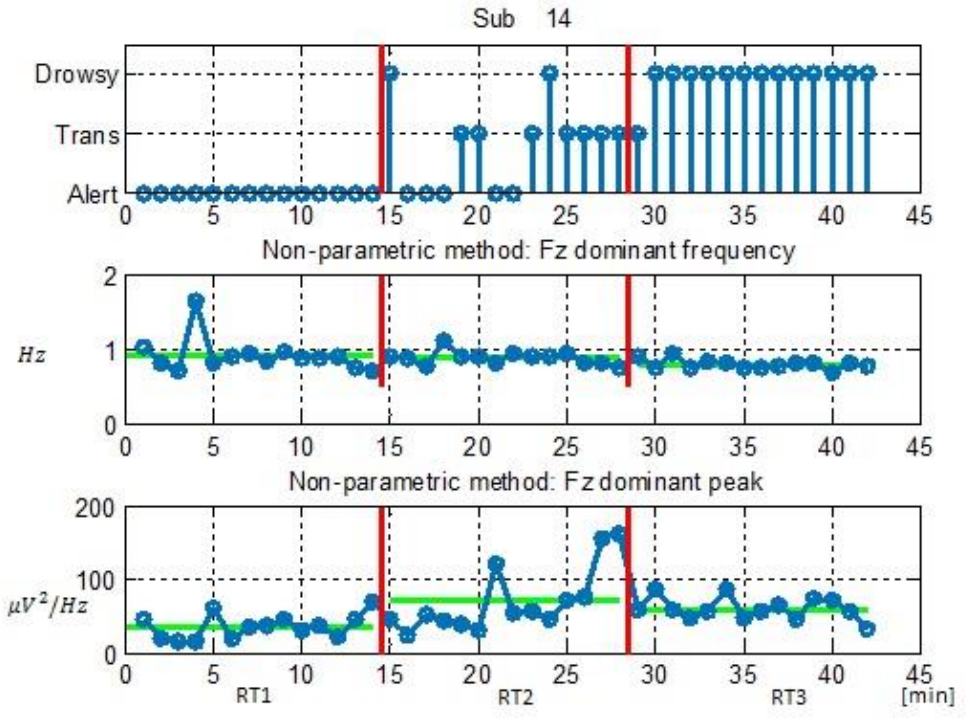

Figure 4.43: starting from the top, there are labels per minutes of test, dominant frequency and dominant peak of the whole range, from the frontal area.

In this figure, the dominant frequency slightly decreases, confirming what was assumed about its meaning, and the dominant peak increases with a not so remarkable difference between the second and the last test. This fact is however justified because, this time, in the second test, there is a mix of states of alertness, according to the labels.

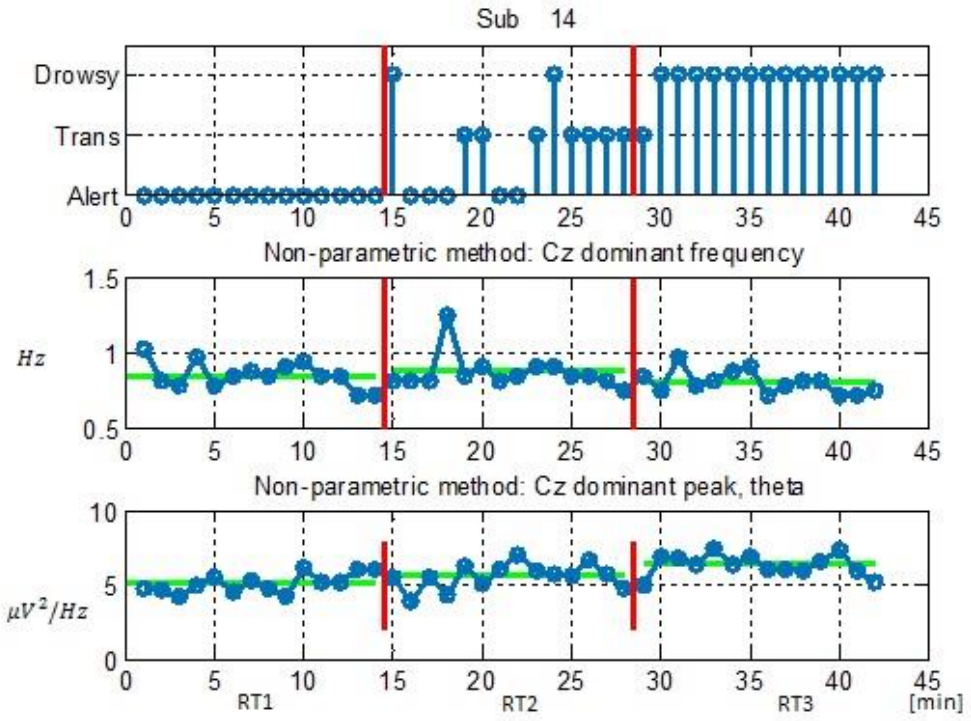

Figure 4.44: starting from the top, there are labels per minutes of test, dominant frequency in the whole range and dominant peak in θ band, from central area.

The trend of a diminution of the dominant frequency in the third test is clearly visible as well as an increment of dominant peak for theta band is still observable in these graphics above. They perfectly mirror what expected for drowsiness and confirm what emerged before, for other subjects.

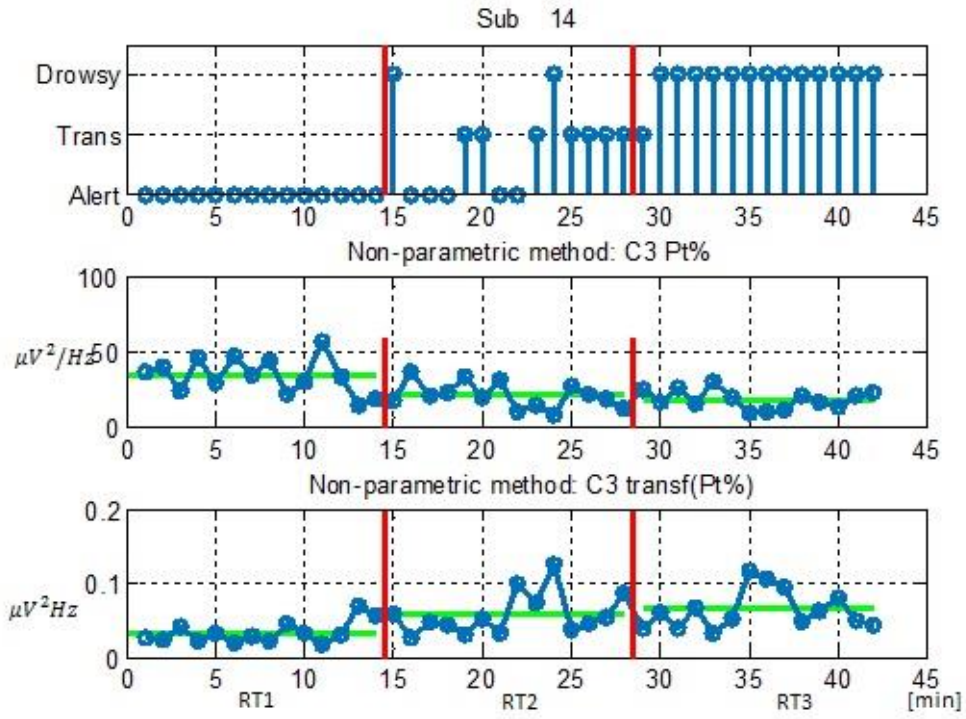

Figure 4.45: starting from the top, there are labels per minutes of test, percentage power and a transformed version of it in θ band, from left central area.

Once again, the second feature results to be more coherent with expectations than the simple percentage power. Indeed, one can observe a slight increment in the third test and generally an increasing trend throughout the three tests, from the first one to the last one.

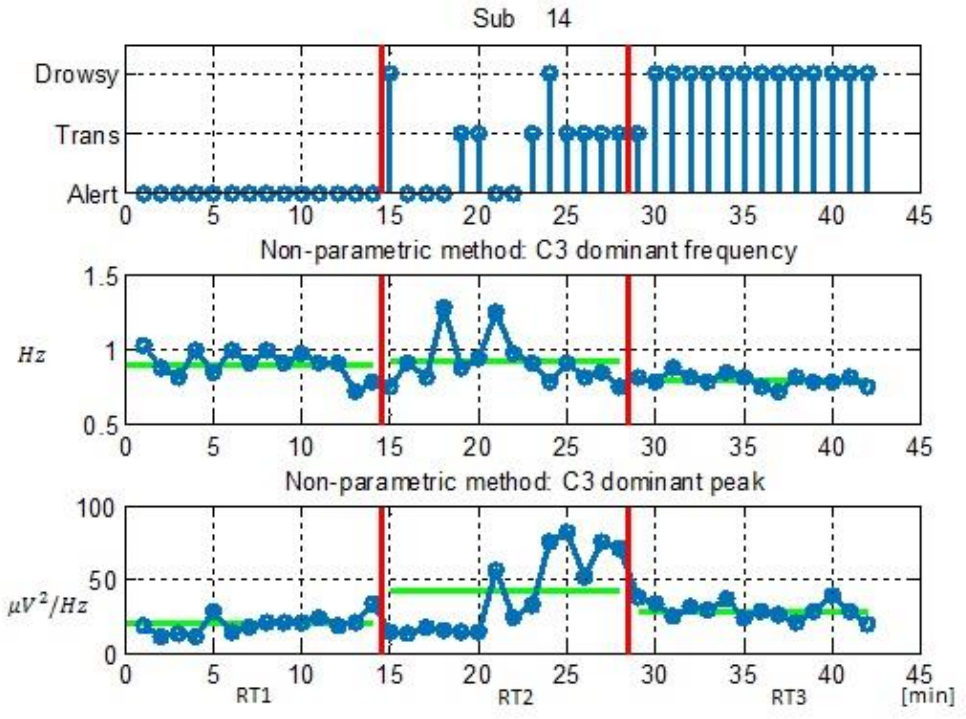

Figure 4.46: starting from the top, there are labels per minutes of test, dominant frequency and dominant peak in the whole range from left central area.

Finally, the last two features confirm what has been already said so far: the dominant frequency decreases as drowsiness occurred and this is what happens in the last test. Concerning dominant peak, it presents an increment in the last test with respect to the first one but here it could be seen a characteristic increase in the middle section, probably related to such peaks towards the end the second test.

5. Discussion and conclusions

This work has firstly aimed at extracting significant spectral features from electroencephalographic signals in order to discriminate three different states of mind: alertness, transition, drowsiness.

The EEG signals have been recorded from volunteers that have performed reaction time tests. In particular, each subject had to carry out three reaction time tests under different conditions of vigilance: the first one was conducted after a normal night of sleep, the second one in the very early morning, without having slept, and the last one after a deprivation sleep night in the later morning/early afternoon. During each test, reaction time data per minute and EEG signals were recorded.

The goal of such a protocol was to detect drowsiness through changes caused by passing from a well-awake condition to less vigilant physiological states. In fact, as emerged from literature, drowsiness is defined as the transition state between awakening and sleep during which a decrease of vigilance is generally observed [1]. It is assumed that, if a subject is going to be drowsy, its vigilance decreases and consequently its capability of detecting a stimulus decreases as well, causing elongated reaction times. Starting from these hypothesis, reaction time data have been utilized to label each minute of test, as it is well-explained in chapter 3, paragraph 3.1. Consequently, epochs of EEG lasting 1 minute have been considered in order to get a perfect correspondence between labels and epochs of signal.

The features have been obtained by implementing three distinct methods of spectral analysis: non-parametric, parametric, singular spectrum analysis, characterized by different advantages and disadvantages. Therefore, the second goal has been to compare performances of each spectral approach. Firstly, a statistical analysis has been realized in order to select the best features to discriminate three classes. Secondly, the comparison involved the employment of a classifier with the purpose of individuating the best method. Finally, once a method has been identified, a further analysis, subject per subject and test per test, has been performed in order to verify if the protocol has been respected and eventually which subjects have well adhered to it. In addition, a correlation between what labels suggested and what features meant has been investigated.

It must be said that, according to the way of data labeling and other considerations, a few cases of drowsiness emerged: the whole dataset consisted of 812 minutes of tests and only 60 cases resulted drowsy, versus a greater and greater number of alert and transition epochs.

Besides, through an analysis subject per subject, only three participants resulted to adhere to the protocol and drowsy epochs were mainly concentrated in those tests performed by these three subjects (no. 2, no. 12, no. 14). Therefore, whoever will read, must be aware that all the following considerations about the behavior of selected features are mainly based on those subjects that correctly adhered to the protocol.

The fact that only 60 drowsy epochs have been collected has inevitably influenced the performance of each method to recognize drowsiness with respect to the other two classes. Indeed, it is difficult to detect a certain physiological state if it rarely happens during an EEG recording because it risks to be masked by the other spectral contributes, that are more dominant in the signal. It is easy to verify what has been said so far if one thinks to what happens in spectral decomposition: each component brings a contribute in terms of amplitude for a certain frequency and the components related to drowsiness are likely shadowed by the other more dominant ones. Vice versa, if drowsiness lasted more or there were more cases of drowsiness per subject, above all in the third test, it should be easier to detect it, with an appropriate frequency resolution that is able to capture the dynamics of the signals.

In addition, since information about reaction time tests were referred to a minute scale, it was appropriate to divide signals into epochs lasting 1 minute. Initially, we also thought to divide signals into epochs lasting 20 seconds and to extract features with three methods, in order to better detect the dynamics of the EEGs. In this case, averaging operations on three epochs of 20 seconds were necessary in order to finally have only one value of each feature, per minute. By averaging features values in groups of three epochs, we observed that this technique did not lead to further improvements in the results. Therefore, the choice of dividing signals into 1 minute epochs was preferred, with the awareness of a small loss of frequency resolution.

Before commenting results, it is convenient to remember below which features have been computed and why:

- percentage power (P%) in each frequency band computed as:

$P_i\% = \frac{PSD_i}{PSD_{EEG}}, \qquad i = \theta, \alpha, \beta$

- $\log(\frac{P_i\%}{1-P_i\%})$
- the ratio between alpha band PSD and beta band PSD: $\frac{P_\alpha}{P_\beta}$
- the ratio between PSD in low frequency (LF) band and in high frequency (HF) band : $\frac{P_\theta + P_\alpha}{P_\beta}$
- dominant frequency and dominant peak for each frequency band and for the whole range.

From literature, it emerged that physiological events, related to drowsiness or generally to sleep, are better detectable, inside EEG signals, in the frequency domain. This is the reason why we focused on spectral features. In particular, each stage of the sleep is related to a certain frequency band: β band indicates alertness and vigilance, α band is associated to wakefulness but with closed eyes, θ band corresponds to falling asleep and deep relaxation, finally δ band is the rhythm of deep sleep. We decided to exclude delta band from the analysis because it is characteristic of the deep sleep and not drowsiness, as already said.

The first two features were considered because it is interesting to know how much the power spectrum in each band is. In particular, the second feature has been considered according to results from a study of the University of Ostrawa [38] about drowsiness detection through EEG processing. The percentage power (referred in the previous study as "relative power") is computed by normalizing the power in a band to the whole PSD.

The third and the forth features were computed because, as explained about physiological meaning of each frequency band, the ratio between bands is a way of knowing how the balance between bands changes as vigilance conditions vary. In particular, the second of the two features was included in order to evaluate if, adding theta band, drowsiness was better detected. These features are typically employed in studies about drowsiness detection through EEG processing. More details about them can be found in [1], [2], [7], [39].

Finally, dominant peak and dominant frequency were used in order to better individuate the contribute in each band and in the whole range. They are useful because they more weight those contributes that "lasted" more in the signal and so those ones that dominate a certain band or the whole range, more than considering the simple amplitude value. A

detailed computation of them can be found in chapter 3, paragraph 3.2.3 and they have been previously used in a study from the University of Singapore [37].

As regards non-parametric method, eleven features resulted to be significant from Kruskal-Wallis test with a significance value of 95%. Even if the number of drowsy epochs is exiguous, this method has however allowed to extract a sufficient number of features to discriminate drowsiness, transition and alertness. This quantity of features is adequate in order to train a classifier. Since non-parametric method resulted to be the most capable to distinguish the three classes, from k-Cohen coefficient, it was possible to evaluate selected features from this method, subject per subject and test per test, and to verify a correlation between labels and features. This analysis, together with the statistical test, stated that the following ones are meaningful:

1. dominant peak in θ band, from parietal area, is adapt to recognize drowsiness indeed it generally increases when drowsiness occurs. Normally when a subject is going to be "drowsy", alpha rhythm trends to disappear and theta power starts to increase; dually, in a vigilant condition, theta contribute should not be present in the spectrum;
2. percentage power in θ band, from frontal area, presented an opposite trend to what expected for drowsiness because it increases during alertness and decreases when a subject is in a "drowsy" state;
3. a transformed version of percentage power, that is the logarithm of the ratio between P% and (1-P%), in θ band, from frontal area, derives from the previous feature. In contrast with the feature no. 2, it becomes greater and greater as passing from the RT1 to RT3, indicating that power spectrum in θ band increases when drowsiness occurs;
4. dominant frequency in the whole range, from frontal area, is greater in RT1 than in the next ones, as going towards conditions of less and less vigilance. As one can observe from figures throughout the chapter of results, it always assumes very small values, more or less from 0.5 to 1.5. It is supposed that this range, belonging to delta band, results to be dominant, when considering the whole range, because the PSD amplitude is greater than in the other bands and so it shadows the contribute of the other frequencies. When PSD increases, it is assumed that it happens because of an increment of amplitude in the other adjacent bands as well

(in particular θ and α are characterized by voltage tensions greater than in β). Consequently, a certain frequency results to be dominant also because of its amplitude: it is expected that if the amplitude increases, the corresponding frequency is dominant. Under these hypothesis, we considered dominant frequency behavior to be coherent with expectations: it increases with alertness because β band should be dominant, and decreases with drowsiness because lower frequencies should predominate, such as θ and α;

5. dominant peak in the whole range, from frontal area, confirms what have been said for the previous feature: when drowsiness occurs, low frequencies contributes should predominate and, since they are characterized by high average voltage tensions, dominant peak increases with respect to vigilant cases;
6. dominant frequency in the whole range, from central area, has the same trend of feature no. 4;
7. dominant peak in θ band, from central area, well explains what happens when drowsiness occurs because it increases when a subject is going to be or is being "drowsy";
8. percentage power in θ band, from left central area, presents an opposite trend with respect to what expected in each condition: it is greater when a subject is "alert", it decreases when the subject is "in transition" and finally it reaches minimum values when the subject is "drowsy";
9. a transformed version of percentage power in θ band, from left central area, correctly explains what happens in alertness, "transition" and drowsiness, respectively;
10. dominant frequency in the whole range, from left central area, confirms what already explained for features no. 4 and 6;
11. dominant peak in the whole range, from left central area, has the same behavior of features no. 5.

As regards parametric method, smoother spectra have been obtained. We tried to keep the same number and the same kind of features, as much as possible, in order to perform a comparison under the same conditions. In this case, only the following four features resulted to be meaningful:

1. percentage power in θ band, from frontal area
2. a transformed version of the percentage power in θ band, from frontal area
3. percentage power in θ band, from left central area
4. a transformed version of the percentage power in θ band, from left central area.

As one can imagine, four features could not be sufficient to train a classifier indeed k-Cohen coefficient was really low for this method and this result has led to not use this approach for the successive step: protocol verification and features evaluation.
The same problem has been encountered with the last approach, singular spectrum analysis. In this case, only three features –listed below- emerged to be statistically significant to discriminate classes:

1. dominant peak in the whole range, from frontal area
2. dominant peak in the whole range, from left central area
3. dominant peak in θ band, from left central area.

These features, that are still less than the previous approach, have been employed as inputs of the classifier. Also in this case, k-Cohen coefficients suggested a weak capability of discrimination for this method that has been consequently excluded for later evaluation.
In conclusion, it is possible to state that the traditional non-parametric method resulted to be robust with respect to the other two ones. This results has demonstrated that it is possible to employ such a simple approach to get features for drowsiness detection, even if only a few cases of drowsiness are available. It could be interesting to repeat this kind of analysis with richer datasets that include more cases of drowsiness in order to verify if the same results are reached by the three above-mentioned methods.
Another tip for future research in this field could be to perform an automatic data labelling at the place of a manual one, as developed in this work. Maybe it could be appropriate to employ for example an unsupervised learning technique in order to individuate automatically the number of classes and which class each minute test belongs, still using a combination of mean reaction times and number of lapses as rules. It could happen that a greater number of classes or a different distribution of the epochs will come up and consequently the performance of each method could change as well.
Finally, since this analysis exploited data from reaction time tests, once the instant of the onset of the stimulus is known, it could be interesting to study the correlation between the

instant when a subject reacts to the stimulus and the related desynchronization into the bands α and β. It emerged from Pfurtsheller's studies [40],[41] that when a stimulus, that causes motor acts, occurs, a decrement of PSD in such bands is noticeable. Therefore, it is interesting to investigate if this desyncronization happens as soon as the stimulus is presented or not. Through this information, some speculations about drowsiness can be developed as well as we have done in this analysis.

APPENDIX A – SLEEP PHYSIOLOGY

In its simplest and most positive terms, sleep is a desired state of unconsciousness. Each evening we willingly and most pleasantly surrender ourselves to a state of disconnection and vulnerability, expecting to be safe, restored, and comforted upon awakening many hours later. It is no small wonder that this state and its unique attributes have long provoked fascination.

The AASM Manual for the scoring of sleep and associated events: rules, terminology and technical specifications, Westchester, 2007 [58]

Sleep is considered as a primary need which takes one third of a person's lifespan. It implies decreased motor activity, reduced sensorial sensibility, altered consciousness and it can be interrupted by appropriate stimulation.

For a long time, it was believed that sleep was a passive process and that brain would shut down its activity and fall asleep when the absence of any sensory inputs occurred, because it caused the inactivation of a brain area called "reticular activating system". This area, if appropriately exited, produces the typical vigilant state waveform. Nowadays instead, it is universally known that brain does not shut down at all while sleeping, rather it shows remarkable and well defined characteristic patterns of activity. Indeed, it was discovered that there are some specific cerebral areas that are responsible for sleep. Anterior hypothalamus stimulation causes sleep, posterior hypothalamus stimulation determines EEG activation and the thalamus influences sleep spindles. Therefore, it is possible to state that brainstem (and neighborhood) contains the so-said "sleep system", which actively provokes sleep by inhibiting the reticular activating system, and that sleep is an active process which involves many parts of the CNS (central nervous system) and PNS (peripheral nervous system), in particular the autonomic nervous system.

Thanks to the possibility of continuous recordings of brain electrical activity by means of the electroencephalogram (EEG), during wakefulness and sleep, it was actually possible to go deeper into the knowledge of sleep. In addition, this fact has allowed to better distinguish wakefulness from sleep and to discover the difference between rapid-eye movement (REM) sleep and non-REM (NREM) sleep [49].

As regards the classification of sleep, there were many efforts of characterizing such patterns of sleep but the rather poor reliability of such methods led to the necessity of a more standardized classification manual of sleep. Since the publication of Rechtschaffen and Kales's scoring sleep manual 38 years ago, the understanding of sleep has been really

accelerated. However, over the years, the science of sleep has evolved a lot therefore newer and newer scoring manuals were needed. In addition, effects of sleep related to arousal, cardiac dysrhythmias, respiratory patterns, movements and behavior increased the interest around this discipline and led to the development of more updated versions of scoring manuals (i.e. AASM manual for scoring sleep, 2007 [58]).

Entering more specifically into the thematic of sleep, when a subject sleeps there is an alternation between a soft sleep and a deep sleep that are typically referred as NREM and REM sleep. The NREM sleep is the resting sleep that occurs after falling asleep and its amount depends on the previous wakefulness. Through EEG, it corresponds to detect synchronous cerebral high-voltage and low frequency rhythms, meaning the co-activation of many neurons. In young people's sleep, it takes the 75% of the night sleep while only the 25% is represented by REM periodic episodes, lasting 5-30 minutes and happening each 90 minutes. The first REM event usually appears 80-100 minutes after falling asleep, when the EEG shows a desynchronized activity characterized by low-voltage and fast frequency waveform. Since REM waveforms are really closed to wakefulness patterns, this phase is also known as "paradoxical sleep", firstly so-defined by Jouvet in 1958.

Sleep stages

As already said, EEG signals allow to detect specific patterns for each vigilance state, which can be observed in Figure A.1. Wakefulness appears as a low voltage and high frequency activity in the EEG, because of the desynchronization of neurons, also known as beta band (13-30)Hz. Subsequently, EEG alpha activity (8-13)Hz becomes dominant, mainly in the occipital areas, when one is going to close eyes for sleeping. When falling asleep and disconnecting from the surrounding, NREM sleep follows. It can be subdivided into three stages. A transitional stage (stage 1 or simply N1), characterized by a gradually disappearing alpha activity and more dominant theta activity (4-8) Hz, that appears with low voltage mixed-frequency EEG pattern. Immediately after, sleep stage 2 (N2) starts, when sleep spindles, that are short-lasting waves at around 12-15 Hz, predominate. Finally, there is the third stage of sleep (N3), where EEG assumes high voltage tensions but with low frequency (1-2 Hz), so that it is also known as "slow wave sleep".

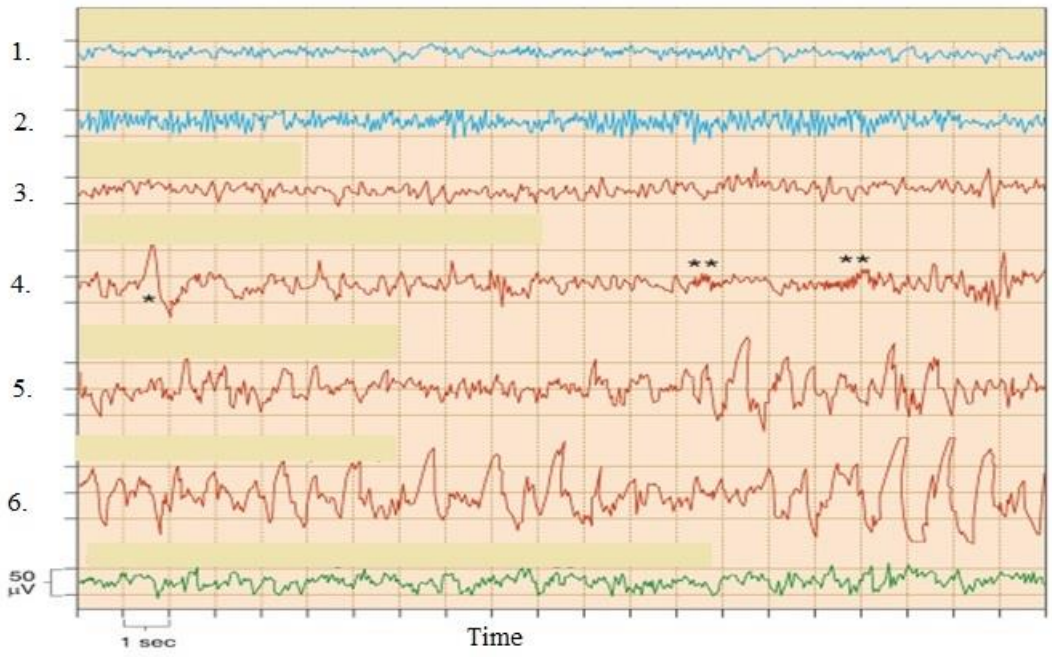

Figure A.1: vigilance states. Starting from the top, the first two signals are related to stage W: track no. 1 indicates EEG associated to wakefulness and it is characterized by low voltage high frequency and irregular rhythm; track no. 2 is related to closed-eyes wakefulness with dominant α activity. The red signals are related to NREM sleep: track no. 3 is typical of stage N1 with dominant θ band; track no. 4 shows K complexes (*) and sleep spindles (**); track no. 5 and no. 6 are related to stage N3. The green one stands for REM sleep.

The transition from low-voltage fast activity, during wakefulness, to NREM sleep is caused by the fact that every cortical neuron is slowly oscillating synchronously across most of the mantle by cortical connections, determining high voltage tensions and low frequencies [49]. During the night, NREM sleep and REM sleep are alternated and when REM sleep occurs, it is possible to observe a fast activity EEG, as it happens in the stage W: for this reason, REM sleep is also called “paradoxical sleep”.

Sleep regulation model

The principle of working of the system that regulates sleep events is based on the correct interaction of two endogenous processes, mutually independent: homeostatic process (S) and circadian process (C). The process S increases when one is awake and decreases while sleeping and corresponds to the amount of low frequencies activity belonging to the range [0.5,4.5]Hz, the delta band, in the NREM sleep EEG. The level of the process S is strictly linked to the duration of the previous wakefulness. Reversely, the process C depends on the so-said “circadian pacemaker”, located in the suprachiasmatic nuclei (SCN) of the

hypothalamus, and more generally it is also related to the ocular retina and the epiphysis (by melatonin influence).

Sleep and wakefulness alternate in fact with a period of 24 hours, from which the term “circadian” derives so that it is influenced by natural stimuli as the light and environmental temperature (Figure A.2). The sleep districts inhibit the reticular activating system, resulting in the transition from sleep to wakefulness. Thereafter, once wakefulness is activated, it naturally endures. After many hours of brain activity, fatigue occurs and leads to sleep.

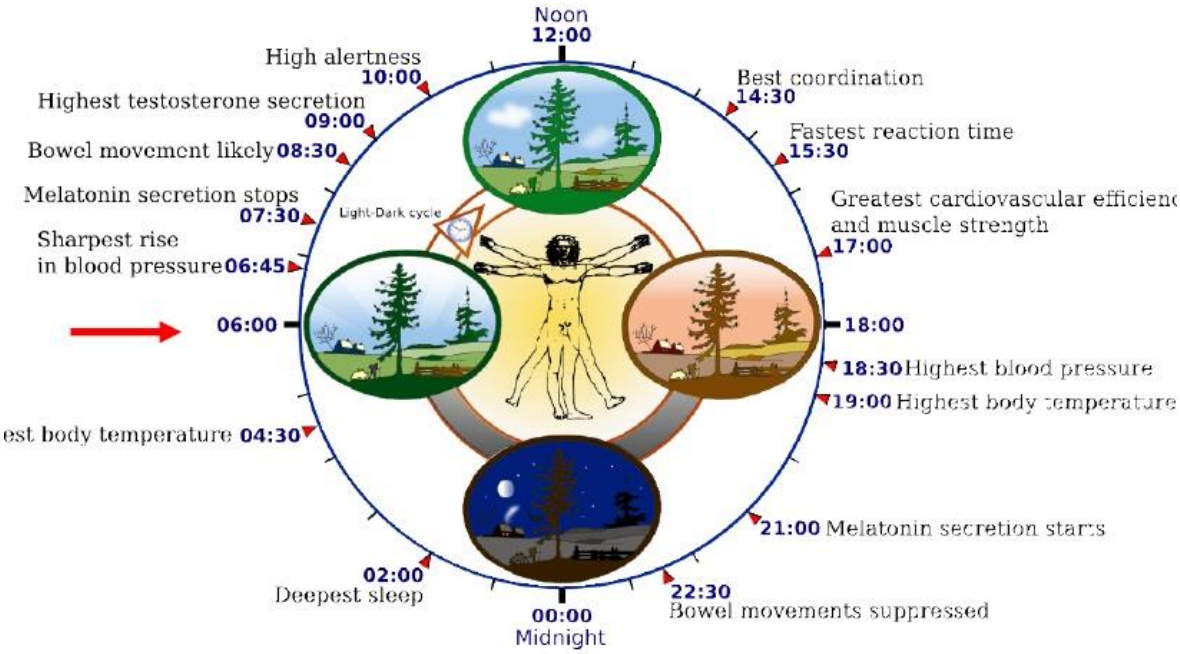

Figure A.2: circadian rhythm diagram of 24 hours.

The function of the process C is then to modulate sleep by controlling a lower and an upper threshold so that if one of these thresholds is reached by process S, one will tend to sleep or wake up. In addition, it must be said that not only the quantity of sleep is important, but also its quality, in fact when a lack of NREM sleep occurs, it can be retrieved by a more intense NREM sleep. Moreover, from some studies it emerged that process S and C act independently indeed sleep-deprived rats, with injured SCN, showed slow-wave activity as well, even if process C no longer existed [49].

Physiological aspects of sleep

Sleep influences so many aspects of human beings' life that its deprivation causes heavy cognitive and physiological impairment. In particular, it allows energetic recovery, temperature regulation, memory and learning enhancement, synaptic homeostasis, and humoral equilibrium.

Several studies have showed that sleep can enhance performance of tasks learned during previous wakefulness. Indeed, the enhancement is not simply a question of time needed to memorize new things, but it is actually linked to sleep [49,50]. Besides, it emerged that the consolidation of new concepts happens during the NREM sleep, while the assimilation and generalization tasks are developed during REM sleep [49].

Another important function of the sleep is the capacity of recovering our organism from fatigue, by restoring physiological levels of activity and metabolic rate and by recharging our forces, lost during wakefulness. For this reason, an elongated awake condition can lead to mental impairment. In fact, while human metabolic savings allow to perform physical tasks despite a sleepless night, brain is the one who mostly suffers sleep deprivation [49]. Indeed, memory consolidation and brain restoration are not conceptually independent according to a new and more complete theory, "the synaptic homeostasis hypothesis" [59]. That theory suggests that plastic processes, occurring during wakefulness, strengthen synaptic connections. What sleep does is then to decrease synaptic strength to a baseline level, being energetically more sustainable, that favors memory and performances. During wakefulness, neuro-modulation intervenes for example by increasing the level of NA (noradrenaline), which enables the storage of information. This fact is due to stronger synapses which mean that a presynaptic neuron fires and thereafter the depolarization of a postsynaptic neuron occurs to indicate remarkable events [49]. During sleep instead, mind is disconnected from the environment and the speed of passing from depolarized to hyperpolarized phases is slower: this fact influences cortical neurons and it appears in the EEG by SWA [60]. These events are caused by changes in neuro-modulation that makes the brain not to interact with environment because no synaptic enhancement occurs.

The reason why the early sleep is still characterized by high amplitude is that, at the end of the wakefulness, synaptic connections are still strong; therefore, neurons can synchronize their firing rate [61]. On the other hand, when synaptic strength decreases, as a consequence of the repetition of depolarization/hyperpolarization phases, the neurons

synchronization decreases as well and a reduced amplitude in slow oscillations results. This fact appears in the EEG as a reduction of SWA [49]. Such cyclic changes of the neural activation influence both the sympathetic activity, during wakefulness, and the parasympathetic one, during sleep. If sympathetic system is over-exited, both because of endogenous or exogenous factors (anxious state or stimulants assumption respectively), this negatively affects the sleep quality because it leads to an excessive increasing vigilance and to an inhibited NREM sleep recovery [14].

Remarkable physiological variations, during sleep, regard also cardiovascular system and respiratory system. In the first case, during NREM sleep, vasodilatation and corresponding reduced heart rate and blood pressure can be detected, while in REM sleep there is vasoconstriction, respectively caused by a reduced and reinforced sympathetic activity. A similar trend regards blood flow to brain during NREM and REM sleep: it decreases during NREM sleep while REM level reaches the same values as in the awake stage [14].

As regards the respiratory system, respiratory rate is constant but there is a slight hypoventilation which leads to increased pCO_2 and decreased pO_2, as a consequence of the muscle relaxation, during NREM sleep. The respiratory rate increases, instead, with REM sleep and here the complete relaxation of the muscle tone causes an increasing resistance to the airflow [14].

Finally, other physiological variations can be observed for kidneys, thermoregulation and important hormones release (like melatonin, present during daylight and absent during darkness).

Sleep quality evaluation

Since sleep plays a very important role from both a physiological and mental point of view, it is clearly useful to evaluate sleep quality, especially in case of pathologies. In addition, it has been proved that bad sleep quality can lead to hypertension and less efficient defense system [14].

Traditionally, sleep is evaluated according to some classification scales: the first one was the R&K scale which involved to divide sleep recordings into 30-seconds epochs and to visually distinguish among AWAKE, NREM (stages 1, 2, 3, 4) and REM sleep, according to polysomnographic signals (ECG, EEG, EMG, EOG). In addition, other parameters can be registered if necessary: thoracic and abdominal movement in order to evaluate

respiratory effort, oxygen saturation (pO_2) and pCO_2 for detecting eventual hypoventilation or sleep apnea, position sensor because some cases of severe upper airway obstruction can affect the body position, pH when gastro-esophageal reflux symptoms are evident. For more information, see "AASM Manual for scoring sleep, 2007" [58], that is the new scale which is recently considered, at the place of the previous R&K scale.

Polysomnographic analysis results in the creation of a characteristic graphic that is known as "hypnogram", where each epoch is labeled by the related sleep stage. Finally, in order to evaluate sleep quality the following parameters are employed: duration of the sleep stage 3, REM latency and duration, frequency and duration of nighttime awakenings and sleep latency, defined as the ratio between time to sleep and time lying on the bed.

APPENDIX B – SPECTRAL ANALYSIS

Non-parametric analysis

The non-parametric analysis is based on the usage of the Discrete Fourier Transform (DFT). It leads to an estimation of the covariance of the process under analysis, or equivalently its spectrum, according to the theorem of Wiener-Khinchin. In particular, non-parametric analysis can be direct or indirect.

The first one employs the periodogram as spectral estimator, which is the squared module of the FFT of the signal normalized to the number of points, defined as below:

$$\hat{S}_y(f) = \frac{1}{NT}|Y(f)|^2,$$

where *N* is the number of data points constituting the signal of interest, *T* the sampling period. Generally, it is preferred to use the faster algorithm of FFT (Fast Fourier Transform) to compute the Fourier Transform. The only constraint is that it is warmly suggested to use a number of points equal to the next power of 2 greater than the length of the signal, because such a choice makes more manageable the computation.

The length of the analyzed signal is generally finite and the signal is not always ergodic, therefore, in order to respect the conditions required to apply DFT, the portion of signal (as if it was windowed) is usually assumed to have an infinite period. In addition, the stationarity is required too. As well known, the big limits of the periodogram are essentially the spectral leakage, the frequency resolution and the large variance of the estimator. The first one is caused by the presence of lateral lobs inside the power spectrum of the signal, resulting in an altered frequency content. The frequency resolution is heavily limited by the number of data points employed for DFT computation. The problems related to spectral leakage and frequency resolution can be partially overcome by applying an appropriate window function to each segment of signal. The third problem derives by the fact that the periodogram is a not statistically consistent spectral estimator, which does not converge to the real spectrum for growing N to infinity.

In order to improve the performance of the traditional periodogram spectral estimation, some devices can be operated, as suggested by Bartlett and Welch method.

This method consists in dividing the signal into K smaller segments of M samples per segment. K periodograms (one per segment), mutually independent, are computed and a

triangular Bartlett window (or eventually other window functions) is applied to each subsequence, so as K modified periodograms are obtained as follows:

$$S_M^{(i)}(f) = \frac{1}{MU} \left| \sum_{n=0}^{M-1} x^{(i)}(n) * w(n) * e^{-\left(\frac{j2\pi kn}{M}\right)} \right|^2, \qquad 1 \leq i \leq K$$

where $x^{(i)}(n)$ is the signal, *w(n)* is the window and *U* is a normalization factor so that the final spectrum estimator P_{xx}, that is then defined, results asymptotically unbiased. The factor *U* is so defined:

$$U = \frac{1}{M} \sum_{n=0}^{M-1} w^2(n)$$

Finally, the spectrum estimator is obtained by averaging on the K modified periodograms as below-indicated:

$$P_{xx}(f) = \frac{1}{K} \sum_{i=1}^{K} S_M^i(f)$$

The indirect method employs the DFT of the autocorrelation function (ACF) of the signal as spectral estimator, according to Wiener-Khinchin theorem, as previously mentioned. The spectral estimation is obtained by applying Blackman-Tuckey method, as follows:

$$\hat{S}_{yy}(f) = T \sum_{k=-M}^{M} r(k)w(k)\, e^{-j2\pi fkT},$$

where *r(k)* is the ACF of the signal, *w(k)* is the window function, *T* the sampling period (the inverse of the sampling frequency F_S).

If on one hand non-parametric analysis presents the above-mentioned limits due to the DFT computation, on the other hand this approach allows to get a simple and fast spectral estimator.

Parametric analysis

The parametric analysis differs from the non-parametric one because it solves the above-mentioned limits about spectral leakage and spectral variance but it requires a heavier computational cost. The parametric approach comes from the concept that a certain process generates the time series under analysis. More specifically, its power spectrum can be computed as the power spectrum of the output signal of a linear time-invariant (LTI) system that receives in input a white noise process (Figure B.1). This is because the power

spectrum of a white noise (WN, the variance of the process) is unitary and so the power spectrum of the output is the squared module of the frequency answer of a system that should be able to represent the signal of interest, if correctly implemented.

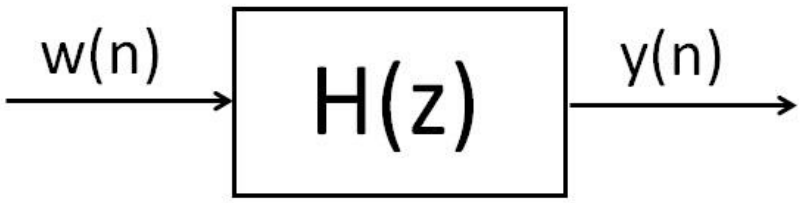

Figure B.1: model of a signal generated by a system receiving in input a stationary white noise WN(0,σ2), with null mean value and standard deviation σ2. The system is completely described by its transfer function.

In particular, implementing a parametric model implies the following three steps:

1. individuation of the appropriate model family of the time series of interest
2. model parameters identification which involves optimum order and coefficients computation
3. PSD estimation by using model coefficients

As regards the first point, it is preferable to take into account the properties of the signal. For instance, an Auto-Regressive (AR) model is appropriate for a signal containing sudden peaks in frequency spectrum. On the contrary, Moving Average (MA) model is used for signals that have no sharp peaks. If the information about the signal is not available to take a decision, the Autoregressive Moving Average (ARMA) model can be used for both cases. As regards EEG signals, AR and ARMA models are preferred because their structure consists of peaks at discrete frequency intervals. In particular, AR model is usually employed because it has more advantages than ARMA in terms of computational costs.

According to the AR model, the amplitude of a signal at a given instant can be obtained by summing up the different amplitudes of previous samples. The relationship between the input and the output of the above-mentioned system, shown in Figure B.1, can be written as in the formula below:

$$y(n) = \sum_{k=1}^{p} a_k y(n-k) + w(n)$$

where *w(n)* is a white noise of variance σ^2 and null mean value.

As regards the second point about the parameters of the model, an important issue is the identification of the optimum order of the AR model. It can be individuated by employing one of the three most famous criteria known as *Akaike Information Criterion* (AIC), *Final Prediction Error* (FPE) and *Minimum Description Length* (MDL), defined respectively as in the formula below:

$$AIC(p) = Nln(\sigma_e^2) + 2p$$

$$FPE(p) = \sigma_e^2 \frac{N + p + 1}{N - p - 1}$$

$$MDL(p) = Nln(\sigma_e^2) + pln(N),$$

where *N* is the total number of samples as well as the length of the signal, *p* is the optimum order, σ_e^2 is the variance of the prediction error as well as an estimator of input noise variance. In particular, each criterion is composed of a term related to the variance of the prediction error and another term linked to the order and so to the number of coefficient. The first term suggests that if the variance of the prediction error decreases the figure of merit decreases as well because it means that the model is well mirroring the signal of interest. However, this fact likely happens when increasing the order of the model so, in order to not risk the problem of overfitting (an excessive adherence of the model to a specific signal, which causes loss of generalization power), the second term balances the behavior of the figure of merit. Indeed, as can be observed in Figure B.2, if the order increases too much, the trend of the figure of merit worsens. The point of intersection between the dotted curve, representing the variance of the prediction error (still going down), and the point where the blue curve of figure of merit starts to grow, indicates the optimum order.

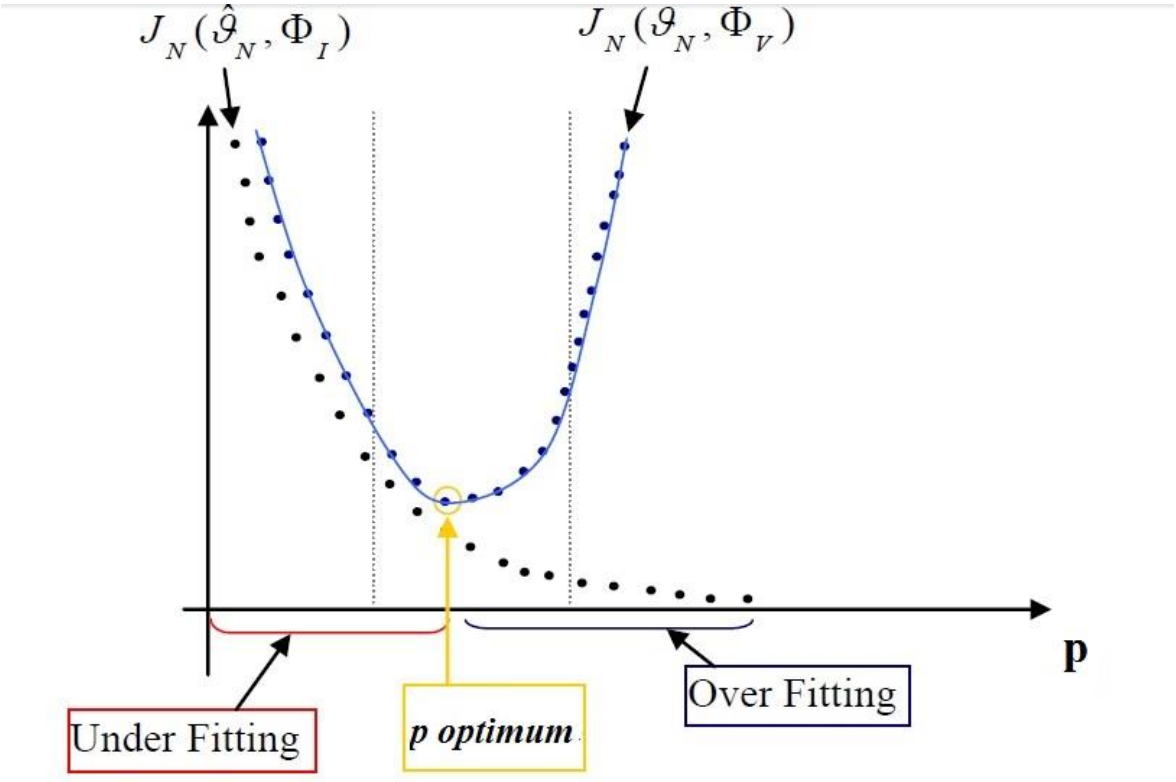

Figure B.2: p is the order of the model, $J_N(\hat{\theta}_N, \Phi_I) and\, J_N(\theta_N, \Phi_V)$ are respectively the variance of the prediction error in the "identification phase" and in the "validation phase". The yellow-circled point indicates the optimum order.

In addition, the Anderson's whiteness test on the prediction error is realized, in order to evaluate the performance of the so-defined model. This test involves to check if the prediction error results to be white and so if its autocorrelation function (ACF), defined below, is maximum at lag=0 and around zero elsewhere.

$$R_e^N(\tau) = \frac{1}{N}\sum_{t=1}^{N} e(t)e(t+\tau),$$

where *N* is the number of samples, *e(t)* is the prediction error and *e(t+τ)* is the error lagged of a certain shift τ , to evaluate the correlation level among samples at such shift.

The whiteness of the prediction error implies that the model well represented and explained the signal. Therefore, if the order suggested by *AIC/FPE/MDL* does not satisfy the condition of the Anderson's test, it needs to be incremented until the residual error becomes white. However, also in this case it is necessary to pay attention not to increment too much the order to avoid the problem of overfitting. Indeed, even if the model seems to

replicate perfectly the signal, it risks losing its capacity of generalization and the model comes up to be inadequate.

As regards the computation of the coefficient, by summing up all the squared values of the prediction errors on the N samples of the signal, a "cost function" called J can be obtained:

$$J = \sum_{n=1}^{N} e(n)^2$$

This figure of merit is a function of the coefficients of the model so that the coefficients are determined through Yule Walker's equations that are based on the minimization of the function *J* using Levinson-Durbin recursion.

Once the estimated coefficients $\hat{a}_k$ of the model have been determined, that are as many as the order of the model, it is possible to move to the third point, the computation of the PSD of the signal, as in the following formula:

$$\hat{S}_y\left(e^{j\omega T}\right) = \sigma^2 T \left|H\left(e^{j\omega T}\right)\right|^2 = \frac{\sigma^2 T}{\left|1 + \sum_{k=1}^{p} a_k e^{-j\omega T k}\right|^2}$$

where σ^2 must be substituted with *J* and a_k with the above-mentioned estimated coefficients $\hat{a}_k$; *T* is the sampling period of the signal.

Singular spectrum analysis

The "Singular spectrum analysis" (SSA) is a technique used for time series analysis and forecasting and it results from a combination of classical time series analysis, multivariate statistics, multivariate geometry, dynamical systems and signal processing.

It aims at decomposing the original series into a sum of a few components that represent the main content of the signal such as a slowly varying trend, oscillatory components and the background noise. It exploits the advantages of both singular value decomposition (SVD) and principal component analysis (PCA). SSA is characterized by the fact that neither a parametric model or stationarity hypothesis are assumed for the time series so it is a model-free technique.

The algorithm can be summarized in 2 principal operations that are the "decomposition stage" and the "reconstruction stage", each of whom consists of other two sub-steps for a total of 4 main passages:

1) Decomposition stage

1.1 Embedding step

The one-dimensional series is embedded into a multidimensional series (lagged vectors) whose dimension is called "*window length*" L. The multidimensional time series, which has become a sequence of vectors as long as the window length, forms the so-called "trajectory matrix" X. The only parameter to determine at this step is the window length L, which is really important for the frequency resolution. In fact, L is linked to the frequency by the relationship:

$$\Delta f = \frac{F_s}{L}$$

Where F_s is the sampling frequency and L should be chosen according to the desired frequency resolution.

If $1 < L < N$, where N is the length of the signal, the embedding step creates $K=N - L+1$ lagged vectors:

$$X_i = (f_{i-1}, \dots, f_{i+L-2})^T, \qquad 1 \leq i \leq K$$

where X_i has dimension equal to L and it is L-lagged. The trajectory matrix is obtained from the sequence of the X_i vectors:

$$X = \begin{pmatrix} f_0 & f_1 & f_2 & \cdots & f_{K-1} \\ f_1 & f_2 & f_3 & \cdots & f_K \\ f_2 & f_3 & f_4 & \cdots & f_{K+1} \\ \vdots & \vdots & \vdots & \ddots & \vdots \\ f_{L-1} & f_L & f_{L+1} & \cdots & f_{N-1} \end{pmatrix}$$

The trajectory matrix is characterized by having equal elements on the diagonals $i+j$ = const. and so it is a *Hankel matrix*.

Then, the real and proper trajectory matrix has been computed and the corresponding covariance matrix C has been obtained as: $\boldsymbol{C = X * X^T}$, of size *LxL*.

1.2 Singular value decomposition (SVD)

The result of this step is the SVD of the trajectory matrix X, but after computing C as the covariance matrix, it is easier to compute its eigenvalues and eigenvectors. $\lambda_1, \dots \dots \dots, \lambda_L$ is the notation of the eigenvalues, considered in a decreasing order of magnitude so as $\lambda_1 \geq \cdots \geq \lambda_L \geq 0$, which represent the squared singular values of X, and $U_1, \dots \dots \dots, U_L$ the notation of the orthonormal system of the related eigenvectors, corresponding to the

left singular vectors of X. These last ones are usually known in literature as "empirical orthogonal functions" (**EOFs**). The right singular vectors can be interpreted instead as the eigenvectors of the matrix $\mathbf{X^T X}$.

Subsequently, it is possible to describe X as a sum of rank-one biorthogonal matrices X_i , where $i = 1.....d$ and $d \leq L$ is the number of nonzero singular values of X, that is $d=max\{I,$ *such that* $\lambda_i > 0\}$.

Then, let's indicate with $V_i = X^T U_i / \sqrt{\lambda_i}$ and X can be now written as $X = X_1 + \ldots\ldots + X_d$, where X_i are defined as $\sqrt{\lambda_i U_i V_i^T}$ and they are rank-one matrices, therefore they can be considered as elementary matrices. Generally $\sqrt{\lambda_i}\, U_i V_i$ are referred as the i-th "*eigentriple*" of the SVD of X.

2) Reconstruction stage

2.1 Grouping step

At this step, the set of indices $I = \{1, \ldots, d\}$ is split into m several groups $I_1, \ldots, I_m$ and some matrices X_i are obtained by summing up within each group. The result of the step is contained into the following statements:

$$X = \sum_{k=1}^{m} X_{I_k}, \quad where\ X_{I_k} = \sum_{i \in I_k} X_i$$

Once d is determined, starting from the **EOFs**, it is possible to compute the principal components (**PCs**) of the signal, by projecting the signal on the EOFs as $V_i = X^T U_i$, with $1 \leq i \leq d$.

2.2 Reconstruction step

This step brings back each matrix X, previously constructed in the grouping step, to the original length N.

Let's denote by **Y** an $L \times K$ matrix, whose elements are y_{ij} , $1 \leq i \leq L$, $1 \leq j \leq K$. Then let's define by $L^* = \min(L,K)$ and by $K^* = \max(L,K)$ so that $N = L + K - 1$. Therefore $y^*_{ij} = y_{ij}$ if L<K and $y^*_{ij} \neq y_{ij}$ otherwise. Thereafter, it is necessary to average on diagonals in order to transfer the matrix Y to the new series $g_o, \ldots\ldots, g_{N-1}$ by using the following formula in Figure B.1:

$$g_k = \begin{cases} \dfrac{1}{k+1} \displaystyle\sum_{m=1}^{k+1} y^*_{m,k-m+2} & \text{for } 0 \le k < L^* - 1, \\ \dfrac{1}{L^*} \displaystyle\sum_{m=1}^{L^*} y^*_{m,k-m+2} & \text{for } L^* - 1 \le k < K^*, \\ \dfrac{1}{N-k} \displaystyle\sum_{m=k-K^*+2}^{N-K^*+1} y^*_{m,k-m+2} & \text{for } K^* \le k < N. \end{cases}$$

"Analysis of Time Series structure: SSA and related techniques", Nina Golyandina, Vladimir Nekrutkin, Anatoly A. Zhigljavsky, 2001 [20]

References

[1] Picot, A., Charbonnier, S., & Caplier, A. (2009). Monitoring drowsiness on-line using a single encephalographic channel. *Recent Advances in Biomedical Engineering*, 145-164.

[2] Jap, B. T., Lal, S., Fischer, P., & Bekiaris, E. (2009). Using EEG spectral components to assess algorithms for detecting fatigue. *Expert Systems with Applications*, *36*(2), 2352-2359.

[3] Huang, R. S., Jung, T. P., & Makeig, S. (2009). Tonic changes in EEG power spectra during simulated driving. In *Foundations of augmented cognition. neuroergonomics and operational neuroscience* (pp. 394-403). Springer Berlin Heidelberg.

[4] Lin, C. T., Wu, R. C., Jung, T. P., Liang, S. F., & Huang, T. Y. (1900). Estimating driving performance based on EEG spectrum analysis. *EURASIP Journal on Advances in Signal Processing*, *2005*(19), 3165-3174.

[5] Eoh, H. J., Chung, M. K., & Kim, S. H. (2005). Electroencephalographic study of drowsiness in simulated driving with sleep deprivation. *International Journal of Industrial Ergonomics*, *35*(4), 307-320.

[6] Anund, A., Kecklund, G., Peters, B., Forsman, Å., Lowden, A., & Åkerstedt, T. (2008). Driver impairment at night and its relation to physiological sleepiness. *Scandinavian journal of work, environment & health*, 142-150.

[7] Fanfulla, F. BIOSENSORS FOR MICROSLEEPS DETECTION DURING DRIVE SIMULATIONS.

[8] Papadelis, C., Kourtidou-Papadeli, C., Bamidis, P. D., Chouvarda, I., Koufogiannis, D., Bekiaris, E., & Maglaveras, N. (2006, August). Indicators of sleepiness in an ambulatory EEG study of night driving. In *Engineering in Medicine and Biology Society, 2006. EMBS'06. 28th Annual International Conference of the IEEE* (pp. 6201-6204). IEEE.

[9] Ungureanu, M., Bigan, C., Strungaru, R., & Lazarescu, V. (2004). Independent component analysis applied in biomedical signal processing. *Measurement Science Review*, *4*(2), 18.

[10] Schlögl, A., Kemp, B., Penzel, T., Kunz, D., Himanen, S. L., Värri, A., ... & Pfurtscheller, G. (1999). Quality control of polysomnographic sleep data by histogram and entropy analysis. *Clinical Neurophysiology*, *110*(12), 2165-2170.

[11] Yue, C. (2011). EOG signals in drowsiness research.

[12] Cerutti, S. (1976). *Analisi del segnale EEG e automazione*. Cooperativa libraria universitaria del politecnico.

[13] Molteni, E., Bianchi, A. M., Butti, M., Reni, G., & Zucca, C. (2008). Combined behavioral and EEG power analysis in DAI improve accuracy in the assessment of sustained attention deficit. *Annals of biomedical engineering*, *36*(7), 1216-1227.

[14] TACCHINO, G. (2011). Estrazione di descrittori per la stadiazione del sonno mediante modelli TVAM su segnali periferici acquisiti con dispositivi wearable.

[15] Collomb, C. Linear prediction and levinson-durbin algorithm, 2009.

[16] Sepehri, A. Levinson-Durbin Algorithm and Signal Modeling.

[17] Akin, M., & Kiymik, M. K. (2000). Application of periodogram and AR spectral analysis to EEG signals. *Journal of Medical Systems*, *24*(4), 247-256.

[18] Moddemeijer, R. (1999, May). An efficient algorithm for selecting optimal configurations of AR-coefficients. In *SYMPOSIUM ON INFORMATION THEORY IN THE BENELUX* (pp. 189-196). Werkgemeenschap voor Informatie-en Communicatietheorie; 1998.

[19] Broomhead, D. S., & King, G. P. (1986). Extracting qualitative dynamics from experimental data. *Physica D: Nonlinear Phenomena*, *20*(2), 217-236.

[20] Golyandina, N., Nekrutkin, V., & Zhigljavsky, A. A. (2010). *Analysis of time series structure: SSA and related techniques*. CRC Press.

[21] Lisi, F., Nicolis, O., & Sandri, M. (1995). Combining singular-spectrum analysis and neural networks for time series forecasting. *Neural Processing Letters*, *2*(4), 6-10.

[22] Golyandina, N., Nekrutkin, V., & Zhigljavsky, A. A. (2010). *Analysis of time series structure: SSA and related techniques*. CRC Press.

[23] Aydın, S., Saraoğlu, H. M., & Kara, S. (2011). Singular spectrum analysis of sleep EEG in insomnia. *Journal of medical systems*, *35*(4), 457-461.

[24] Atoufi, B., Zakerolhosseini, A., & Lucas, C. (2009, October). Improving EEG signal prediction via SSA and channel selection. In *Computer Conference, 2009. CSICC 2009. 14th International CSI* (pp. 349-354). IEEE.

[25] Hassani, H. (2007). Singular spectrum analysis: methodology and comparison.

[26] Claessen, D.,Groth, A. A beginner's guide to SSA.

[27] Mineva, A., & Popivanov, D. (1996). Method for single-trial readiness potential identification, based on singular spectrum analysis. *Journal of neuroscience methods*, *68*(1), 91-99.

[28] Storey, B. (2002). Computing Fourier series and power spectrum with Matlab. *TEX Paper*.

[29] Cerna, M., & Harvey, A. F. (2000). The fundamentals of FFT-based signal analysis and measurement. *National Instruments, Junho*.

[30] Chang, D. C. Nonparametric Spectrum Estimation .

[31] McNames, J.Spectral Estimation Overview.

[32] Sadiq, I., & Khan, S. A. (2010, March). Fuzzification of the Analysis of Heart Rate Variability Using ECG in Time, Frequency and Statistical Domains. In *Computer Engineering and Applications (ICCEA), 2010 Second International Conference on* (Vol. 1, pp. 481-485). IEEE.

[33] Orlando, T.ANALISI NUMERICA IN FREQUENZA.

[34] Oppenheim, A. V., Willsky, A. S., & Nawab, S. H. (1983). *Signals and systems* (Vol. 2). Englewood Cliffs, NJ: Prentice-Hall.

[35] Achermann, P. (2009). EEG analysis applied to sleep. *Epileptologie*, *26*, 28-33.

[36] Acharya U, R., Faust, O., Kannathal, N., Chua, T., & Laxminarayan, S. (2005). Non-linear analysis of EEG signals at various sleep stages. *Computer methods and programs in biomedicine*, *80*(1), 37-45.

[37] Yeo, M. V., Li, X., Shen, K., & Wilder-Smith, E. P. (2009). Can SVM be used for automatic EEG detection of drowsiness during car driving?. *Safety Science*, *47*(1), 115-124.

[38] Zoubek, L., Charbonnier, S., Lesecq, S., Buguet, A., & Chapotot, F. (2007). Feature selection for sleep/wake stages classification using data driven methods. *Biomedical Signal Processing and Control*, *2*(3), 171-179.

[39] Eoh, H. J., Chung, M. K., & Kim, S. H. (2005). Electroencephalographic study of drowsiness in simulated driving with sleep deprivation. *International Journal of Industrial Ergonomics*, *35*(4), 307-320.

[40] Pfurtscheller, G., Neuper, C., Brunner, C., & da Silva, F. L. (2005). Beta rebound after different types of motor imagery in man. *Neuroscience letters*, *378*(3), 156-159.

[41] Solis-Escalante, T., Müller-Putz, G. R., Pfurtscheller, G., & Neuper, C. (2012). Cue-induced beta rebound during withholding of overt and covert foot movement. *Clinical Neurophysiology*, *123*(6), 1182-1190.

[42] Zaepffel, M., Trachel, R., Kilavik, B. E., & Brochier, T. (2013). Modulations of EEG Beta Power during Planning and Execution of Grasping Movements. *PloS one*, *8*(3), e60060.

[43] Leocani, L., Toro, C., Manganotti, P., Zhuang, P., & Hallett, M. (1997). Event-related coherence and event-related desynchronization/synchronization in the 10 Hz and 20 Hz EEG during self-paced movements. *Electroencephalography and Clinical Neurophysiology/Evoked Potentials Section*, *104*(3), 199-206.

[44] Makeig, S., Bell, A. J., Jung, T. P., & Sejnowski, T. J. (1996). Independent component analysis of electroencephalographic data. *Advances in neural information processing systems*, 145-151.

[45] Lin, C. T., Wu, R. C., Jung, T. P., Liang, S. F., & Huang, T. Y. (1900). Estimating driving performance based on EEG spectrum analysis. *EURASIP Journal on Advances in Signal Processing*, *2005*(19), 3165-3174.

[46] Santamaria, J., & Chiappa, K. H. (1987). The EEG of drowsiness in normal adults. *Journal of clinical Neurophysiology*, *4*(4), 327-382.

[47] Åkerstedt, T., & Gillberg, M. (1990). Subjective and objective sleepiness in the active individual. *International Journal of Neuroscience*, *52*(1-2), 29-37.

[48] Kay, A. M. A. N. D. A., Trinder, J. O. H. N., Bowes, G. L. E. N. N., & Kim, Y. O. U. N. G. (1994). Changes in airway resistance during sleep onset. *Journal of Applied Physiology*, *76*(4), 1600-1607.

[49] Huber, R. Functional aspects of EEG sleep, Epileptologie 2009; 26: 34 – 41

[50] Achermann, P. (2009). EEG analysis applied to sleep. *Epileptologie*, *26*, 28-33.

[51] Silber, M. H., Ancoli-Israel, S., Bonnet, M. H., Chokroverty, S., Grigg-Damberger, M. M., Hirshkowitz, M., ... & Iber, C. (2007). The visual scoring of sleep in adults. *J Clin Sleep Med*, *3*(2), 121-131.

[52] Quanten, S., De Valck, E., Cluydts, R., & Berckmans, D. (2006). Thermoregulatory changes at driver sleepiness. *International journal of vehicle design*, *42*(1), 87-100.

[53] Bianchi, A. M., Mendez, M. O., & Cerutti, S. (2010). Processing of signals recorded through smart devices: sleep-quality assessment. *Information Technology in Biomedicine, IEEE Transactions on*, *14*(3), 741-747.

[54] Törnros, J., Peters, B., and Östlund, J. (2000) .Heart rate measures as drowsiness indicators. Swedish National Road and Transport Research Institute.

[55] Mathew, R., & Dutt, N. D. (1991). Spectral Estimation of Short Segments of EEG Signals Using Least Squares Waveshaping Filters.

[56] «Measurement in health and disease: Cohen's kappa », University of York Department of Health Sciences.

[57] Wertz, J., François, C., & Verly, J. G. (2013). Drowsiness monitoring for road safety.

[58] American Academy of Sleep Medicine, & Iber, C. (2007). *The AASM manual for the scoring of sleep and associated events: rules, terminology and technical specifications*. American Academy of Sleep Medicine.

[59] Tononi, G., & Cirelli, C. (2006). Sleep function and synaptic homeostasis. *Sleep medicine reviews*, *10*(1), 49-62.

[60] Steriade, M., & Timofeev, I. (2003). Neuronal plasticity in thalamocortical networks during sleep and waking oscillations. *Neuron*, *37*(4), 563-576.

[61] Esser, S. K., Hill, S. L., & Tononi, G. (2007). Sleep homeostasis and cortical synchronization: I. Modeling the effects of synaptic strength on sleep slow waves. *Sleep*, *30*(12), 1617.

[62] Pfurtscheller, G., Neuper, C., Pichler-Zalaudek, K., Edlinger, G., & Lopes da Silva, F. H. (2000). Do brain oscillations of different frequencies indicate interaction between cortical areas in humans?. *Neuroscience letters*, *286*(1), 66-68.

[63] Chouvarda, I., Rosso, V., Mendez, M. O., Bianchi, A. M., Parrino, L., Grassi, A., ... & Cerutti, S. (2011). Assessment of the EEG complexity during activations from sleep. *Computer methods and programs in biomedicine*, *104*(3), e16-e28.

[64] Johns, M. W. (1991). A new method for measuring daytime sleepiness: the Epworth sleepiness scale. *sleep*, *14*(6), 540-545.

[65] POPIVANOV, D. (1999). Assessment of EEG frequency dynamics using complex demodulation. *Physiol. Res*, *48*, 157-165.

[66] Anguita, D. Business Intelligence.

[67] McKeown, M., Humphries, C., Achermann, P., Borbély, A., & Sejnowsk, T. (1998). A new method for detecting state changes in the EEG: Exploratory application to sleep data. *Journal of sleep research*, *7*(S1), 48-56.

[68] Isaksson, A., Lagergren, K., & Wennberg, A. (1976). Visible and non-visible EEG changes demonstrated by spectral parameter analysis. Electroencephalography and clinical neurophysiology, 41(3), 225-236.

[69] Isaksson, A., Wennberg, A., & Zetterberg, L. H. (1981). Computer analysis of EEG signals with parametric models. Proceedings of the IEEE, 69(4), 451-461.

[70] Cerutti, S., Baselli, G., Liberati, D., & Pavesi, G. (1987). Single sweep analysis of visual evoked potentials through a model of parametric identification. Biological cybernetics, 56(2-3), 111-120.

[71] Cerutti, S., Chiarenza, G., Liberati, D., Mascellani, P., & Pavesi, G. (1988). A parametric method of identification of single-trial event-related potentials in the brain. *Biomedical Engineering, IEEE Transactions on*, *35*(9), 701-711.

[72] Liberati, D., Cursi, M., Locatelli, T., Comi, G., & Cerutti, S. (1997). Total and partial coherence analysis of spontaneous and evoked EEG by means of multi-variable autoregressive processing. *Medical and Biological Engineering and Computing*, *35*(2), 124-130.